Linear Parameter-Varying Sliding Mode Control of State Delayed Systems with Application to Delta Wing Vortex Coupled Dynamics

Ming Yang

A Thesis

in

The Department

of

Mechanical and Industrial Engineering

Presented in Partial Fulfillment of the Requirements
for the Degree of Master of Applied Science (Mechanical Engineering) at
Concordia University
Montreal, Quebec, Canada

December, 2005

Your file Votre référence
ISBN: 0-494-14316-9
Our file Notre référence
ISBN: 0-494-14316-9

ABSTRACT

Linear Parameter-Varying Sliding Mode Control of State Delayed Systems with Application to Delta Wing Vortex Coupled Dynamics

Ming Yang

In this thesis a new linear parameter-varying sliding mode control (LPVSMC) approach is developed for linear parameter-varying time-delayed systems (LPVTDS). This approach combines sliding mode control (SMC), linear parameter-varying (LPV) control theory, and time delay stability analysis to solve an LPVTDS control problem. A new linear parameter-varying sliding surface is proposed to achieve the control objectives. The time-varying parameters of the sliding surface are calculated according to a parameter-dependent Lyapunov-Krasovskiĭ functional analysis which ensures asymptotic stability of the closed-loop system. It is anticipated that this method will lead to significant improvement over existing SMC approaches in aerospace applications with parameter variations.

ACKNOWLEDGEMENTS

I would like to take this opportunity to thank everyone who has helped me during the completion of this thesis.

I am grateful to my supervisor Dr. Brandon W. Gordon. It is his vast knowledge, considerable enthusiasm and great patience that guided me throughout the development of the project. His careful reviews of my manuscript helped me a lot in this project. I also enjoyed and appreciated the thoughtful insights and advice from the defence scientist C. A. Rabbath of Defence Research and Development Canada since I have especially benefited from many discussions with him.

I must acknowledge a company named the Numérica Technologies for providing financial support for the delta wing project. In addition, I would like to thank all the people currently and formerly at the Department of Mechanical and Industrial Engineering for providing a great social and professional environment.

I would also like to express my appreciations to all the members of Control and Information Systems (CIS) laboratory, especially Merhdad Pakmehr and Wei Wei Liu who helped me develop my understanding and knowledge of the delta wing systems, and Vijay Prakash, Zhi Qian Ren, Behnood Gholami, Jiang Lu and Bin Liu, who provided useful suggestions on the draft version of my thesis.

Finally, I am grateful to my wife, who has stood by my side and always supported me in all of my endeavours, and my parents for their constant support and encouragement, in spite of the distance.

TABLE OF CONTENTS

LIST OF FIGURES

NOMENCLATURE

$\mathbf{A},\mathbf{B},\mathbf{C},\mathbf{D}$	parameter matrices of system
$\hat{\mathbf{A}},\hat{\mathbf{B}},\hat{\mathbf{C}},\hat{\mathbf{D}}$	parameter matrices of regular form
$\tilde{\mathbf{A}},\tilde{\mathbf{B}},\tilde{\mathbf{C}},\tilde{\mathbf{D}}$	parameter matrices of reduced form
Cl	roll moment coefficient of delta wing systems
e	output error
f_c	bearing friction coefficient of delta wing systems
$\mathbf{F},\mathbf{G},\mathbf{H},\mathbf{L}$	time-varying parameters of sliding surface
h	constant time delay
I	moment of inertia of delta wing systems
$\mathbf{I}$	identity matrix of appropriate dimension
k	boundary layer thickness of sliding surface
m, p	time-varying parameters of the delta wing model
q	dynamic air pressure of delta wing system
r	reference signal
$\mathbf{P},\mathbf{Q},\mathbf{R}$	positive definite symmetric matrices
IR	real number
s_a	wing element area of delta wing systems
$\mathbf{s}$	sliding surface
$\mathbf{S}$	linear parameter-varying operator

$\mathcal{S}^{n \times n}$	symmetric matrices
t	present time
T	time period of decay of delta wing systems
T^*	release time of delta wing systems
$\mathbf{u}$	control input
$\mathbf{u}_{eq}$	Equilibrium control input
U	input torque of delta wing systems
V	Lyapunov function
$\mathbf{x}$	state vector
X_q	quasi-steady term in X_{vb} of delta wing systems
X_s	static term in X_{vb} of delta wing systems
X_{vb}	vortex breakdown location
$\mathbf{y}$	measured output
$\mathbf{z}$	state of normal form
α	angle of attack of delta wing systems
δ	approximation of time delays
ε	boundary layer width of sliding surface
ϕ	roll angle of delta wing systems
φ	structure angle of delta wing systems
λ_0	half apex angle of delta wing systems
$\boldsymbol{\sigma}(t)$	time-varying parameter
τ	time at step onset

Γ	leading edge sweep angle of delta wing systems
Λ	effective sweep back angle of delta wing systems

Subscripts:

h	time-delayed vector
l	left vortex
q	quasi-steady term
r	right vortex
s	static term
vb	vortex breakdown

Notation:

$\mathbb{R}$ denotes the set of real numbers and $\mathbb{R}^{n \times m}$ the set of $n \times m$ real matrices. The transpose and inverse of the real matrix $\mathbf{M}$ are denoted by $\mathbf{M}^{T}$ and $\mathbf{M}^{-1}$ respectively. A square matrix $\mathbf{M}$ is symmetric if $\mathbf{M} = \mathbf{M}^{T}$, and a square matrix $\mathbf{M}$ is skew-symmetric if $\mathbf{M} = -\mathbf{M}^{T}$. $\mathbf{I}$ is used to represent an identity matrix of appropriate dimensions. $\mathrm{diag}\{\cdots\}$ denotes a block-diagonal matrix. $\mathbf{M}(\cdot)$ is used to denote a matrix function. We use $\boldsymbol{S}^{n}$ to denote the set of $n \times n$ real symmetric matrix. $\mathbf{M} \in \boldsymbol{S}^{n}$ and $\mathbf{M} > \mathbf{0}$ ($\mathbf{M} \geq \mathbf{0}$) means that $\mathbf{M}$ is a positive definite symmetric matrix (positive semi-definite symmetric matrix), this is $\mathbf{x}^{T}\mathbf{M}\mathbf{x} > \mathbf{0}$ ($\mathbf{x}^{T}\mathbf{M}\mathbf{x} \geq \mathbf{0}$) for all nonzero vectors $\mathbf{x}$. Similarly, $\mathbf{M} \in \boldsymbol{S}^{n}$ and $\mathbf{M} < \mathbf{0}$ ($\mathbf{M} \leq \mathbf{0}$) means that $\mathbf{M}$ is a negative definite symmetric matrix (negative semi-definite symmetric matrix), this is $\mathbf{x}^{T}\mathbf{M}\mathbf{x} < \mathbf{0}$ ($\mathbf{x}^{T}\mathbf{M}\mathbf{x} \leq \mathbf{0}$) for all nonzero vectors $\mathbf{x}$. In a symmetric block matrix, the expression $(*)$ will be used to denote the sub-matrices that lie below the diagonal.

LIST OF ACRONYMS

LMI	linear matrix inequality
LPV	linear parameter-varying
LPVSMC	linear parameter-varying sliding mode control
LPVTDS	linear parameter-varying time-delayed system
SMC	sliding mode control
NIRISS	nonlinear indicial response and internal state-space

Chapter 1

Introduction

1.1. Motivation

The delta wing aircraft has become a favoured design for advanced fighters because of two main advantages. The first advantage is that the delta wing leading edge remains behind the shock wave generated by the nose of the aircraft when flying faster than the speed of sound. If the shock wave hits the wings of the aircraft, the high-pressure variation across a shock could cause structural fatigue. The second reason is that the delta wing has a very high stall angle [54]. An increase in the angle of attack results in an increase in the lift force. The angle of attack can continue to increase up to a point where maximum lift is generated. This point is the so-called stall angle. The delta wing can also generate a vortex that remains attached to the upper surface of the wing, even if the aircraft has a very high angle of attack. This large vortex can make the delta wing have a larger stall angle than other kinds of aircraft configurations. The delta wing has been used for the design of numerous fighter aircrafts such as the Mirage and MiG aircraft. It has also been used for the design of unmanned aerial vehicles (UAVs) such as the Stingray developed by Boeing in 2002, and the Cutlass a cruise missile used by Israel's military force since 1999.

Controller design for delta wing systems, when modelled using the nonlinear indicial response and internal state-space (NIRISS) modelling approach, is difficult since this description includes two highly nonlinear terms: the nonlinear static terms and the unsteady convolution term involving delayed states [20], [21] and [22]. A control problem for roll motion of delta wing systems can be characterized by time-varying nonlinear terms and complex time-delayed components. To address the nonlinearity and parameter variations of the model, a standard linear parameter-varying (LPV) controller has been developed based on a linear parameter-varying approximation of the system [54]. However, the standard LPV controller response to a fast changing input signal is characterized by a large overshoot and long setting time. This is a result of the system parameters varying too rapidly which results in conservative LPV control designs.

The sliding mode control (SMC) approach has been effectively used for systems that are nonlinear with rapid parameter variations [8]. It is a powerful control method with increasing applications in many areas of control engineering. The purpose of SMC is to drive the plant's state trajectory onto a pre-designed surface in the state space and to maintain the plant's state trajectory on this surface for all subsequent time. The pre-designed surface is called a "sliding surface." Many approaches have been proposed for the design of the sliding surface. These include pole placement, eigen-structure assignment and linear/optimal quadratic techniques, etc. Linear matrix inequality (LMI) based methods have also been explored in [13], which proposes SMC strategies for systems with time delays. However, these sliding mode control approaches are not well suited for application to linear parameter-varying time delayed systems (LPVTDS) such as the vortex-coupled delta wing system. In particular, they don't include parameter varying sliding surfaces or manifold stability analysis based on the LPVTDS description.

This thesis presents a new linear parameter-varying sliding mode control (LPVSMC) design approach for an LPVTDS. The organization of the thesis is as follows. In chapter 2, the background material is presented such as the quasi-LPV modelling approach, LMI-based control and convex optimization, Lyapunov-Krasovskiĭ theorems for time-delayed systems, SMC design approach, and NIRISS model of delta wing systems. In chapter 3, an LPVSMC is developed for an LPVTDS by means of solving the stability equation of a parameter-dependent Lyapunov-Krasovskiĭ functional. The controller synthesis conditions are formulated in terms of LMI that can be solved via LMI solvers. This result is then generalized to multiple time-delayed LPV systems. Chapter 4 describes the quasi-LPV modelling and LPVSMC synthesis procedure for the delta wing roll motion problem. Finally, chapter 5 presents conclusions and future work.

1.2. Previous Work

Three main topics of previous work relate to this thesis. They are LPV systems and model development, time-delayed system analysis, and the SMC approach. Research results from these areas are reviewed in the following paragraphs.

The LPV approach, which has received increasing attention since it was initially studied in 1991 [41], is defined as a linear system whose dynamics depend on time-varying parameters whose trajectories are unknown *a priori* but can be measured in real-time. Since the controller is synthesized based on an LPV model, it is important to carefully select the LPV representation to avoid conservative results. There are two main approaches to the LPV modelling of nonlinear systems. Jacobian linearization approach is presented in [12], [30], [40] and [55]. This approach assumes the nonlinear system behaves similarly to a linear system in a small range around certain points that are defined as equilibrium points, so the deviations around equilibrium points will be small. By setting the deviations equal to zero, a Jacobian Matrix can be obtained. An LPV model arises from computing the Jacobian Matrix. The other approach is the quasi-LPV linearization method, which is introduced in [1], [5], [29], [31], [42], [55] and [48]. The quasi-LPV approach focuses on linearizing the nonlinear systems by defining nonlinear terms as time-varying parameters. This approach can guarantee stability and performance properties, but we may not always find the controller for the LPV plant because of conservative nature of this approach.

Time delays are often encountered in control systems, so stability criteria for time-delayed system have become a critical problem in controller design. The existing criteria can be classified into two types: delay-independent and delay-dependent stabilization, as in [32], [38], [51] and [52]. If the delay terms are unknown or unbounded, the delay-independent stability criteria are used since the controller is synthesized without considering the information of the delay. It has been studied in [23], [26] and [35]. Recently, many studies focus on the delay-dependent stability criteria, for example [7], [10], [16], [24], [33], [49], [52] and [59]. The delay-dependent approaches make use of the bound of delay terms, so it can give less conservative than the delay-independent ones.

SMC is also called variable structure control (VSC), which is an effective robust control approach for the nonlinear model, see [45] and [56]. The idea of SMC is based on the use of discontinuous control laws. It breaks down into two steps. Firstly, the sliding mode controller drives the state trajectory onto the pre-designed sliding surface. Once on the surface, the state trajectory slides along the surface toward a designed point. SMC has been applied to various systems. For example, [15], [17], [37] and [53] are applied to flight control problems; [27] designs a sliding mode controller for brushless direct drive servo motors; [43] introduces a SMC application of active magnetic bearings;

[9] and [58] are applied for rigid manipulators; and [36] is for an underwater vehicle prototype. In addition, SMC research concepts have been extended to time-delayed systems, see [14], [18], [28], [39], [44] and [46]. In [14], the authors introduce the SMC of uncertain systems with single or multiple time delays, and use LMI for the optimization procedure. There are very few papers discussing the parameter-varying SMC approach. We only found one paper [43] that presents the approach for dealing with sliding mode hyperplane for a single time-varying parameter second-order LPV model.

1.3. Thesis Contributions

The main original contributions of this thesis are as follows:

1) A new LPVSMC synthesis procedure for LPVTDS

A linear parameter-varying sliding surface is proposed to achieve the requirement of tracking or regulation. Using this surface a parameter-dependent Lyapunov-Krasovskiĭ functional analysis is used to guarantee asymptotic stability of the closed-loop system. The time-varying controller parameters are calculated from a set of LMIs, which can be readily solved using LMI solvers such as YALMIP, SeDuMi, or LMITool. Furthermore, the results are extended to the more general case of multiple time delay systems. This original contribution represents the first approach for LPV based SMC of time delay systems.

2) A new multiple time delay LPV model for vortex-coupled delta wing systems

This model is developed based on an approximation of an NIRISS representation of vortex-coupled dynamics proposed in the literature. This model is characterized by time-varying nonlinear terms and complex time-delayed components. Through curve fitting of the various coefficients and delay terms a new LPV description is developed. It is shown that the LPV model agrees closely with the full nonlinear model representation. This new LPV model can be used to develop and test new LPV, LPVSMC, and other nonlinear control methods. This work represents the first LPV based model for vortex coupled delta wing systems.

3) Application of the LPVSMC method to vortex-coupled delta wing systems

The LPVSMC approach is applied to an LPV representation of vortex-coupled delta wing system dynamics to demonstrate the validity of the approach. The approach presented is one of the first applications of nonlinear control for vortex-coupled delta wing systems.

Chapter 2

Background Material

In this chapter, the background material, which associates to this study, is introduced such as the quasi-LPV modelling approach, LMI-based control and convex optimization, Lyapunov-Krasovskiĭ theorems for time-delayed systems, SMC design approach, and NIRISS model of delta wing systems.

2.1. Quasi-LPV Modelling Approach

A quasi-LPV modelling approach is used in this thesis to develop a control oriented model for delta wing systems. This approached was used since it can directly obtain an LPV model from the aerodynamic model of vortex-coupled delta wing systems by using several simple approximations of the nonlinear terms. Before we develop the LPV model for delta wing systems, the background of quasi-LPV modelling is introduced in this section. Related references are given by [1], [5], [29], [31], [42], [55] and [48]. Consider the nonlinear system

$$\begin{aligned} \dot{\mathbf{x}} &= \mathbf{a}\,(\mathbf{x},\mathbf{u},\mathbf{w},\mathbf{v}) \\ \mathbf{y} &= \mathbf{c}\,(\mathbf{x},\mathbf{u},\mathbf{w},\mathbf{v}) \end{aligned} \tag{1}$$

where $\mathbf{x} \in I\!R^{n}$ is the state, $\mathbf{u} \in I\!R^{m}$ is the control input, and $\mathbf{y} \in I\!R^{p}$ is the measured output. The symbol $\mathbf{w}$ represents the parameter-dependent external input, and the symbol $\mathbf{v}$ represents the parameter-independent external input, such as reference commands, disturbances and noises. Equations (1) are linearized by replacing the nonlinear terms by the time-varying parameters $\boldsymbol{\sigma}(t)$. The boundary of $\boldsymbol{\sigma}(t)$ can be determined according to the nonlinear terms, but the exact value of $\boldsymbol{\sigma}(t)$ can only be calculated on-line. Therefore, the open-loop LPV description for the nonlinear system can be given as

$$\begin{aligned}\dot{\mathbf{x}}(t) &= \mathbf{A}(\boldsymbol{\sigma}(t))\,\mathbf{x}(t) + \mathbf{B}(\boldsymbol{\sigma}(t))\,\mathbf{u}(t)\\ \mathbf{y}(t) &= \mathbf{C}(\boldsymbol{\sigma}(t))\,\mathbf{x}(t) + \mathbf{D}(\boldsymbol{\sigma}(t))\,\mathbf{u}(t)\end{aligned} \tag{2}$$

The state-space matrix functions $\mathbf{A}(\cdot) \in \mathbb{R}^{n\times n}$, $\mathbf{B}(\cdot) \in \mathbb{R}^{n\times m}$, $\mathbf{C}(\cdot) \in \mathbb{R}^{p\times n}$ and $\mathbf{D}(\cdot) \in \mathbb{R}^{p\times m}$ are assumed to be bounded continuous functions of a time-varying parameter vector $\boldsymbol{\sigma}(t) \in \Theta$. The constraints Θ are defined as

$$\Theta = \left\{\boldsymbol{\sigma} : \boldsymbol{\sigma}(t) \in \mathbb{R}^{s}, \left|\dot{\boldsymbol{\sigma}}_i(t)\right| \le \upsilon_i, i = 1,2,\cdots s, \forall t \in \mathbb{R}\right\} \tag{3}$$

When it will not cause an ambiguity, we use $\boldsymbol{\sigma}$ to denote the vector of time-varying parameter $\boldsymbol{\sigma}(t)$ for the rest of the thesis. For the same reason, subscript 'h' is used to denote the time-delayed vector, e.g., $\mathbf{x}_h := \mathbf{x}(t-h)$ and $\boldsymbol{\sigma}_h := \boldsymbol{\sigma}(t-h)$.

Example 1. Consider a linear time-varying plant

$$\begin{aligned}\begin{bmatrix}\dot{x}_1\\ \dot{x}_2\end{bmatrix} &= \begin{bmatrix}0 & 0.6+0.2(2+\sin(t))\\ -2 & -3.2+0.1(2+\sin(t))\end{bmatrix}\begin{bmatrix}x_1\\ x_2\end{bmatrix} + \begin{bmatrix}0\\ 1\end{bmatrix}u\\ y &= \begin{bmatrix}1 & 0\end{bmatrix}\begin{bmatrix}x_1\\ x_2\end{bmatrix}\end{aligned} \tag{4}$$

If the time-varying parameter $\sigma(t)$ is used to replace the time-varying component $(2+\sin(t))$, the linear time-varying plant can be modelled using the LPV system

$$\begin{bmatrix} \dot{x}_1 \\ \dot{x}_2 \end{bmatrix} = \left(\begin{bmatrix} 0 & 0.6 \\ -2 & -3.2 \end{bmatrix} + \begin{bmatrix} 0 & 0.2 \\ 0 & 0.1 \end{bmatrix} \sigma \right) \begin{bmatrix} x_1 \\ x_2 \end{bmatrix} + \begin{bmatrix} 0 \\ 1 \end{bmatrix} u \tag{5}$$

where the time-varying parameter is

$$\begin{aligned} &\sigma(t) = 2+\sin(t), \qquad 1 \le \sigma(t) \le 3 \\ &|\dot{\sigma}(t)| = |\cos(t)| \le 1 \end{aligned} \tag{6}$$

The quasi-LPV representation for a nonlinear system is not unique, so we should choose a suitable quasi-LPV representation that can be implemented readily.

2.2. LMI based Control and Convex Optimization

Most of recent control theories usually lead to solve some LMIs. A LMI can be represented as the following, as in [3] and [4]

$$\mathbf{M}(\mathbf{x}) = \mathbf{M}_0 + x_1\mathbf{M}_1 + \cdots + x_n\mathbf{M}_n > \mathbf{0} \tag{7}$$

where $\mathbf{x} \in \mathbb{R}^n$ and $\mathbf{M} \in \mathcal{S}^n$. The LMI is convex constraints, that is

$$\lambda\mathbf{M}(\mathbf{x}) + (1-\lambda)\mathbf{M}(\mathbf{y}) \ge \mathbf{M}(\lambda\mathbf{x} + (1-\lambda)\mathbf{y}) > \mathbf{0} \tag{8}$$

if

$$\mathbf{M}(\mathbf{x}) > \mathbf{0} \quad \text{and} \quad \mathbf{M}(\mathbf{y}) > \mathbf{0} \tag{9}$$

for all $\lambda \in [0,\ 1]$. If $\mathbf{x}$ can be found for the given LMI $\mathbf{M}(\mathbf{x}) > \mathbf{0}$, $\mathbf{x}$ is called the feasible solution of the LMI, otherwise, the LMI is called infeasibile. Lyapunov functional for a linear system is an example of LMI. Given the following linear system

$$\begin{aligned} \dot{\mathbf{x}}(t) &= \mathbf{A}\mathbf{x}(t) + \mathbf{B}\mathbf{u}(t) \\ \mathbf{y}(t) &= \mathbf{C}\mathbf{x}(t) + \mathbf{D}\mathbf{u}(t) \end{aligned} \tag{10}$$

we choose the following Lyapunov functional

$$V = \mathbf{x}^T(t)\mathbf{P}\mathbf{x}(t) > 0 \tag{11}$$

According to the definition of positive definite matrix, the above equation implies that

$$\mathbf{P} > \mathbf{0} \tag{12}$$

where $\mathbf{P} \in \boldsymbol{S}^n$ is symmetric positive definite matrix. Calculating the derivative of $\mathbf{V}$ yields

$$\frac{dV}{dt} = \mathbf{x}^T(t)\mathbf{A}^T\mathbf{P}\mathbf{x}(t) + \mathbf{x}^T(t)\mathbf{P}\mathbf{A}\mathbf{x}(t) = \mathbf{x}^T(t)\left(\mathbf{A}^T\mathbf{P} + \mathbf{P}\mathbf{A}\right)\mathbf{x}(t) \tag{13}$$

If the following LMI is feasible, the system is stable.

$$\mathbf{A}^T\mathbf{P} + \mathbf{P}\mathbf{A} < \mathbf{0} \tag{14}$$

where $\mathbf{A}$ is given and $\mathbf{P}$ is the variable. If we study $\mathbf{H}_\infty$ in [60] or LPV control in [2], it might lead to convex optimization problems [4], such as

$$\begin{aligned} &\text{minimize} \quad \gamma \\ &\text{subject to} \begin{bmatrix} \mathbf{A}^T\mathbf{X}+\mathbf{X}\mathbf{A} & \mathbf{X}\mathbf{B} & \mathbf{C}^T \\ (*) & -\gamma\mathbf{I} & \mathbf{D}^T \\ (*) & (*) & -\gamma\mathbf{I} \end{bmatrix} < \mathbf{0} \end{aligned} \tag{15}$$

where γ is an induced $\mathbf{H}_\infty$ – norm of closed-loop system. In order to efficiently solve the LMI and convex optimization problems, several conic programming solvers were developed based on interior point methods [4], such as YALMIP, SeDuMi, SOSTools or LMITool. YALMIP is a MATLAB toolbox for rapid solving of optimization problems [59]. It focused on semi-definite programming, convex linear, quadratic, and second order cone. We select YALMIP to solve a LMI, because it is not only easy to learn but also easy to use. Now, we give an example to demonstrate how to solve Lyapunov equation using YALMIP.

Example 2. Consider a second-order system

$$\begin{aligned} \dot{x}_1 &= -4x_2 \\ \dot{x}_2 &= x_1 - 2x_2 \end{aligned} \tag{16}$$

The state space equation of the system is

$$\mathbf{A} = \begin{bmatrix} 0 & -4 \\ 1 & -2 \end{bmatrix} \tag{17}$$

The system is stable, if there exist matrices $\mathbf{P}, \mathbf{Q} > \mathbf{0}$ with the LMI

$$\mathbf{A}^T\mathbf{P} + \mathbf{P}\mathbf{A} - \mathbf{Q} < \mathbf{0} \tag{18}$$

Let us take $\mathbf{Q} = \mathbf{I}$ and use YALMIP

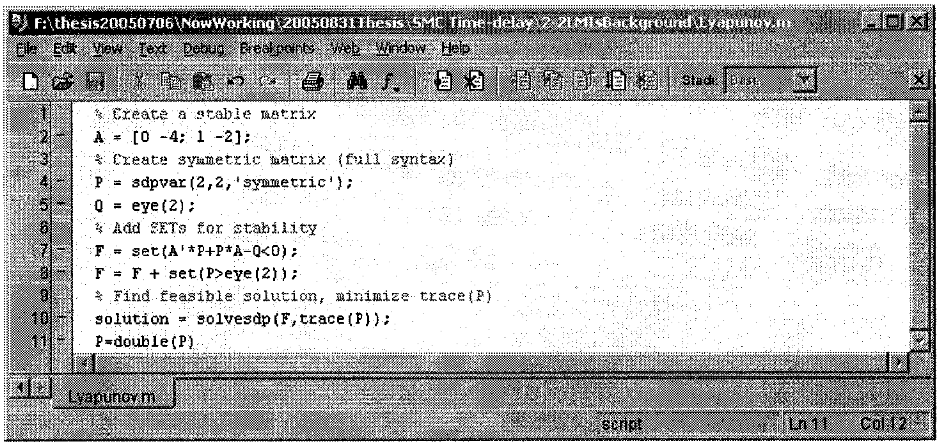

Figure 2-1 Interface of YALMIP to solve Lyapunov function

The solutions are

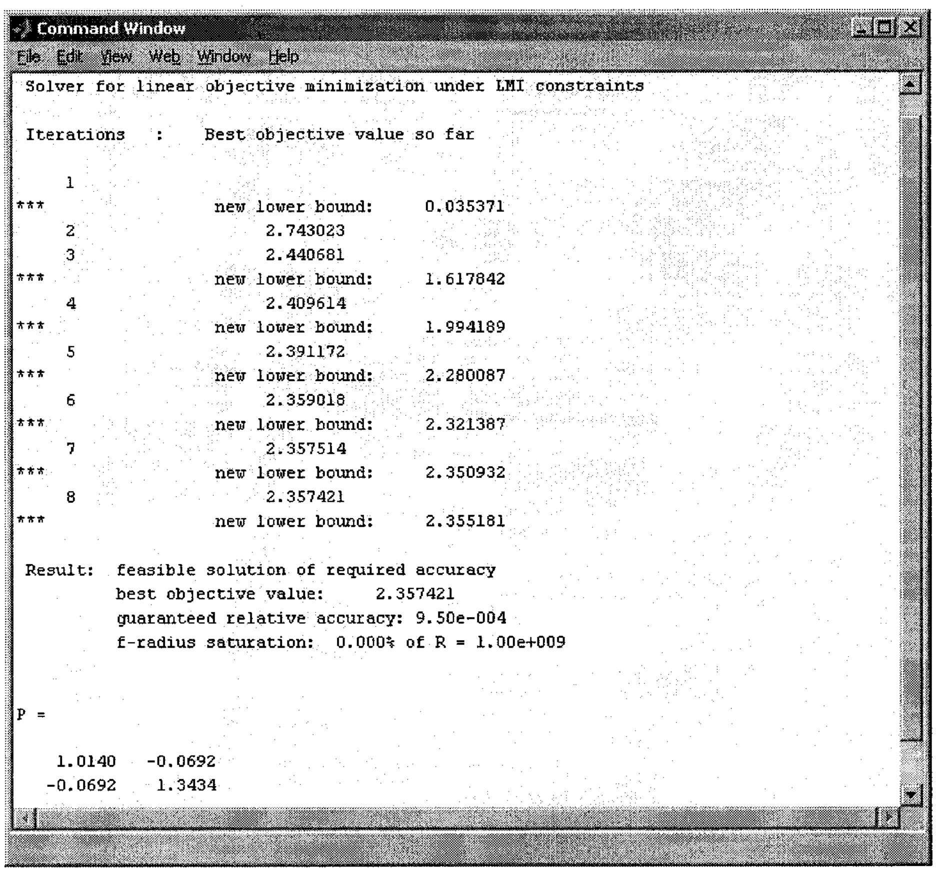

Figure 2-2 YALMIP results for Lyapunov function

The LMI is feasible, so the system is stable.

The above solutions can be checked using an eigenvalue test method. We know that any matrix $\mathbf{M} \in \mathbb{R}^{n \times n}$ can be decomposed as the sum of a symmetric matrix and a skew-symmetric matrix as the following equation [5] and [45]

$$\mathbf{M} = \frac{\mathbf{M}+\mathbf{M}^{\mathrm{T}}}{2} + \frac{\mathbf{M}-\mathbf{M}^{\mathrm{T}}}{2} \tag{19}$$

where the fist part is symmetric

$$\left(\frac{\mathbf{M}+\mathbf{M}^{\mathrm{T}}}{2}\right)^{\mathrm{T}} = \frac{\mathbf{M}+\mathbf{M}^{\mathrm{T}}}{2} \tag{20}$$

and the second part is skew-symmetric.

$$\left(\frac{\mathbf{M}-\mathbf{M}^{\mathrm{T}}}{2}\right)^{\mathrm{T}} = -\frac{\mathbf{M}-\mathbf{M}^{\mathrm{T}}}{2} \tag{21}$$

Assuming $\mathbf{x}$ as an arbitrary $n \times 1$ vector, we have

$$\mathbf{x}^{\mathrm{T}} \frac{\mathbf{M}-\mathbf{M}^{\mathrm{T}}}{2} \mathbf{x} = -\left(\mathbf{x}^{\mathrm{T}} \frac{\mathbf{M}-\mathbf{M}^{\mathrm{T}}}{2} \mathbf{x}\right)^{\mathrm{T}} \tag{22}$$

Then, it leads to

$$\mathbf{x}^{\mathrm{T}} \frac{\mathbf{M}-\mathbf{M}^{\mathrm{T}}}{2} \mathbf{x} = 0 \tag{23}$$

The quadratic function of the skew-symmetric part is zero, so we obtain a quadratic function of any matrix can be replaced by its symmetric term.

$$\mathbf{x}^{\mathrm{T}}\mathbf{M}\mathbf{x} = \mathbf{x}^{\mathrm{T}}\left(\frac{\mathbf{M}+\mathbf{M}^{\mathrm{T}}}{2}+\frac{\mathbf{M}-\mathbf{M}^{\mathrm{T}}}{2}\right)\mathbf{x} = \mathbf{x}^{\mathrm{T}}\frac{\mathbf{M}+\mathbf{M}^{\mathrm{T}}}{2}\mathbf{x}+\mathbf{0} \tag{24}$$

Therefore, a general matrix is positive definite if and only if its symmetric part has all positive eigenvalues [5].

Example 3. Testing of the YALMIP results in Example 2. From that example we have

$$\mathbf{P} = \begin{bmatrix} 1.0140 & -0.0692 \\ -0.0692 & 1.3434 \end{bmatrix} \tag{25}$$

where $\mathbf{P}$ is a symmetric matrix, so it is not necessary to decompose it as the sum of a symmetric matrix and a skew-symmetric matrix. We can directly use the eigenvalues of $\mathbf{P}$ to check the positive definiteness. The eigenvalues are given by

$$|\mathbf{P}-\lambda\mathbf{I}| = \begin{vmatrix} 1.0140-\lambda & -0.0692 \\ -0.0692 & 1.3434-\lambda \end{vmatrix} = 0 \tag{26}$$

From the above equation we can calculate the eigenvalues of $\mathbf{P}$ as

$$\lambda_1 = 1 > 0 \quad \text{and} \quad \lambda_2 = 1.3574 > 0 \tag{27}$$

Therefore the solution $\mathbf{P}$ of the LMI is positive definite. The LMI solution can be verified from

$$\mathbf{A}^{T}\mathbf{P}+\mathbf{P}\mathbf{A}-\mathbf{Q} \tag{28}$$
$$=\begin{bmatrix}0 & -4\\ 1 & -2\end{bmatrix}^{T}\begin{bmatrix}1.0140 & -0.0692\\ -0.0692 & 1.3434\end{bmatrix}+\begin{bmatrix}1.0140 & -0.0692\\ -0.0692 & 1.3434\end{bmatrix}\begin{bmatrix}0 & -4\\ 1 & -2\end{bmatrix}-\begin{bmatrix}1 & 0\\ 0 & 1\end{bmatrix}$$
$$=\begin{bmatrix}-1.1384 & -2.5740\\ -2.5740 & 5.82\end{bmatrix}$$

The eigenvalues of this expression are given by

$$\lambda_{1}=-6.9584<0 \quad \text{and} \quad \lambda_{2}=-0.00002<0 \tag{29}$$

The solution matrix **P** is positive definite and the LMI expression is negative definite. Therefore the YALMIP solution is feasible and the system is asymptotically stable.

2.3. Lyapunov-Krasovskiĭ Theorems for Time-Delayed Systems

Recently, the Lyapunov-Krasovskiĭ approach has received increasing attention for analysis of the delay-dependent stabilization of time-delayed systems. It was used to analyze the LPVTDS in [47], [50] and [51], in which the stability, $\mathbf{L}_2$ and $\mathbf{L}_2$-to-$\mathbf{L}_\infty$ gain performance for these systems are explored using quadratic single Lyapunov-Krasovskiĭ functional equations. The Lyapunov-Krasovskiĭ functional is chosen as

$$V=\mathbf{x}^{T}\mathbf{P}(\boldsymbol{\sigma}(t))\mathbf{x}+\int_{t-h}^{t}\mathbf{x}^{T}(\theta)\mathbf{Q}(\boldsymbol{\sigma}(\theta))\mathbf{x}(\theta)d\theta \tag{30}$$

In [16], a new method for dealing with a time-delayed system is presented. In this method, the derivative terms of the state, which is in the derivative of the Lyapunov functional, are retained and some free weighting matrices are used to express the relationships among the system variables, and among the terms in the Leibniz-Newton formula. In [7] and [10], the authors develop efficient delay-dependent conditions for the stability of time-delayed systems. These conditions are parameter-dependent. Also, these conditions improve the results that were derived using a single Lyapunov-Krasovskiĭ functional. The functional is chosen as

$$V = \mathbf{x}^T\mathbf{P}(\boldsymbol{\sigma}(t))\mathbf{x} + \int_{t-h}^{t} \mathbf{x}^T(\theta)\mathbf{R}\mathbf{x}(\theta)d\theta + \int_{-h}^{0}\int_{t+s}^{t} \mathbf{x}^T(\theta)\mathbf{Q}\mathbf{x}(\theta)d\theta ds \tag{31}$$

Now, we introduce the two most important Lyapunov-Krasovskiĭ theorems given in [25].

Lyapunov-Krasovskiĭ Theorem 1. If there is a differential equation with time delay

$$\frac{dx_i}{dt} = f_i(x_1(t-h),\cdots,x_n(t-h),t) \qquad i=1,\cdots,n \tag{32}$$

for $h > 0$, there corresponds a functional $\mathbf{V}(x,t)$ which is positive definite for

$$\|x(t)\| \le H, \quad t \in [-h \quad 0] \tag{33}$$

and has an infinitely small upper bound, and if the value

$$\left(\limsup_{\Delta t \to +0} \frac{\Delta V}{\Delta t}\right) = \limsup_{\Delta t \to +0}\left(\frac{V(x(x_0(-h),t_0,t+\Delta t-h),t+\Delta t) - V(x(x_0(-h),t_0,t-h),t)}{\Delta t}\right) \tag{34}$$

is negative definite along Equation (32), then the system of Equation (32) is asymptotically stable.

Lyapunov-Krasovskiĭ Theorem 2. Suppose there is an upper-bounded functional $V(x(t), x(t-h), t)$ that satisfies the conditions [25]

$$V \geq 0 \tag{35}$$

$$\lim_{\Delta t \to +0} \sup\left(\frac{\Delta V}{\Delta t}\right) < 0 \tag{36}$$

Then, the following multiple time delay system is asymptotically stable

$$\frac{dx_i}{dt} = f_i(x_1(t-h_{i1}), \cdots, x_n(t-h_{in}); x_1(t), \cdots, x_n(t), t)), \quad i = 1, \cdots, n; \; 0 \leq h_{ij}(t) \leq h \tag{37}$$

Next, we present the procedure of using the Lyapunov-Krasovskiĭ approach to analyze the stability of time-delayed systems. Consider the following time-delayed system

$$\dot{\mathbf{x}} = \mathbf{A}\mathbf{x}(t) + \mathbf{A}_h \mathbf{x}(t-h) \tag{38}$$

Choosing the following Lyapunov-Krasovskiĭ functional

$$V = \mathbf{x}^T(t)\mathbf{P}\mathbf{x}(t) + \int_{t-h}^{t} \mathbf{x}^T(\theta)\mathbf{Q}\mathbf{x}(\theta)d\theta \tag{39}$$

where $\mathbf{P}, \mathbf{Q} \in \boldsymbol{S}^n$ are symmetric positive definite matrices. Calculating the derivative of V along the trajectory of Equation (38) yields

$$\frac{dV}{dt}=\mathbf{x}^T(t)\mathbf{A}^T\mathbf{P}\mathbf{x}(t)+\mathbf{x}^T(t-h)\mathbf{A}_h^T\mathbf{P}\mathbf{x}(t)+\mathbf{x}^T(t)\mathbf{P}\mathbf{A}\mathbf{x}(t)+\mathbf{x}^T(t)\mathbf{P}\mathbf{A}_h\mathbf{x}(t-h)$$
$$+\mathbf{x}^T(t)\mathbf{Q}\mathbf{x}(t)-\mathbf{x}^T(t-h)\mathbf{Q}\mathbf{x}(t-h)$$
$$=\begin{bmatrix}\mathbf{x}(t)\\ \mathbf{x}(t-h)\end{bmatrix}^T\begin{bmatrix}\mathbf{A}^T\mathbf{P}+\mathbf{P}\mathbf{A}+\mathbf{Q} & \mathbf{P}\mathbf{A}_h\\ (*) & -\mathbf{Q}\end{bmatrix}\begin{bmatrix}\mathbf{x}(t)\\ \mathbf{x}(t-h)\end{bmatrix} \quad (40)$$

If the following LMI is feasible, the system is stable.

$$\begin{bmatrix}\mathbf{A}^T\mathbf{P}+\mathbf{P}\mathbf{A}+\mathbf{Q} & \mathbf{P}\mathbf{A}_h\\ (*) & -\mathbf{Q}\end{bmatrix}\leq 0 \quad (41)$$

The Lyapunov-Krasovskiĭ approach is illustrated using the following example.

Example 4. Consider the time-delayed system (38) with

$$\mathbf{A}=\begin{bmatrix}-2 & 0\\ 1.75 & -0.25\end{bmatrix}, \mathbf{A}_h=\begin{bmatrix}-1 & 0\\ -0.1 & -0.25\end{bmatrix} \text{ and } h=1.65 \quad (42)$$

The results of YALMIP below in Figure 2-3 indicate the Lyapunov-Krasovskiĭ LMI is feasible. After 36 iterations, we obtain the positive definite matrices

$$\mathbf{P}=\begin{bmatrix}0.1008 & 0.0134\\ (*) & 0.0073\end{bmatrix} \text{ and } \mathbf{Q}=\begin{bmatrix}0.2570 & 0.0141\\ (*) & 0.0018\end{bmatrix} \quad (43)$$

Therefore the system is stable, which is confirmed by its regulation plot from the initial values $x_1(0)=1$ and $x_2(0)=1$ (see Figure 2-4).

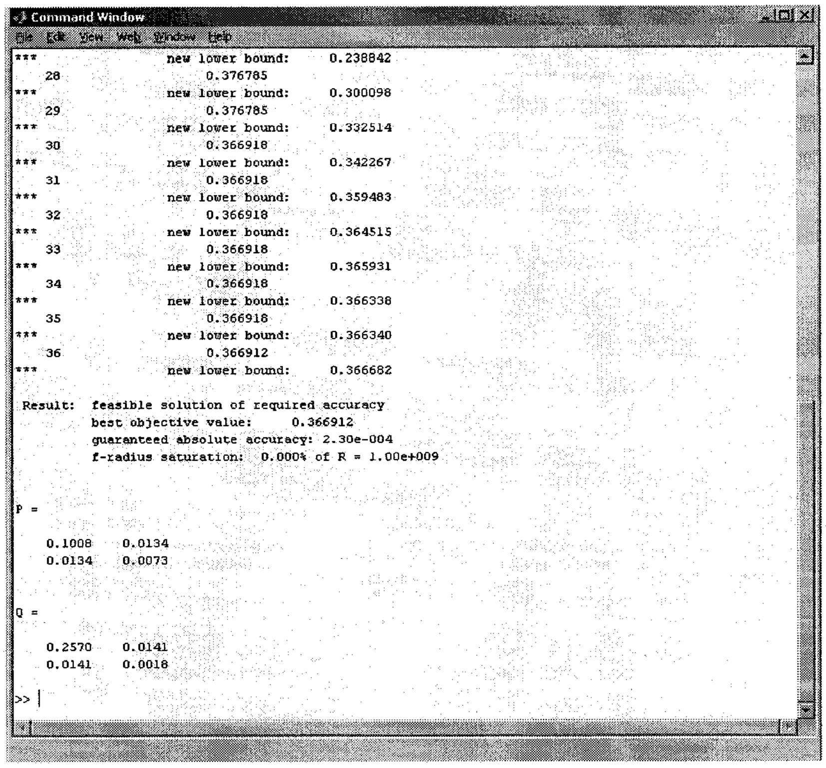

Figure 2-3 Feasible results of LMI for a stable system

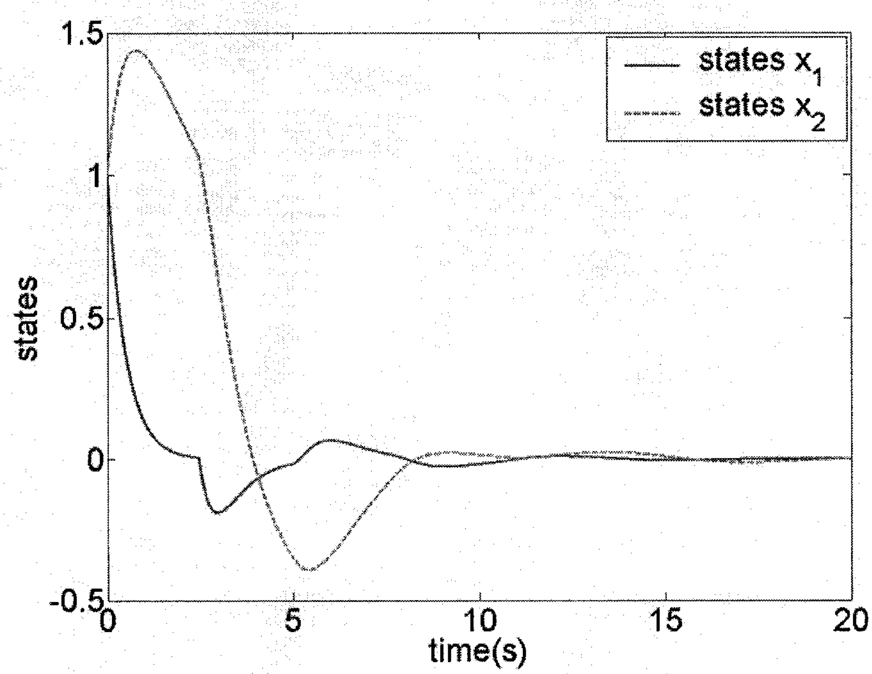

Figure 2-4 Regulation of a stable time-delayed system

2.4. Sliding Mode Control

Consider the dynamic system

$$\begin{bmatrix} \dot{\mathbf{z}}_1 \\ \dot{\mathbf{z}}_2 \end{bmatrix} = \begin{bmatrix} \hat{\mathbf{A}}_{11} & \hat{\mathbf{A}}_{12} \\ \hat{\mathbf{A}}_{21} & \hat{\mathbf{A}}_{22} \end{bmatrix} \begin{bmatrix} \mathbf{z}_1 \\ \mathbf{z}_2 \end{bmatrix} + \begin{bmatrix} \mathbf{0} \\ \hat{\mathbf{B}} \end{bmatrix} \mathbf{u} \tag{44}$$

where $\mathbf{z}_1 \in IR^{n-m}$, $\mathbf{z}_2 \in IR^{m}$, $\hat{\mathbf{A}}_{11}$ and $\hat{\mathbf{A}}_{12}$ are real matrices of appropriate dimensions, $\hat{\mathbf{B}} \in IR^{m \times m}$ is a full rank real matrix, and $\hat{\mathbf{A}}_{21}$, $\hat{\mathbf{A}}_{22}$ can be any bounded nonlinear matrices. A non-dynamic sliding surface can be defined by [21]

$$\mathbf{s} = \mathbf{L}\mathbf{z}_1 + \mathbf{z}_2 \tag{45}$$

When the state trajectory is on the sliding surface $\mathbf{s} = \mathbf{0}$, $\mathbf{z}_2$ can be obtained as

$$\mathbf{z}_2 = -\mathbf{L}\mathbf{z}_1 \tag{46}$$

The system (44) can be reduced to

$$\dot{\mathbf{z}}_1(t) = \left(\hat{\mathbf{A}}_{11} - \hat{\mathbf{A}}_{12}\mathbf{L}\right)\mathbf{z}_1 \tag{47}$$

Stability of the linear time-invariant systems depends on the location of the position of poles of $\left(\hat{\mathbf{A}}_{11} - \hat{\mathbf{A}}_{12}\mathbf{L}\right)$ in the complex plane. It has been proven that if the open-loop system $\left(\hat{\mathbf{A}}_{11}, \hat{\mathbf{A}}_{12}\right)$ is completely controllable, any set of desire closed-loop poles can be achieved using the constant matrix $\mathbf{L}$ [57]. Then using the known Equation for sliding mode $\dot{\mathbf{s}} = \mathbf{0}$, we have the representation of the system (44) around the equilibrium points as

$$\begin{aligned}\mathbf{0} &= \dot{\mathbf{s}} \\ &= \mathbf{L}\dot{\mathbf{z}}_1 + \dot{\mathbf{z}}_2 \\ &= \mathbf{L}\hat{\mathbf{A}}_{11}\mathbf{z}_1 - \mathbf{L}\hat{\mathbf{A}}_{12}\mathbf{L}\mathbf{z}_1 + \hat{\mathbf{A}}_{21}\mathbf{z}_1 - \hat{\mathbf{A}}_{22}\mathbf{L}\mathbf{z}_1 + \hat{\mathbf{B}}\mathbf{u}_{eq}\end{aligned} \tag{48}$$

Substituting (46) into the above equation, it is necessary to calculate the equilibrium control input as

$$\mathbf{u}_{eq} = -\hat{\mathbf{B}}^{-1}\left(\mathbf{L}\hat{\mathbf{A}}_{11} - \mathbf{L}\hat{\mathbf{A}}_{12}\mathbf{L} + \hat{\mathbf{A}}_{21} - \hat{\mathbf{A}}_{22}\mathbf{L}\right)\mathbf{z}_1 \tag{49}$$

If the initial states do not lie on the sliding surface, we can prove that surface is globally attractive [43]. From any initial condition out of the sliding surface, the square of distance to the sliding surface is measured by $(\mathbf{s}-\mathbf{0})^T(\mathbf{s}-\mathbf{0})$. For simplicity, we define the function

$$\mathrm{V} = \frac{1}{2}(\mathbf{s}-\mathbf{0})^T(\mathbf{s}-\mathbf{0}) = \frac{1}{2}\mathbf{s}^T\mathbf{s} \geq 0 \tag{50}$$

The state trajectory will reach the sliding surface in a finite time smaller than $\|\mathbf{s}\|/\mathrm{k}$, in which k is a strictly positive constant [45]. Then, the derivative of V will be

$$\dot{\mathrm{V}} = \mathbf{s}^T\dot{\mathbf{s}} = \mathbf{s}^T\left(\mathbf{L}\dot{\mathbf{z}}_1 + \dot{\mathbf{z}}_2\right) = \mathbf{s}^T\hat{\mathbf{B}}(\mathbf{u} - \mathbf{u}_{eq}) \leq -\mathrm{k}\|\mathbf{s}\| < 0 \tag{51}$$

and a unit vector sliding control law is proposed as the following [34]

$$\mathbf{u}(t) = \begin{cases}\mathbf{u}_{eq} - \mathbf{u}_n & \mathbf{s}^T\hat{\mathbf{B}} > \mathbf{0} \\ \mathbf{u}_{eq} + \mathbf{u}_n & \mathbf{s}^T\hat{\mathbf{B}} < \mathbf{0}\end{cases} \tag{52}$$

$$\mathbf{u}_n = \left| \frac{k\|\mathbf{s}\|}{\|\mathbf{s}^T\hat{\mathbf{B}}\| + \varepsilon} \left(\mathbf{s}^T\hat{\mathbf{B}}\right)^T \right| \tag{53}$$

where ε is a strictly positive constant vector. Form above equations, it is apparent that k is in inverse proportion to the setting time and in direct proportion to the control input. The coefficient ε is called boundary layer width, which is used to achieve an optimal trade-off between chattering frequency and tracking precision.

Example 5. Given a nonlinear system

$$\begin{bmatrix} \dot{z}_1 \\ \dot{z}_2 \end{bmatrix} = \begin{bmatrix} 0 & 1 \\ -\dfrac{\sin(z_1)}{z_1} & 0 \end{bmatrix} \begin{bmatrix} z_1 \\ z_2 \end{bmatrix} + \begin{bmatrix} 0 \\ 1 \end{bmatrix} u \tag{54}$$

Now, supposing the desired pole of the closed-loop system is '–2', we can select matrix $L = 2$. The reduced system becomes stable and can be written as

$$\dot{z}_1(t) = \left(\hat{\mathbf{A}}_{11} - L\hat{\mathbf{A}}_{12}\right) z_1 = -2z_1 \tag{55}$$

Then, we can obtain the sliding surface as

$$s = Lz_1 + z_2 = 2z_1 + z_2 \tag{56}$$

and the equilibrium control input as

$$u_{eq} = -\hat{\mathbf{B}}^{-1}\left(L\hat{\mathbf{A}}_{11} - L\hat{\mathbf{A}}_{12}L + \hat{\mathbf{A}}_{21} - \hat{\mathbf{A}}_{22}L\right) z_1 = \left(\frac{\sin(z_1)}{z_1} + 4\right) z_1 = \sin(z_1) + 4z_1 \tag{57}$$

Supposing the initial values are $\mathbf{z}_1(0) = 1$ and $\mathbf{z}_2(0) = 1$, the simulation results show that the system is stable with $k = 10$ and $\varepsilon = 0.001$.

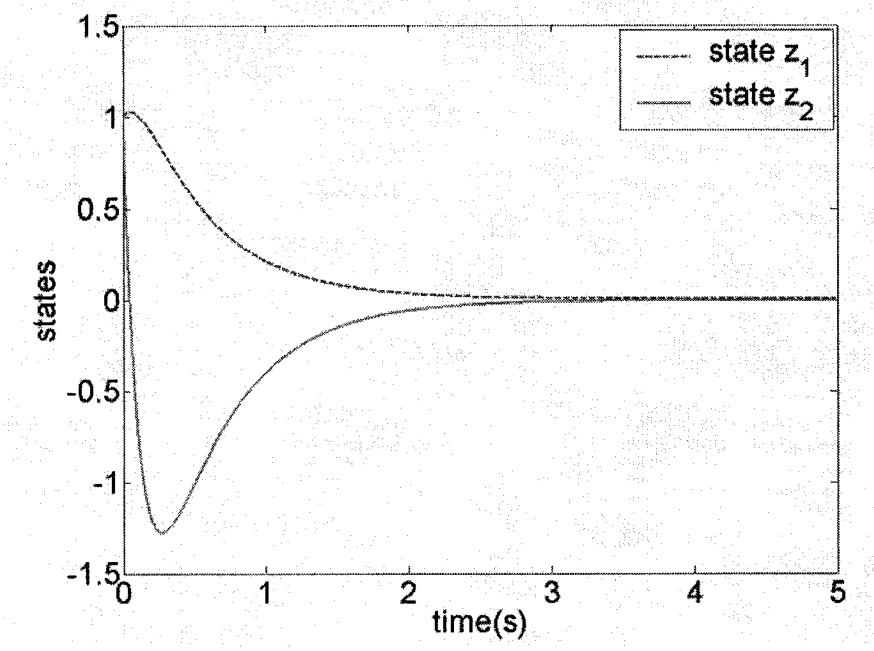

Figure 2-5 States of a controlled system

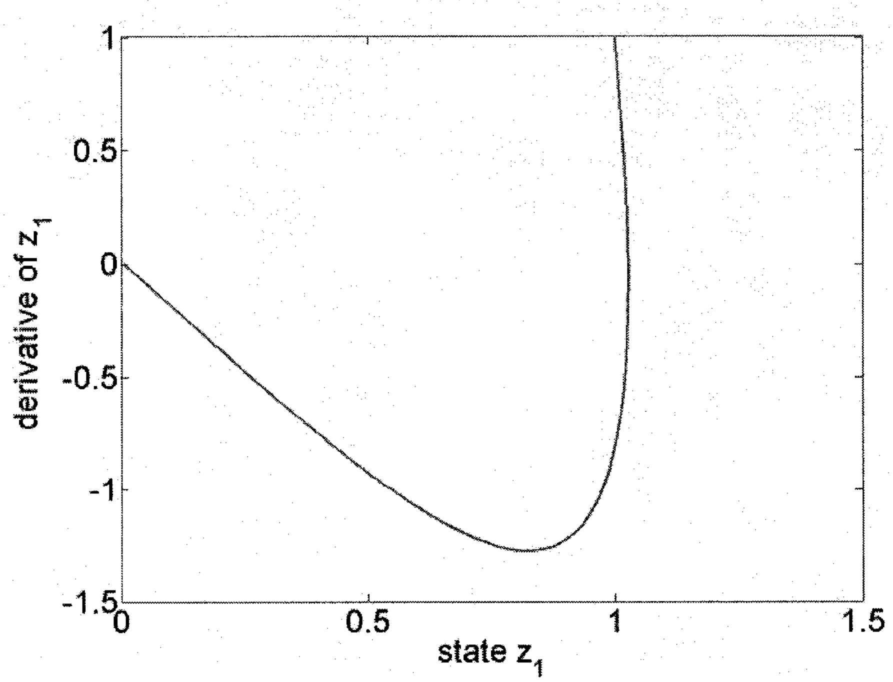

Figure 2-6 Phase diagram of a controlled system

From the simulation results, the SMC controller can stabilize this nonlinear system by placing the poles of the closed-loop system at the desired points.

2.5. NIRISS Modelling of Delta Wing Systems

A NIRISS representation of rotation motion provides a realistic example of the control problem in delta wing systems. An airplane has three rotations: roll, pitch and yaw. In this thesis, only aerodynamics of the roll motion is considered.

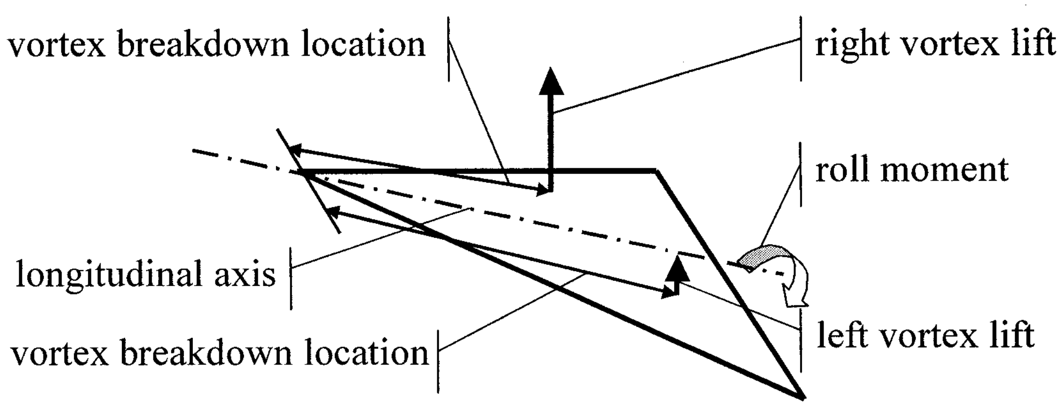

Figure 2-7 Vortex-coupled model of delta wing systems

The different left and right vortex breakdown location produced two different lifts on the left and right wings. Then, the roll moment is produced. Newton's second law is applied to the delta wing system of Figure 2-7, giving [20]

$$I\ddot{\Phi}(t) = -f_c\dot{\Phi}(t) + qs_a bCl(X_{vbl}, X_{vbl}) + U(t) \tag{58}$$

where the constants I, q, s_a and b represent the moment of inertia, the dynamic air pressure, the wing element area, and the wingspan, respectively. f_c is the bearing friction coefficient produced by the support bearing of the experimental setup. In the real system, f_c will be very small, and the roll damping of the real system will be less than experimental model. Under such condition, a low level PD controller can increase the roll damping of the real system before LPV controller synthesis. The dependent field variables $\Phi(t)$, $\dot{\Phi}(t)$, $\ddot{\Phi}(t)$ and $Cl(X_{vbl}, X_{vbl})$ are the roll angle, the roll angular velocity, the roll angular acceleration, and the roll moment coefficient, respectively. $U(t)$ is the input torque of vortex-coupled delta wing systems. In these systems, because the air loads are dependent on the vortex breakdown locations, the roll moment coefficient $Cl(X_{vbl}, X_{vbl})$ can be represented as a function of difference of the left and right vortex breakdown locations. In [13], the relationship between the roll moment coefficient and vortex breakdown locations is given as

$$Cl = e_0 + e_1(X_{vbl} - X_{vbr}) \tag{59}$$

where e_0 and e_1 are determined from the experimental data [19]. Also, the left and right vortex breakdown locations X_{vbl} and the right one X_{vbr} can be obtained from the following equations [20]

$$X_{vbl} = X_{sl}(\phi(t)) + X_q(\dot{\phi}(t))X_{sl}(\phi(t)) + \int_{t-T}^{t} X_u(t-\tau)\dot{\phi}(\tau)d\tau \tag{60}$$

$$X_{vbr} = X_{sr}(\phi(t)) + X_q(\dot{\phi}(t))X_{sr}(\phi(t)) - \int_{t-T}^{t} X_u(t-\tau)\dot{\phi}(\tau)d\tau \tag{61}$$

From the equations above, we see that each vortex breakdown location is determined by three terms: the first term represents the static value for the roll angle at t, and the second and the third terms are the quasi-steady and the unsteady effects respectively. Experimental results have shown that the quasi-steady terms are often negligible [19].

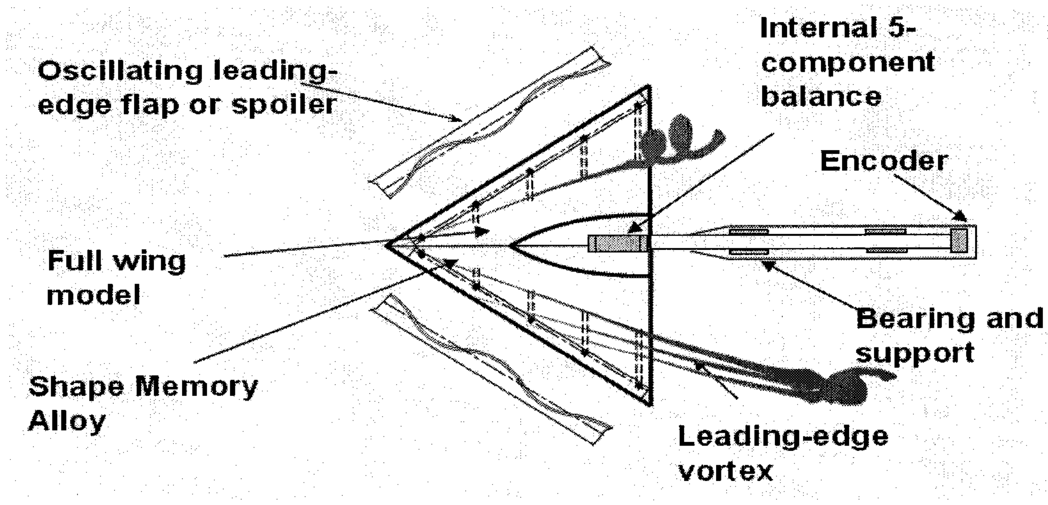

Figure 2-8 Conceptual design of full wing experimental set-up

For simplicity, the quasi-steady terms are ignored. The equations can then be written as

$$X_{vbl} = X_{sl}(\phi(t)) + \int_{t-T}^{t} X_u(t-\tau)\dot{\phi}(\tau)d\tau \tag{62}$$

$$X_{vbr} = X_{sr}(\phi(t)) - \int_{t-T}^{t} X_u(t-\tau)\dot{\phi}(\tau)d\tau \tag{63}$$

The static term X_s can be obtained by solving a second-order equation in [20] given by

$$C_0 + BX_s - AX_s^2 = \Gamma \tag{64}$$

From Equation (64), the static term X_s depends on the leading edge sweep angle Γ, and the parameters $A_{l,r}$ and $B_{l,r}$. The formulation of $A_{l,r}$ and $B_{l,r}$ for the left and right vortices is as follows [20]

$$A_l = 1.1\sin(\alpha(t))\sin(\Lambda_l), \quad B_l = 4A_l \tag{65}$$

$$A_r = 1.1\sin(\alpha(t))\sin(\Lambda_r), \quad B_r = 4A_r \tag{66}$$

where $\alpha(t)$ is the angle of attack. The effective sweep back angles are given by

$$\Lambda_l = \lambda_0 - \mathrm{atan}(\tan(\varphi)\sin(\phi(t))) \tag{67}$$

$$\Lambda_r = \lambda_0 + \mathrm{atan}(\tan(\varphi)\sin(\phi(t))) \tag{68}$$

with λ_0 and φ being the half apex angle and the structure angle respectively. Critical circulation can be represented as

$$\Gamma_{cl} = 0.8\cos[4(\Lambda_l - \Lambda_e)] \tag{69}$$

$$\Gamma_{cr} = 0.8\cos[4(\Lambda_r - \Lambda_e)] \tag{70}$$

where Λ_e is obtained from experimental results. The non-dimensional circulation at trailing edge (non-dimensional chord $X = 1$) is used to determine the distributions of circulation in chord wise in parabolic [20].

$$\Gamma_l = 5.11\cos(\Lambda_l + \frac{2.65}{57.3})(\alpha - \frac{3.5}{57.3}) \tag{71}$$

$$C_{l0} = \Gamma_l - B_l + A_l \tag{72}$$

$$\Gamma_r = 5.11\cos(\Lambda_r + \frac{2.65}{57.3})(\alpha - \frac{3.5}{57.3}) \tag{73}$$

$$C_{r0} = \Gamma_r - B_r + A_r \tag{74}$$

The solution of the static term X_s is determined as follows. If $B_l^2 + 4A_lC_{l0} - 4A_l\Gamma_{cl}$ is greater than or equal to 0, then

$$X_{sl} = \frac{B_l - \sqrt{B_l^2 + 4A_l C_{l0} - 4A_l \Gamma_{cl}}}{2A_l} \tag{75}$$

otherwise,

$$X_{sl} = \frac{B_l - \sqrt{-\left(B_l^2 + 4A_l C_{l0} - 4A_l \Gamma_{cl}\right)}}{2A_l} \tag{76}$$

If $B_r^2 + 4A_r C_{r0} - 4A_r \Gamma_{cr}$ is greater than or equal to 0, then

$$X_{sr} = \frac{B_r - \sqrt{B_r^2 + 4A_r C_{r0} - 4A_r \Gamma_{cr}}}{2A_r} \tag{77}$$

otherwise,

$$X_{sr} = \frac{B_r - \sqrt{-\left(B_r^2 + 4A_r C_{r0} - 4A_r \Gamma_{cr}\right)}}{2A_r} \tag{78}$$

Also the representation for the unsteady effects is

$$\int_{t-T}^{t} X_u(t-\tau)\dot{\Phi}(\tau)d\tau = \frac{1.65}{\tan\alpha(t)} \int_{t-T}^{t} \sin\left(\frac{\pi(t-\tau)}{T^*}\right)\dot{\Phi}(\tau)d\tau \tag{79}$$

where T is the time period of decay, and T^* is the release time. The experimental results in [20] show that the time period of decay is equal to the release time.

$$T = T^* = 0.16s \tag{80}$$

Hence, we use T to represent both time periods of decay and release time.

The NIRISS model that results from the aerodynamic characteristics of the roll motion presents significant problems in the context of a real-time simulation and control. Most of the existing analysis methods for time-varying nonlinear models require the replacement of the time-varying parameter by a constant parameter and the linearization of the nonlinear system around the equilibrium points. This replacement usually changes the dynamic behaviour of the original system. Furthermore, the series expansion linearization method to linearize the nonlinear system is only valid near the equilibrium points. Sometimes, the approximation is not valid since it cannot guarantee the stability of the closed-loop system. In chapter 4, a modelling approach based on LPV technology is introduced to solve the nonlinear time-varying problem in a more systematic and efficient manner.

Chapter 3

Linear Parameter-Varying Sliding Mode Control

In this chapter, we synthesize a linear parameter-varying sliding mode controller for an LPVTDS. The time-varying parameters of sliding surface are determined by the means of solving a parameter-dependent Lyapunov-Krasovskiĭ functional, which can guarantee the asymptotic stability of the closed-loop system. This theorem is generalized to multiple time delay systems. Finally, a typical time-delayed LPV example is presented to demonstrate the controller synthesis procedure.

3.1. Problem Statement

We consider the following LPVTDS

$$\begin{aligned} \dot{\mathbf{x}} &= \mathbf{A}(\boldsymbol{\sigma}(t))\mathbf{x}(t) + \mathbf{A}_h(\boldsymbol{\sigma}(t))\mathbf{x}(t-h) + \mathbf{B}(\boldsymbol{\sigma}(t))u(t) \\ \mathbf{y} &= \mathbf{C}(\boldsymbol{\sigma}(t))\mathbf{x}(t) \end{aligned} \tag{81}$$

$$\mathbf{x}(t) = 0, \quad t \in [-h \quad 0]$$

where $\mathbf{x} \in \mathit{IR}^{n}$ is the state, $\mathbf{u} \in \mathit{IR}^{m}$ is the control input, and $\mathbf{y} \in \mathit{IR}^{p}$ is the measured output, and $h > 0$ is the constant time delay. The state-space matrix functions $\mathbf{A}(\cdot) \in \mathit{IR}^{n\times n}$, $\mathbf{A}_h(\cdot) \in \mathit{IR}^{n\times n}$, $\mathbf{B}(\cdot) \in \mathit{IR}^{n\times m}$ and $\mathbf{C}(\cdot) \in \mathit{IR}^{p\times n}$ are assumed to be bounded continuous functions of a time-varying parameter vector $\boldsymbol{\sigma}(t) \in \Theta$.

We first transform the original system into the so-called regular form by using a linear state transformation approach of [8]. The regular form can be represented as

$$\begin{bmatrix}\dot{\mathbf{z}}_1(t)\\ \dot{\mathbf{z}}_2(t)\end{bmatrix}=\begin{bmatrix}\hat{\mathbf{A}}_{11}(\boldsymbol{\sigma}) & \hat{\mathbf{A}}_{12}(\boldsymbol{\sigma})\\ \hat{\mathbf{A}}_{21}(\boldsymbol{\sigma}) & \hat{\mathbf{A}}_{22}(\boldsymbol{\sigma})\end{bmatrix}\begin{bmatrix}\mathbf{z}_1(t)\\ \mathbf{z}_2(t)\end{bmatrix}+\begin{bmatrix}\hat{\mathbf{A}}_{h11}(\boldsymbol{\sigma}) & \hat{\mathbf{A}}_{h12}(\boldsymbol{\sigma})\\ \hat{\mathbf{A}}_{h21}(\boldsymbol{\sigma}) & \hat{\mathbf{A}}_{h22}(\boldsymbol{\sigma})\end{bmatrix}\begin{bmatrix}\mathbf{z}_1(t-h)\\ \mathbf{z}_2(t-h)\end{bmatrix}+\begin{bmatrix}\mathbf{0}\\ \hat{\mathbf{B}}\end{bmatrix}\mathbf{u}\quad \boldsymbol{\sigma}(t)\in\boldsymbol{\Theta} \tag{82}$$

$$\mathbf{y}=\hat{\mathbf{C}}(\boldsymbol{\sigma})\mathbf{z}_1(\mathbf{t})$$

$$\mathbf{z}_1(t)=0 \text{ and } \mathbf{z}_2(t)=0,\quad t\in[-h\quad 0]$$

where $\mathbf{z}_1\in \mathit{IR}^{n-m}$, $\mathbf{z}_2\in \mathit{IR}^{m}$, and $\hat{\mathbf{B}}(\cdot)\in \mathit{IR}^{m\times m}$ is full rank. Now, we introduce an assumption that will be used in our proof.

Assumption 1. The sub-matrix $\hat{\mathbf{A}}_{h12}(\boldsymbol{\sigma})$ is zero, so that we can design a memoryless time-varying sliding surface for an LPVTDS.

$$\hat{\mathbf{A}}_{h12}(\boldsymbol{\sigma})=\mathbf{0} \tag{83}$$

The objective of this thesis is to develop a systemitic procedure to design a linear parameter-varying sliding mode controller for (81) such that the closed-loop system is asymptotically stable. Before moving on, we introduce two lemmas, which are essential for the development of our results.

Lemma 1. Assume that $\mathbf{a}(\cdot)\in \mathit{IR}^{n_a}$, $\mathbf{b}(\cdot)\in \mathit{IR}^{n_b}$ and $\mathbf{N}(\cdot)\in \mathit{IR}^{n_b\times n_b}$ are defined on the interval Ω. Then for any bounded matrix functions $\mathbf{X}(\cdot)\in \mathit{IR}^{n_a\times n_a}$, $\mathbf{Y}(\cdot)\in \mathit{IR}^{n_a\times n_b}$ and $\mathbf{Z}(\cdot)\in \mathit{IR}^{n_b\times n_b}$, the following inequality holds [1]

$$-2\int_\Omega \mathbf{a}(s)\mathbf{N}(t)\mathbf{b}(s)ds\le \int_\Omega \begin{bmatrix}\mathbf{a}(s)\\ \mathbf{b}(s)\end{bmatrix}^T\begin{bmatrix}\mathbf{X}(t) & \mathbf{Y}(t)-\mathbf{N}(t)\\ (*) & \mathbf{Z}(s)\end{bmatrix}\begin{bmatrix}\mathbf{a}(s)\\ \mathbf{b}(s)\end{bmatrix}ds \tag{84}$$

where

$$\begin{bmatrix} \mathbf{X}(t) & \mathbf{Y}(t) \\ (*) & \mathbf{Z}(s) \end{bmatrix} \geq \mathbf{0} \tag{85}$$

Lemma 2. Let $\mathbf{x}(t) \in \mathit{IR}^n$ be a vector-valued function with first-order continuous-derivative entries. Then, the following integral inequality holds for any bounded matrix functions $\mathbf{Y}_1(\cdot), \mathbf{Y}_2(\cdot) \in \mathit{IR}^{n\times n}$ and a symmetric positive definite matrix function $\mathbf{Z}(\cdot) \in \boldsymbol{S}^n$, and a scalar $h > 0$

$$\begin{aligned} -\int_{t-h}^{t} \dot{\mathbf{x}}^T(s)\mathbf{Z}(s)\dot{\mathbf{x}}^T(s)ds \leq & \begin{bmatrix} \mathbf{x}(t) \\ \mathbf{x}(t-h) \end{bmatrix}^T \begin{bmatrix} \mathbf{Y}_1^T(t)+\mathbf{Y}_1(t) & -\mathbf{Y}_1^T(t)+\mathbf{Y}_2(t) \\ (*) & -\mathbf{Y}_2^T(t)-\mathbf{Y}_2(t) \end{bmatrix} \begin{bmatrix} \mathbf{x}(t) \\ \mathbf{x}(t-h) \end{bmatrix} \\ & + h\begin{bmatrix} \mathbf{x}(t) \\ \mathbf{x}(t-h) \end{bmatrix}^T \begin{bmatrix} \mathbf{Y}_1^T(t) \\ \mathbf{Y}_2^T(t) \end{bmatrix} \mathbf{Z}^{-1}(\boldsymbol{\sigma}(t)) \begin{bmatrix} \mathbf{Y}_1^T(t) \\ \mathbf{Y}_2^T(t) \end{bmatrix}^T \begin{bmatrix} \mathbf{x}(t) \\ \mathbf{x}(t-h) \end{bmatrix} \end{aligned} \tag{86}$$

Proof. See **APPENDIX** A.

3.2. Linear Parameter-Varying Sliding Mode Controller Design

Now, we begin to design a linear parameter-varying sliding surface for regulation based on the regular form (82) and synthesize a sliding mode controller with global attractivity. The error signal is defined by

$$\mathbf{e} = \mathbf{r}(t) - \hat{\mathbf{C}}(\boldsymbol{\sigma})\mathbf{z}_1(t) \tag{87}$$

where $\mathbf{r}(t)$ is the reference input signal. The linear parameter-varying sliding surface is chosen as

$$\mathbf{s}(\boldsymbol{\sigma})=\mathbf{S}(\boldsymbol{\sigma},\mathbf{z}_1)+\mathbf{z}_2 \tag{88}$$

where $\mathbf{S}(\boldsymbol{\sigma},\mathbf{z}_1)$ is a linear parameter-varying operator of $\mathbf{z}_1$. The LPV operator $\mathbf{S}(\boldsymbol{\sigma},\mathbf{z}_1)$ is similar to the function $\mathbf{S}(\mathbf{z}_1)$ of [57], but $\mathbf{S}(\boldsymbol{\sigma},\mathbf{z}_1)$ adds time-varying parameters of the plant. The parameter-varying controller can adjust to the variation of the system parameters on-line. Therefore the LPVSMC approach can potentially obtain better control performance and less conservative results than standard SMC with a constant parameter sliding surface. The chosen switching function $\mathbf{s}$ will have some dynamics compared to a conventional switching function in terms of the defined new variable $\mathbf{z}_w$

$$\begin{aligned}\dot{\mathbf{z}}_w &= \mathbf{F}(\boldsymbol{\sigma})\mathbf{z}_w+\mathbf{G}(\boldsymbol{\sigma})\mathbf{r}-\mathbf{G}(\boldsymbol{\sigma})\hat{\mathbf{C}}(\boldsymbol{\sigma})\mathbf{z}_1 \\ \mathbf{S}(\boldsymbol{\sigma},\mathbf{z}_1) &= \mathbf{H}(\boldsymbol{\sigma})\mathbf{z}_w+\mathbf{L}(\boldsymbol{\sigma})\mathbf{r}-\mathbf{L}(\boldsymbol{\sigma})\hat{\mathbf{C}}(\boldsymbol{\sigma})\mathbf{z}_1\end{aligned} \tag{89}$$

If we combine the regular form (82) and the above switching function, we obtain the composite system represented as

$$\begin{aligned}\begin{bmatrix}\dot{\mathbf{z}}_w\\ \dot{\mathbf{z}}_1\\ \dot{\mathbf{z}}_2\end{bmatrix} &= \begin{bmatrix}\mathbf{F}(\boldsymbol{\sigma}) & -\mathbf{G}(\boldsymbol{\sigma})\hat{\mathbf{C}}(\boldsymbol{\sigma}) & \mathbf{0}\\ \mathbf{0} & \hat{\mathbf{A}}_{11}(\boldsymbol{\sigma}) & \hat{\mathbf{A}}_{12}(\boldsymbol{\sigma})\\ \mathbf{0} & \hat{\mathbf{A}}_{21}(\boldsymbol{\sigma}) & \hat{\mathbf{A}}_{22}(\boldsymbol{\sigma})\end{bmatrix}\begin{bmatrix}\mathbf{z}_w\\ \mathbf{z}_1\\ \mathbf{z}_2\end{bmatrix}+\begin{bmatrix}\mathbf{0} & \mathbf{0} & \mathbf{0}\\ \mathbf{0} & \hat{\mathbf{A}}_{h11}(\boldsymbol{\sigma}) & \hat{\mathbf{A}}_{h12}(\boldsymbol{\sigma})\\ \mathbf{0} & \hat{\mathbf{A}}_{h21}(\boldsymbol{\sigma}) & \hat{\mathbf{A}}_{h22}(\boldsymbol{\sigma})\end{bmatrix}\begin{bmatrix}\mathbf{z}_w(t-h)\\ \mathbf{z}_1(t-h)\\ \mathbf{z}_2(t-h)\end{bmatrix}+\begin{bmatrix}\mathbf{0}\\ \mathbf{0}\\ \hat{\mathbf{B}}\end{bmatrix}\mathbf{u}+\begin{bmatrix}\mathbf{G}(\boldsymbol{\sigma})\\ \mathbf{0}\\ \mathbf{0}\end{bmatrix}\mathbf{r}\\ \mathbf{s}(\boldsymbol{\sigma}) &= \mathbf{H}(\boldsymbol{\sigma})\mathbf{z}_w+\mathbf{L}(\boldsymbol{\sigma})\mathbf{r}-\mathbf{L}(\boldsymbol{\sigma})\hat{\mathbf{C}}(\boldsymbol{\sigma})\mathbf{z}_1+\mathbf{z}_2\end{aligned} \tag{90}$$

Assuming the sliding mode occurs on $\mathbf{s}(\boldsymbol{\sigma})=\mathbf{0}$ and solving for the vector $\mathbf{z}_2$, we have

$$\mathbf{z}_2=-\mathbf{H}(\boldsymbol{\sigma})\mathbf{z}_w-\mathbf{L}(\boldsymbol{\sigma})\mathbf{r}+\mathbf{L}(\boldsymbol{\sigma})\hat{\mathbf{C}}(\boldsymbol{\sigma})\mathbf{z}_1 \tag{91}$$

Also using the known equation for sliding mode $\dot{\mathbf{s}}(\boldsymbol{\sigma}) = \mathbf{0}$, we have the following representation for the system around the equilibrium points

$$
\begin{aligned}
\mathbf{0} &= \dot{\mathbf{s}}(\boldsymbol{\sigma}) \qquad (92)\\
&= \frac{\partial \mathbf{H}(\boldsymbol{\sigma})}{\partial \boldsymbol{\sigma}}\dot{\boldsymbol{\sigma}}\mathbf{z}_w + \mathbf{H}(\boldsymbol{\sigma})\dot{\mathbf{z}}_w + \frac{\partial \mathbf{L}(\boldsymbol{\sigma})}{\partial \boldsymbol{\sigma}}\dot{\boldsymbol{\sigma}}\mathbf{r} + \mathbf{L}(\boldsymbol{\sigma})\dot{\mathbf{r}}(t) - \frac{\partial \mathbf{L}(\boldsymbol{\sigma})}{\partial \boldsymbol{\sigma}}\dot{\boldsymbol{\sigma}}\mathbf{C}(\boldsymbol{\sigma})\mathbf{z}_1 - \mathbf{L}(\boldsymbol{\sigma})\frac{\partial \mathbf{C}(\boldsymbol{\sigma})}{\partial \boldsymbol{\sigma}}\dot{\boldsymbol{\sigma}}\mathbf{z}_1 - \mathbf{L}(\boldsymbol{\sigma})\mathbf{C}(\boldsymbol{\sigma})\dot{\mathbf{z}}_1 + \dot{\mathbf{z}}_2\\
&= \frac{\partial \mathbf{H}(\boldsymbol{\sigma})}{\partial \boldsymbol{\sigma}}\dot{\boldsymbol{\sigma}}\mathbf{z}_w + \mathbf{H}(\boldsymbol{\sigma})\mathbf{F}(\boldsymbol{\sigma})\mathbf{z}_w - \mathbf{H}(\boldsymbol{\sigma})\mathbf{G}(\boldsymbol{\sigma})\mathbf{C}(\boldsymbol{\sigma})\mathbf{z}_1 + \mathbf{H}(\boldsymbol{\sigma})\mathbf{G}(\boldsymbol{\sigma})\mathbf{r}\\
&\quad + \frac{\partial \mathbf{L}(\boldsymbol{\sigma})}{\partial \boldsymbol{\sigma}}\dot{\boldsymbol{\sigma}}\mathbf{r} + \mathbf{L}(\boldsymbol{\sigma})\dot{\mathbf{r}}(t)\\
&\quad - \frac{\partial \mathbf{L}(\boldsymbol{\sigma})}{\partial \boldsymbol{\sigma}}\dot{\boldsymbol{\sigma}}\mathbf{C}(\boldsymbol{\sigma})\mathbf{z}_1 - \mathbf{L}(\boldsymbol{\sigma})\frac{\partial \mathbf{C}(\boldsymbol{\sigma})}{\partial \boldsymbol{\sigma}}\dot{\boldsymbol{\sigma}}\mathbf{z}_1 - \mathbf{L}(\boldsymbol{\sigma})\mathbf{C}(\boldsymbol{\sigma})\hat{\mathbf{A}}_{11}(\boldsymbol{\sigma})\mathbf{z}_1 - \mathbf{L}(\boldsymbol{\sigma})\mathbf{C}(\boldsymbol{\sigma})\hat{\mathbf{A}}_{12}(\boldsymbol{\sigma})\mathbf{z}_2\\
&\quad - \mathbf{L}(\boldsymbol{\sigma})\mathbf{C}(\boldsymbol{\sigma})\hat{\mathbf{A}}_{h12}(\boldsymbol{\sigma})\mathbf{z}_2(t-h) - \mathbf{L}(\boldsymbol{\sigma})\mathbf{C}(\boldsymbol{\sigma})\hat{\mathbf{A}}_{h11}(\boldsymbol{\sigma})\mathbf{z}_1(t-h)\\
&\quad + \hat{\mathbf{A}}_{21}(\boldsymbol{\sigma})\mathbf{z}_1 + \hat{\mathbf{A}}_{22}(\boldsymbol{\sigma})\mathbf{z}_2 + \hat{\mathbf{A}}_{h21}(\boldsymbol{\sigma})\mathbf{z}_1(t-h) + \hat{\mathbf{A}}_{h22}(\boldsymbol{\sigma})\mathbf{z}_2(t-h) + \hat{\mathbf{B}}\mathbf{u}
\end{aligned}
$$

Substituting (91) and using **Assumption 1**, the equilibrium control input is obtained as

$$
\begin{aligned}
\mathbf{u}_{eq} = -\hat{\mathbf{B}}^{-1}\Big\{ &\Big[\frac{\partial \mathbf{H}(\boldsymbol{\sigma})}{\partial \boldsymbol{\sigma}}\dot{\boldsymbol{\sigma}} + \mathbf{H}(\boldsymbol{\sigma})\mathbf{F}(\boldsymbol{\sigma}) + \mathbf{L}(\boldsymbol{\sigma})\mathbf{C}(\boldsymbol{\sigma})\hat{\mathbf{A}}_{12}(\boldsymbol{\sigma})\mathbf{H}(\boldsymbol{\sigma}) - \hat{\mathbf{A}}_{22}(\boldsymbol{\sigma})\mathbf{H}(\boldsymbol{\sigma})\Big]\mathbf{z}_w \qquad (93)\\
&+\Big[-\mathbf{H}(\boldsymbol{\sigma})\mathbf{G}(\boldsymbol{\sigma})\mathbf{C}(\boldsymbol{\sigma}) - \frac{\partial \mathbf{L}(\boldsymbol{\sigma})}{\partial \boldsymbol{\sigma}}\dot{\boldsymbol{\sigma}}\mathbf{C}(\boldsymbol{\sigma}) - \mathbf{L}(\boldsymbol{\sigma})\frac{\partial \mathbf{C}(\boldsymbol{\sigma})}{\partial \boldsymbol{\sigma}}\dot{\boldsymbol{\sigma}} - \mathbf{L}(\boldsymbol{\sigma})\mathbf{C}(\boldsymbol{\sigma})\hat{\mathbf{A}}_{11}(\boldsymbol{\sigma})\\
&\quad - \mathbf{L}(\boldsymbol{\sigma})\mathbf{C}(\boldsymbol{\sigma})\hat{\mathbf{A}}_{12}(\boldsymbol{\sigma})\mathbf{L}(\boldsymbol{\sigma})\mathbf{C}(\boldsymbol{\sigma}) + \hat{\mathbf{A}}_{21}(\boldsymbol{\sigma}) + \hat{\mathbf{A}}_{22}(\boldsymbol{\sigma})\mathbf{L}(\boldsymbol{\sigma})\mathbf{C}(\boldsymbol{\sigma})\Big]\mathbf{z}_1\\
&+\Big[\frac{\partial \mathbf{L}(\boldsymbol{\sigma})}{\partial \boldsymbol{\sigma}}\dot{\boldsymbol{\sigma}} + \mathbf{L}(\boldsymbol{\sigma})\mathbf{C}(\boldsymbol{\sigma})\hat{\mathbf{A}}_{12}(\boldsymbol{\sigma})\mathbf{L}(\boldsymbol{\sigma}) - \hat{\mathbf{A}}_{22}(\boldsymbol{\sigma})\mathbf{L}(\boldsymbol{\sigma}) + \mathbf{H}(\boldsymbol{\sigma})\mathbf{G}(\boldsymbol{\sigma})\Big]\mathbf{r}\\
&+\Big[-\mathbf{L}(\boldsymbol{\sigma})\mathbf{C}(\boldsymbol{\sigma})\hat{\mathbf{A}}_{h11}(\boldsymbol{\sigma}) + \hat{\mathbf{A}}_{h21}(\boldsymbol{\sigma})\Big]\mathbf{z}_1(t-h)\\
&+\hat{\mathbf{A}}_{h22}(\boldsymbol{\sigma})\mathbf{z}_2(t-h)\\
&+\mathbf{L}(\boldsymbol{\sigma})\dot{\mathbf{r}}(t)\Big\}
\end{aligned}
$$

In order to guarantee the global attractivity of the linear parameter-varying sliding surface, the Lyapunov function is chosen as

$$V = \frac{1}{2}\mathbf{s}^T\mathbf{s} \tag{94}$$

The derivative of V is

$$\dot{V} = \mathbf{s}^T\dot{\mathbf{s}} = \mathbf{s}^T(\mathbf{L}\dot{\mathbf{z}}_1 + \dot{\mathbf{z}}_2) = \mathbf{s}^T\hat{\mathbf{B}}(\mathbf{u} - \mathbf{u}_{eq}) \le -k\|\mathbf{s}\| < 0 \tag{95}$$

where the state trajectory will reach the sliding surface in a finite time smaller than $\|\mathbf{s}\|/k$. Thus, the sliding mode controller is identical to the unit vector control law

$$\mathbf{u}(t) = \begin{cases} \mathbf{u}_{eq} - \mathbf{u}_n & \mathbf{s}^T\hat{\mathbf{B}} > \mathbf{0} \\ \mathbf{u}_{eq} + \mathbf{u}_n & \mathbf{s}^T\hat{\mathbf{B}} < \mathbf{0} \end{cases} \tag{96}$$

where

$$\mathbf{u}_n = \left| \frac{k\|\mathbf{s}\|}{\|\mathbf{s}^T\hat{\mathbf{B}}\| + \varepsilon} (\mathbf{s}^T\hat{\mathbf{B}})^T \right| \tag{97}$$

3.3. Stability of the Reduced Form

The linear parameter-varying coefficients $\mathbf{F}(\boldsymbol{\sigma})$, $\mathbf{G}(\boldsymbol{\sigma})$, $\mathbf{H}(\boldsymbol{\sigma})$ and $\mathbf{L}(\boldsymbol{\sigma})$ in Equation (93) are unknown, but it is clear that these linear parameter-varying coefficients should be determined to guarantee the stability of the composite system (90). In this section, we will calculate these linear parameter-varying coefficients from LMI-based stability of an unforced reduced form of an LPVTDS.

From Equation (90), the unforced composite system is represented as

$$\begin{bmatrix}\dot{\mathbf{z}}_w\\ \dot{\mathbf{z}}_1\\ \dot{\mathbf{z}}_2\end{bmatrix}=\begin{bmatrix}\mathbf{F}(\boldsymbol{\sigma}) & -\mathbf{G}(\boldsymbol{\sigma})\mathbf{C}(\boldsymbol{\sigma}) & \mathbf{0}\\ \mathbf{0} & \hat{\mathbf{A}}_{11}(\boldsymbol{\sigma}) & \hat{\mathbf{A}}_{12}(\boldsymbol{\sigma})\\ \mathbf{0} & \hat{\mathbf{A}}_{21}(\boldsymbol{\sigma}) & \hat{\mathbf{A}}_{22}(\boldsymbol{\sigma})\end{bmatrix}\begin{bmatrix}\mathbf{z}_w\\ \mathbf{z}_1\\ \mathbf{z}_2\end{bmatrix}+\begin{bmatrix}\mathbf{0} & \mathbf{0} & \mathbf{0}\\ \mathbf{0} & \hat{\mathbf{A}}_{h11}(\boldsymbol{\sigma}) & \hat{\mathbf{A}}_{h12}(\boldsymbol{\sigma})\\ \mathbf{0} & \hat{\mathbf{A}}_{h21}(\boldsymbol{\sigma}) & \hat{\mathbf{A}}_{h22}(\boldsymbol{\sigma})\end{bmatrix}\begin{bmatrix}\mathbf{z}_w(t-h)\\ \mathbf{z}_1(t-h)\\ \mathbf{z}_2(t-h)\end{bmatrix} \tag{98}$$

Substituting Equation (91) into Equation (98), the reduced system becomes

$$\begin{aligned}\begin{bmatrix}\dot{\mathbf{z}}_w\\ \dot{\mathbf{z}}_1\end{bmatrix}&=\begin{bmatrix}\mathbf{F}(\boldsymbol{\sigma}) & -\mathbf{G}(\boldsymbol{\sigma})\mathbf{C}(\boldsymbol{\sigma})\\ -\hat{\mathbf{A}}_{12}(\boldsymbol{\sigma})\mathbf{H}(\boldsymbol{\sigma}) & \hat{\mathbf{A}}_{11}(\boldsymbol{\sigma})+\hat{\mathbf{A}}_{12}(\boldsymbol{\sigma})\mathbf{L}(\boldsymbol{\sigma})\mathbf{C}(\boldsymbol{\sigma})\end{bmatrix}\begin{bmatrix}\mathbf{z}_w\\ \mathbf{z}_1\end{bmatrix}\\ &\quad+\begin{bmatrix}\mathbf{0} & \mathbf{0}\\ -\hat{\mathbf{A}}_{h12}(\boldsymbol{\sigma})\mathbf{H}(\boldsymbol{\sigma}(t-h)) & \hat{\mathbf{A}}_{h11}(\boldsymbol{\sigma})+\hat{\mathbf{A}}_{h12}(\boldsymbol{\sigma})\mathbf{L}(\boldsymbol{\sigma}(t-h)\mathbf{C}(\boldsymbol{\sigma}(t-h)\end{bmatrix}\begin{bmatrix}\mathbf{z}_w(t-h)\\ \mathbf{z}_1(t-h)\end{bmatrix}\\ &=\left(\tilde{\mathbf{A}}_0+\tilde{\mathbf{A}}_1\tilde{\mathbf{A}}_F\right)\begin{bmatrix}\mathbf{z}_w\\ \mathbf{z}_1\end{bmatrix}+\left(\tilde{\mathbf{A}}_{h0}+\tilde{\mathbf{A}}_{h1}\tilde{\mathbf{A}}_{hF}\right)\begin{bmatrix}\mathbf{z}_w(t-h)\\ \mathbf{z}_1(t-h)\end{bmatrix}\end{aligned} \tag{99}$$

where

$$\begin{aligned}&\tilde{\mathbf{A}}_0=\begin{bmatrix}\mathbf{0} & \mathbf{0}\\ \mathbf{0} & \hat{\mathbf{A}}_{11}(\boldsymbol{\sigma})\end{bmatrix}, &&\tilde{\mathbf{A}}_1=\begin{bmatrix}\mathbf{I} & \mathbf{0}\\ \mathbf{0} & \hat{\mathbf{A}}_{12}(\boldsymbol{\sigma})\end{bmatrix},\\ &\tilde{\mathbf{A}}_{h0}=\begin{bmatrix}\mathbf{0} & \mathbf{0}\\ \mathbf{0} & \hat{\mathbf{A}}_{h11}(\boldsymbol{\sigma})\end{bmatrix}, &&\tilde{\mathbf{A}}_{h1}=\begin{bmatrix}\mathbf{0} & \mathbf{0}\\ \mathbf{0} & \hat{\mathbf{A}}_{h12}(\boldsymbol{\sigma})\end{bmatrix},\\ &\tilde{\mathbf{A}}_F=\begin{bmatrix}\mathbf{F}(\boldsymbol{\sigma}) & -\mathbf{G}(\boldsymbol{\sigma})\hat{\mathbf{C}}(\boldsymbol{\sigma})\\ -\mathbf{H}(\boldsymbol{\sigma}) & \mathbf{L}(\boldsymbol{\sigma})\hat{\mathbf{C}}(\boldsymbol{\sigma})\end{bmatrix}, &&\tilde{\mathbf{A}}_{hF}=\begin{bmatrix}\mathbf{F}(\boldsymbol{\sigma}_h) & -\mathbf{G}(\boldsymbol{\sigma}_h)\hat{\mathbf{C}}(\boldsymbol{\sigma}_h)\\ -\mathbf{H}(\boldsymbol{\sigma}_h) & \mathbf{L}(\boldsymbol{\sigma}_h)\hat{\mathbf{C}}(\boldsymbol{\sigma}_h)\end{bmatrix}\end{aligned} \tag{100}$$

Based on the **Assumption 1**, we set $\hat{\mathbf{A}}_{h12}(\boldsymbol{\sigma})=\mathbf{0}$. The reduced system now becomes

$$\begin{bmatrix}\dot{\mathbf{z}}_w\\ \dot{\mathbf{z}}_1\end{bmatrix}=\left(\tilde{\mathbf{A}}_0+\tilde{\mathbf{A}}_1\tilde{\mathbf{A}}_F\right)\begin{bmatrix}\mathbf{z}_w\\ \mathbf{z}_1\end{bmatrix}+\left(\tilde{\mathbf{A}}_{h0}\right)\begin{bmatrix}\mathbf{z}_w(t-h)\\ \mathbf{z}_1(t-h)\end{bmatrix} \tag{101}$$

where

$$\widetilde{\mathbf{A}}_0 = \begin{bmatrix} \mathbf{0} & \mathbf{0} \\ \mathbf{0} & \hat{\mathbf{A}}_{11}(\boldsymbol{\sigma}) \end{bmatrix}, \qquad \widetilde{\mathbf{A}}_1 = \begin{bmatrix} \mathbf{I} & \mathbf{0} \\ \mathbf{0} & \hat{\mathbf{A}}_{12}(\boldsymbol{\sigma}) \end{bmatrix},$$
$$\widetilde{\mathbf{A}}_{h0} = \begin{bmatrix} \mathbf{0} & \mathbf{0} \\ \mathbf{0} & \hat{\mathbf{A}}_{h11}(\boldsymbol{\sigma}) \end{bmatrix}, \qquad \widetilde{\mathbf{A}}_F = \begin{bmatrix} \mathbf{F}(\boldsymbol{\sigma}) & -\mathbf{G}(\boldsymbol{\sigma})\hat{\mathbf{C}}(\boldsymbol{\sigma}) \\ -\mathbf{H}(\boldsymbol{\sigma}) & \mathbf{L}(\boldsymbol{\sigma})\hat{\mathbf{C}}(\boldsymbol{\sigma}) \end{bmatrix} \tag{102}$$

Using a parameter-dependent Lyapunov-Krasovskiĭ approach for the stability analysis of the system, we have the following theorem:

Theorem 1. Consider the unforced LPVTDS

$$\dot{\mathbf{z}}(t) = \widetilde{\mathbf{A}}(\boldsymbol{\sigma}(t))\mathbf{z}(t) + \widetilde{\mathbf{A}}_h(\boldsymbol{\sigma}(t))\mathbf{z}(t-h) \quad \boldsymbol{\sigma}(t) \in \Theta \tag{103}$$

The constraints Θ have the form as

$$\Theta = \left\{ \boldsymbol{\sigma} : \boldsymbol{\sigma}(t) \in \boldsymbol{R}^s, \left|\dot{\boldsymbol{\sigma}}_i(t)\right| \le \upsilon_i, i = 1,2,\cdots s, \forall t \in \boldsymbol{R} \right\} \tag{104}$$

If there exist symmetric positive definite matrix functions $\mathbf{P}(\cdot), \mathbf{Q}(\cdot), \mathbf{R}(\cdot) \in \boldsymbol{S}^n$ with $\mathbf{P}(\cdot) > \mathbf{0}$, $\mathbf{Q}(\cdot) > \mathbf{0}$, $\mathbf{R}(\cdot) > \mathbf{0}$, and any bounded matrices $\mathbf{Y}_1, \mathbf{Y}_2 \in /\boldsymbol{R}^{n \times n}$ and a positive scalar $h > 0$ such that

$$\begin{bmatrix} \boldsymbol{\Xi}_{11} & \boldsymbol{\Xi}_{12} & h\mathbf{Y}_1^T(\boldsymbol{\sigma}) \\ (*) & \boldsymbol{\Xi}_{22} & h\mathbf{Y}_2^T(\boldsymbol{\sigma}) \\ (*) & (*) & -h\mathbf{Q}(\boldsymbol{\sigma}) \end{bmatrix} \le \mathbf{0} \tag{105}$$

where

$$\Xi_{11} = \widetilde{\mathbf{A}}^T(\boldsymbol{\sigma})\mathbf{P}(\boldsymbol{\sigma}) + \mathbf{P}(\boldsymbol{\sigma})\widetilde{\mathbf{A}}(\boldsymbol{\sigma}) + \left(\sum_{i=1}^{s} \dot{\boldsymbol{\sigma}}_i \frac{\partial \mathbf{P}(\boldsymbol{\sigma}_i)}{\partial \boldsymbol{\sigma}_i}\right) + \mathbf{R}(\boldsymbol{\sigma}) + \mathbf{Y}_1^T(\boldsymbol{\sigma}) + \mathbf{Y}_1(\boldsymbol{\sigma})$$
$$\Xi_{12} = \mathbf{P}(\boldsymbol{\sigma})\widetilde{\mathbf{A}}_h(\boldsymbol{\sigma}) - \mathbf{Y}_1^T(\boldsymbol{\sigma}) + \mathbf{Y}_2(\boldsymbol{\sigma})$$
$$\Xi_{22} = \mathbf{R}(\boldsymbol{\sigma}_h) - \mathbf{Y}_2^T(\boldsymbol{\sigma}) - \mathbf{Y}_2(\boldsymbol{\sigma}) \tag{106}$$

for all independent parameter vectors $\boldsymbol{\sigma}, \boldsymbol{\sigma}_h \in \Theta$ then the unforced system is asymptotically stable.

Proof. Choose a parameter-dependent Lyapunov-Krasovskiĭ functional candidate as

$$V = V_1(\boldsymbol{\sigma}(t)) + V_2(\boldsymbol{\sigma}(t)) + V_3(\boldsymbol{\sigma}(t)) \tag{107}$$

where

$$V_1(\boldsymbol{\sigma}(t), t) = \mathbf{z}^T(t)\mathbf{P}(\boldsymbol{\sigma}(t))\mathbf{z}(t)$$
$$V_2(\boldsymbol{\sigma}(t), t) = \int_{t-h}^{t} \mathbf{z}^T(\theta)\mathbf{R}(\boldsymbol{\sigma}(\theta))\mathbf{z}(\theta)d\theta$$
$$V_3(\boldsymbol{\sigma}(t), t) = \int_{t-h}^{t}\int_{s}^{t} \dot{\mathbf{z}}^T(\theta)\mathbf{Q}(\boldsymbol{\sigma}(\theta))\dot{\mathbf{z}}(\theta)d\theta ds \tag{108}$$

And $\mathbf{P}(\cdot), \mathbf{Q}(\cdot), \mathbf{R}(\cdot) \in \boldsymbol{S}^n$ are symmetric positive definite matrix functions with $\mathbf{P}(\cdot) > \mathbf{0}$, $\mathbf{Q}(\cdot) > \mathbf{0}$ and $\mathbf{R}(\cdot) > \mathbf{0}$. This parameter-dependent Lyapunov-Krasovskiĭ functional is less conservative than one with constant parameters [38], since it considers the variation of the system parameters. Three Lyapunov functional components V_1, V_2, and V_3 are used to allow more variables and flexibility for the LMI equations. This makes it easier to find a feasible and less conservative solution compared to a one or two component Lyapunov functional.

Calculating the derivative of V_1 along the trajectory of Equation (103) yields

$$\frac{dV_1}{dt}=\mathbf{z}^T\tilde{\mathbf{A}}^T\mathbf{P}\mathbf{z}+\mathbf{z}_h^T\tilde{\mathbf{A}}_h^T\mathbf{P}\mathbf{z}+\mathbf{z}^T\mathbf{P}\tilde{\mathbf{A}}\mathbf{z}+\mathbf{z}^T\mathbf{P}\tilde{\mathbf{A}}_h\mathbf{z}_h+\mathbf{z}^T\left(\sum_{i=1}^{s}\dot{\boldsymbol{\sigma}}_i\frac{\partial\mathbf{P}(\boldsymbol{\sigma}_i)}{\partial\boldsymbol{\sigma}_i}\right)\mathbf{z} \tag{109}$$

$\frac{dV_2}{dt}$ is represented as follows

$$\frac{dV_2}{dt}=\mathbf{z}^T\mathbf{R}\mathbf{z}-\mathbf{z}_h^T\mathbf{R}_h\mathbf{z}_h \tag{110}$$

and

$$\frac{dV_3}{dt}=\dot{\mathbf{z}}^T h\mathbf{Q}\dot{\mathbf{z}}-\int_{t-h}^{t}\dot{\mathbf{z}}^T(s)\mathbf{Q}(\boldsymbol{\sigma}(s))\dot{\mathbf{z}}(s)ds \tag{111}$$

By approximation the integral in the above equation and using **Lemma 2**,

$$-\int_{t-h}^{t}\dot{\mathbf{z}}^T(s)\mathbf{Q}(\boldsymbol{\sigma}(s))\dot{\mathbf{z}}(s)ds\le\begin{bmatrix}\mathbf{z}\\ \mathbf{z}_h\end{bmatrix}^T\begin{bmatrix}\mathbf{Y}_1^T+\mathbf{Y}_1 & -\mathbf{Y}_1^T+\mathbf{Y}_2\\ (*) & -\mathbf{Y}_2^T-\mathbf{Y}_2\end{bmatrix}\begin{bmatrix}\mathbf{z}\\ \mathbf{z}_h\end{bmatrix}+h\begin{bmatrix}\mathbf{z}\\ \mathbf{z}_h\end{bmatrix}^T\begin{bmatrix}\mathbf{Y}_1^T\\ \mathbf{Y}_2^T\end{bmatrix}\mathbf{Q}^{-1}\begin{bmatrix}\mathbf{Y}_1^T\\ \mathbf{Y}_2^T\end{bmatrix}^T\begin{bmatrix}\mathbf{z}\\ \mathbf{z}_h\end{bmatrix} \tag{112}$$

we obtain the following inequality

$$\frac{dV_3}{dt}\le\dot{\mathbf{z}}^T h\mathbf{Q}\dot{\mathbf{z}}+\begin{bmatrix}\mathbf{z}\\ \mathbf{z}_h\end{bmatrix}^T\begin{bmatrix}\mathbf{Y}_1^T+\mathbf{Y}_1 & -\mathbf{Y}_1^T+\mathbf{Y}_2\\ (*) & -\mathbf{Y}_2^T-\mathbf{Y}_2\end{bmatrix}\begin{bmatrix}\mathbf{z}\\ \mathbf{z}_h\end{bmatrix}+h\begin{bmatrix}\mathbf{z}\\ \mathbf{z}_h\end{bmatrix}^T\begin{bmatrix}\mathbf{Y}_1^T\\ \mathbf{Y}_2^T\end{bmatrix}\mathbf{Q}^{-1}\begin{bmatrix}\mathbf{Y}_1^T\\ \mathbf{Y}_2^T\end{bmatrix}^T\begin{bmatrix}\mathbf{z}\\ \mathbf{z}_h\end{bmatrix} \tag{113}$$

The quadratic form of the derivative of this parameter-dependent Lyapunov-Krasovskiĭ functional can be written as

$$\frac{dV}{dt} \leq \begin{bmatrix} \mathbf{z} \\ \mathbf{z}_h \end{bmatrix}^T \left\{ \begin{bmatrix} \widetilde{\mathbf{A}}^T\mathbf{P} + \mathbf{P}\widetilde{\mathbf{A}} + \left(\sum_{i=1}^{s} \dot{\boldsymbol{\sigma}}_i \frac{\partial \mathbf{P}(\boldsymbol{\sigma}_i)}{\partial \boldsymbol{\sigma}_i} \right) + \mathbf{R} & \mathbf{P}\widetilde{\mathbf{A}}_h \\ (*) & -\mathbf{R}_h \end{bmatrix} + \begin{bmatrix} \mathbf{Y}_1^T + \mathbf{Y}_1 & -\mathbf{Y}_1^T + \mathbf{Y}_2 \\ (*) & -\mathbf{Y}_2^T - \mathbf{Y}_2 \end{bmatrix} + h \begin{bmatrix} \mathbf{Y}_1^T \\ \mathbf{Y}_2^T \end{bmatrix} \mathbf{Q}^{-1} \begin{bmatrix} \mathbf{Y}_1^T \\ \mathbf{Y}_2^T \end{bmatrix}^T \right\} \begin{bmatrix} \mathbf{z} \\ \mathbf{z}_h \end{bmatrix} \tag{114}$$

Thus we have

$$\begin{bmatrix} \widetilde{\mathbf{A}}^T\mathbf{P} + \mathbf{P}\widetilde{\mathbf{A}} + \left(\sum_{i=1}^{s} \dot{\boldsymbol{\sigma}}_i \frac{\partial \mathbf{P}(\boldsymbol{\sigma}_i)}{\partial \boldsymbol{\sigma}_i} \right) + \mathbf{R} & \mathbf{P}\widetilde{\mathbf{A}}_h \\ (*) & -\mathbf{R}_h \end{bmatrix} + \begin{bmatrix} \mathbf{Y}_1^T + \mathbf{Y}_1 & -\mathbf{Y}_1^T + \mathbf{Y}_2 \\ (*) & -\mathbf{Y}_2^T - \mathbf{Y}_2 \end{bmatrix} + h \begin{bmatrix} \mathbf{Y}_1^T \\ \mathbf{Y}_2^T \end{bmatrix} \mathbf{Q}^{-1} \begin{bmatrix} \mathbf{Y}_1^T \\ \mathbf{Y}_2^T \end{bmatrix}^T \leq \mathbf{0} \tag{115}$$

Now using the Schur complement (see **APPENDIX B**) for the above inequality, the above equation can be rewritten as

$$\begin{bmatrix} \left\{ \begin{matrix} \widetilde{\mathbf{A}}^T(\boldsymbol{\sigma})\mathbf{P}(\boldsymbol{\sigma}) + \mathbf{P}(\boldsymbol{\sigma})\widetilde{\mathbf{A}}(\boldsymbol{\sigma}) + \left(\sum_{i=1}^{s} \dot{\boldsymbol{\sigma}}_i \frac{\partial \mathbf{P}(\boldsymbol{\sigma}_i)}{\partial \boldsymbol{\sigma}_i} \right) \\ + \mathbf{R}(\boldsymbol{\sigma}) + \mathbf{Y}_1^T(\boldsymbol{\sigma}) + \mathbf{Y}_1(\boldsymbol{\sigma}) \end{matrix} \right\} & \mathbf{P}(\boldsymbol{\sigma})\widetilde{\mathbf{A}}_h(\boldsymbol{\sigma}) - \mathbf{Y}_1^T(\boldsymbol{\sigma}) + \mathbf{Y}_2(\boldsymbol{\sigma}) & h\mathbf{Y}_1^T(\boldsymbol{\sigma}) \\ (*) & -\mathbf{R}(\boldsymbol{\sigma}_h) - \mathbf{Y}_2^T(\boldsymbol{\sigma}) - \mathbf{Y}_2(\boldsymbol{\sigma}) & \mathbf{Y}_2^T(\boldsymbol{\sigma}) \\ (*) & (*) & -h\mathbf{Q}(\boldsymbol{\sigma}) \end{bmatrix} \leq \mathbf{0} \tag{116}$$

This completes the proof. □

Remark 1. According to **Theorem 1,** the reduced system (101) is asymptotically stable if there exist symmetric positive definite matrix functions $\mathbf{P}(\cdot), \mathbf{Q}(\cdot), \mathbf{R}(\cdot) \in \boldsymbol{S}^n$ with $\mathbf{P}(\cdot) > \mathbf{0}$, $\mathbf{Q}(\cdot) > \mathbf{0}$, $\mathbf{R}(\cdot) > \mathbf{0}$, any bounded matrices $\mathbf{Y}_1, \mathbf{Y}_2 \in I\!\!R^{n \times n}$ and a positive scalar $h > 0$ such that

$$\begin{bmatrix} \left\{ \begin{array}{l} \left(\widetilde{\mathbf{A}}_0 + \widetilde{\mathbf{A}}_1 \widetilde{\mathbf{A}}_F\right)^T \mathbf{P} + \mathbf{P}\left(\widetilde{\mathbf{A}}_0 + \widetilde{\mathbf{A}}_1 \widetilde{\mathbf{A}}_F\right) \\ + \left(\sum_{i=1}^{s} \dot{\boldsymbol{\sigma}}_i \dfrac{\partial \mathbf{P}(\boldsymbol{\sigma}_i)}{\partial \boldsymbol{\sigma}_i} \right) + \mathbf{R} + \mathbf{Y}_1 + \mathbf{Y}_1^T \end{array} \right\} & \mathbf{P}\widetilde{\mathbf{A}}_{h0} - \mathbf{Y}_1^T + \mathbf{Y}_2 & h\mathbf{Y}_1^T \\ (*) & -\mathbf{R}(\boldsymbol{\sigma}_h) - \mathbf{Y}_2 - \mathbf{Y}_2^T & h\mathbf{Y}_2^T \\ (*) & (*) & -h\mathbf{Q} \end{bmatrix} \leq \mathbf{0} \tag{117}$$

Theorem 2. If there exist symmetric positive definite matrix functions $\widetilde{\mathbf{P}}(\cdot), \widetilde{\mathbf{Q}}(\cdot), \widetilde{\mathbf{R}}(\cdot) \in \boldsymbol{S}^n$ with $\widetilde{\mathbf{P}}(\cdot) > \mathbf{0}$, $\widetilde{\mathbf{Q}}(\cdot) > \mathbf{0}$, $\widetilde{\mathbf{R}}(\cdot) > \mathbf{0}$, any bounded matrices $\widetilde{\mathbf{Y}}_1, \widetilde{\mathbf{Y}}_2 \in I\!\!R^{n \times n}$ and scalar a positive $h > 0$ such that

$$\begin{bmatrix} \left\{ \begin{array}{l} \widetilde{\mathbf{P}}\widetilde{\mathbf{A}}_0^T + \widetilde{\mathbf{A}}_0 \widetilde{\mathbf{P}} + \widetilde{\mathbf{F}}^T \widetilde{\mathbf{A}}_1^T + \widetilde{\mathbf{A}}_1 \widetilde{\mathbf{F}} \\ + \left(\sum_{i=1}^{s} \dot{\boldsymbol{\sigma}}_i \dfrac{\partial \widetilde{\mathbf{P}}(\boldsymbol{\sigma}_i)}{\partial \boldsymbol{\sigma}_i} \right) + \widetilde{\mathbf{R}} + \widetilde{\mathbf{Y}}_1 + \widetilde{\mathbf{Y}}_1^T \end{array} \right\} & \widetilde{\mathbf{A}}_{h0}\widetilde{\mathbf{P}} - \widetilde{\mathbf{Y}}_1^T + \widetilde{\mathbf{Y}}_2 & h\widetilde{\mathbf{Y}}_1^T \\ (*) & -\widetilde{\mathbf{R}} - \widetilde{\mathbf{Y}}_2 - \widetilde{\mathbf{Y}}_2^T & h\widetilde{\mathbf{Y}}_2^T \\ (*) & (*) & -h\widetilde{\mathbf{Q}} \end{bmatrix} \leq \mathbf{0} \tag{118}$$

The system with $\widetilde{\mathbf{A}}_F = \begin{bmatrix} \mathbf{F}(\boldsymbol{\sigma}) & -\mathbf{G}(\boldsymbol{\sigma})\hat{\mathbf{C}}(\boldsymbol{\sigma}) \\ -\mathbf{H}(\boldsymbol{\sigma}) & \mathbf{L}(\boldsymbol{\sigma})\hat{\mathbf{C}}(\boldsymbol{\sigma}) \end{bmatrix} = \widetilde{\mathbf{F}}\widetilde{\mathbf{P}}^{-1}$ is asymptotically stable.

Proof. Pre- and post-multiplying Equation (117) with $\mathrm{diag}(\mathbf{P}^{-1},\mathbf{P}^{-1},\mathbf{P}^{-1})$, we have

$$\begin{bmatrix} \left\{ \begin{array}{l} \mathbf{P}^{-1}\widetilde{\mathbf{A}}_0^T + \widetilde{\mathbf{A}}_0\mathbf{P}^{-1} + \left(\widetilde{\mathbf{A}}_F\mathbf{P}^{-1}\right)^T\widetilde{\mathbf{A}}_1^T + \widetilde{\mathbf{A}}_1\left(\widetilde{\mathbf{A}}_F\mathbf{P}^{-1}\right) \\ +\mathbf{P}^{-1}\left(\sum_{i=1}^{s}\dot{\boldsymbol{\sigma}}_i\dfrac{\partial\mathbf{P}(\boldsymbol{\sigma}_i)}{\partial\boldsymbol{\sigma}_i}\right)\mathbf{P}^{-1} + \mathbf{P}^{-1}\mathbf{R}\mathbf{P}^{-1} + 2\mathbf{P}^{-1}\mathbf{Y}_1\mathbf{P}^{-1} \end{array} \right\} & \widetilde{\mathbf{A}}_{h0}\mathbf{P}^{-1} - \mathbf{P}^{-1}\mathbf{Y}_1\mathbf{P}^{-1} + \mathbf{P}^{-1}\mathbf{Y}_2\mathbf{P}^{-1} & \mathrm{h}\mathbf{P}^{-1}\mathbf{Y}_1\mathbf{P}^{-1} \\ (*) & -\mathbf{P}^{-1}\mathbf{R}(\boldsymbol{\sigma}(t-h))\mathbf{P}^{-1} - 2\mathbf{P}^{-1}\mathbf{Y}_2\mathbf{P}^{-1} & \mathrm{h}\mathbf{P}^{-1}\mathbf{Y}_2\mathbf{P}^{-1} \\ (*) & (*) & -\mathrm{h}\mathbf{P}^{-1}\mathbf{Q}\mathbf{P}^{-1} \end{bmatrix} \leq \tag{119}$$

It is apparent that the parameter box of $\mathbf{R}(\boldsymbol{\sigma}(t))$ is identical to the parameter box of $\mathbf{R}(\boldsymbol{\sigma}(t-h))$, when we convert the affine linear parameter-varying systems to polytopic parameters, then we can set $\mathbf{P}^{-1}\mathbf{R}(\boldsymbol{\sigma}(t-h))\mathbf{P}^{-1} = \mathbf{P}^{-1}\mathbf{R}(\boldsymbol{\sigma}(t))\mathbf{P}^{-1} = \widetilde{\mathbf{R}}$. Defining $\widetilde{\mathbf{P}} = \mathbf{P}^{-1}$, we have

$$\frac{\partial\widetilde{\mathbf{P}}}{\partial\boldsymbol{\sigma}_i} = \mathbf{P}^{-1}\frac{\partial\mathbf{P}}{\partial\boldsymbol{\sigma}_i}\mathbf{P}^{-1} \tag{120}$$

Also, defining $\widetilde{\mathbf{F}} = \widetilde{\mathbf{A}}_F\mathbf{P}^{-1}$, $\widetilde{\mathbf{Y}}_1 = \mathbf{P}^{-1}\mathbf{Y}_1\mathbf{P}^{-1}$, $\widetilde{\mathbf{Y}}_2 = \mathbf{P}^{-1}\mathbf{Y}_2\mathbf{P}^{-1}$ and $\widetilde{\mathbf{Q}} = \mathbf{P}^{-1}\mathbf{Q}\mathbf{P}^{-1} \leq \mathbf{0}$, we have

$$
\begin{bmatrix}
\left\{\begin{array}{l}\tilde{\mathbf{P}}\tilde{\mathbf{A}}_0^T+\tilde{\mathbf{A}}_0\tilde{\mathbf{P}}+\tilde{\mathbf{F}}^T\tilde{\mathbf{A}}_1^T+\tilde{\mathbf{A}}_1\tilde{\mathbf{F}}\\ +\left(\sum_{i=1}^{s}\dot{\boldsymbol{\sigma}}_i\dfrac{\partial\tilde{\mathbf{P}}(\boldsymbol{\sigma}_i)}{\partial\boldsymbol{\sigma}_i}\right)+\tilde{\mathbf{R}}+\tilde{\mathbf{Y}}_1+\tilde{\mathbf{Y}}_1^T\end{array}\right\} & \tilde{\mathbf{A}}_{h0}\tilde{\mathbf{P}}-\tilde{\mathbf{Y}}_1^T+\tilde{\mathbf{Y}}_2 & h\tilde{\mathbf{Y}}_1^T\\
(*) & -\tilde{\mathbf{R}}-\tilde{\mathbf{Y}}_2-\tilde{\mathbf{Y}}_2^T & h\tilde{\mathbf{Y}}_2^T\\
(*) & (*) & -h\tilde{\mathbf{Q}}
\end{bmatrix}\leq\mathbf{0} \tag{121}
$$

This completes the proof. □

Remark 2. Using the similar approach, for the multiple time delay LPV system

$$
\begin{bmatrix}\dot{\mathbf{z}}_w\\ \dot{\mathbf{z}}_1\end{bmatrix}=\left(\tilde{\mathbf{A}}_0+\tilde{\mathbf{A}}_1\tilde{\mathbf{A}}_F\right)\begin{bmatrix}\mathbf{z}_w\\ \mathbf{z}_1\end{bmatrix}+\sum_{i=1}^{n}\left(\tilde{\mathbf{A}}_{hi}\right)\begin{bmatrix}\mathbf{z}_w(t-h_i)\\ \mathbf{z}_1(t-h_i)\end{bmatrix} \tag{122}
$$

, the LMI-based asymptotic stability analysis results in the following

$$
\begin{bmatrix}
\left\{\begin{array}{l}\tilde{\mathbf{P}}\tilde{\mathbf{A}}_0^T+\tilde{\mathbf{A}}_0\tilde{\mathbf{P}}+\tilde{\mathbf{F}}^T\tilde{\mathbf{A}}_1^T+\tilde{\mathbf{A}}_1\tilde{\mathbf{F}}\\ +\left(\sum_{i=1}^{s}\dot{\boldsymbol{\sigma}}_i\dfrac{\partial\tilde{\mathbf{P}}(\boldsymbol{\sigma}_i)}{\partial\boldsymbol{\sigma}_i}\right)+n\left(\tilde{\mathbf{R}}+\tilde{\mathbf{Y}}_1+\tilde{\mathbf{Y}}_1^T\right)\end{array}\right\} & \tilde{\mathbf{A}}_{h1}\tilde{\mathbf{P}}-\tilde{\mathbf{Y}}_1^T+\tilde{\mathbf{Y}}_2 & \cdots & \tilde{\mathbf{A}}_{hn}\tilde{\mathbf{P}}-\tilde{\mathbf{Y}}_1^T+\tilde{\mathbf{Y}}_2 & \tilde{\mathbf{Y}}_1^T\sum_{i=1}^{n}h_i\\
(*) & -\tilde{\mathbf{R}}-\tilde{\mathbf{Y}}_2-\tilde{\mathbf{Y}}_2^T & \mathbf{0} & \mathbf{0} & h_1\tilde{\mathbf{Y}}_2^T\\
\vdots & \mathbf{0} & \ddots & \mathbf{0} & \vdots\\
(*) & \mathbf{0} & \mathbf{0} & -\tilde{\mathbf{R}}-\tilde{\mathbf{Y}}_2-\tilde{\mathbf{Y}}_2^T & h_n\tilde{\mathbf{Y}}_2^T\\
(*) & (*) & \cdots & (*) & -\tilde{\mathbf{Q}}\sum_{i=1}^{n}h_i
\end{bmatrix}\leq\mathbf{0} \tag{123}
$$

where

$$\widetilde{\mathbf{A}}_0=\begin{bmatrix}\mathbf{0} & \mathbf{0}\\ \mathbf{0} & \hat{\mathbf{A}}_{11}(\boldsymbol{\sigma})\end{bmatrix},\qquad \widetilde{\mathbf{A}}_1=\begin{bmatrix}\mathbf{I} & \mathbf{0}\\ \mathbf{0} & \hat{\mathbf{A}}_{12}(\boldsymbol{\sigma})\end{bmatrix},$$
$$\widetilde{\mathbf{A}}_{hi}=\begin{bmatrix}\mathbf{0} & \mathbf{0}\\ \mathbf{0} & \hat{\mathbf{A}}_{h11i}(\boldsymbol{\sigma})\end{bmatrix},\qquad \widetilde{\mathbf{A}}_F=\begin{bmatrix}\mathbf{F}(\boldsymbol{\sigma}) & -\mathbf{G}(\boldsymbol{\sigma})\hat{\mathbf{C}}(\boldsymbol{\sigma})\\ -\mathbf{H}(\boldsymbol{\sigma}) & \mathbf{L}(\boldsymbol{\sigma})\hat{\mathbf{C}}(\boldsymbol{\sigma})\end{bmatrix},$$
$$i=1,2,\cdots,n \tag{124}$$

Proof. See **APPENDIX C**.

3.4. Numerical Example

To conclude this chapter we present an example, in which apply the LPVSMC synthesis technique is applied to an LPVTDS.

Example 6. An LPVTDS adopted from [50] and [51] with constant time delay 2.5 second

$$\begin{bmatrix}\dot{x}_1\\ \dot{x}_2\end{bmatrix}=\begin{bmatrix}0 & 1+0.2\sin(t)\\ -2 & -3+0.1\sin(t)\end{bmatrix}\begin{bmatrix}x_1(t)\\ x_2(t)\end{bmatrix}+\begin{bmatrix}0.2\sin(t) & 0\\ -0.2+0.1\sin(t) & -0.3\end{bmatrix}\begin{bmatrix}x_1(t-2.5)\\ x_2(t-2.5)\end{bmatrix}+\begin{bmatrix}0\\ 1\end{bmatrix}u$$
$$y=\begin{bmatrix}1 & 0\end{bmatrix}\begin{bmatrix}x_1(t)\\ x_2(t)\end{bmatrix} \tag{125}$$

By slightly modifying the previous model, we have

$$\begin{aligned}\begin{bmatrix}\dot{x}_1\\ \dot{x}_2\end{bmatrix}&=\left(\begin{bmatrix}0 & 0.6\\ -2 & -3.2\end{bmatrix}+\begin{bmatrix}0 & 0.2\\ 0 & 0.1\end{bmatrix}\sigma(t)\right)\begin{bmatrix}x_1(t)\\ x_2(t)\end{bmatrix}\\ &+\left(\begin{bmatrix}-0.4 & 0\\ -0.4 & -0.3\end{bmatrix}+\begin{bmatrix}0.2 & 0\\ 0.1 & 0\end{bmatrix}\sigma(t)\right)\begin{bmatrix}x_1(t-2.5)\\ x_2(t-2.5)\end{bmatrix}+\begin{bmatrix}0\\ 1\end{bmatrix}u\end{aligned} \tag{126}$$

where the time-varying parameter is

$$\sigma(t)=2+\sin(t), \qquad 1\le\sigma(t)\le 3 \tag{127}$$
$$|\dot{\sigma}(t)|=|\cos(t)|\le 1$$

In order to find a parameter-dependent controller, we set the positive definite matrix functions as

$$\begin{aligned}\widetilde{\mathbf{P}}(\cdot)&=\widetilde{\mathbf{P}}_0+\widetilde{\mathbf{P}}_1 m(x_1)>\mathbf{0}\\ \widetilde{\mathbf{Q}}(\cdot)&=\widetilde{\mathbf{Q}}_0+\widetilde{\mathbf{Q}}_1 m(x_1)>\mathbf{0}\\ \widetilde{\mathbf{R}}(\cdot)&=\widetilde{\mathbf{R}}_0+\widetilde{\mathbf{R}}_1 m(x_1)>\mathbf{0}\end{aligned} \tag{128}$$

In order to make it easy to calculate the inverse of $\widetilde{\mathbf{P}}$, we choose

$$\widetilde{\mathbf{P}}_1=\begin{bmatrix}1 & 0\\ 0 & 1\end{bmatrix} \tag{129}$$

After solving the Equation (118) on each vertex of the parameter box, we have

$$\begin{aligned}\widetilde{\mathbf{P}}_0&=\begin{bmatrix}0.5 & 0\\ 0 & 0.5\end{bmatrix},\\ \widetilde{\mathbf{F}}&=\begin{bmatrix}-0.75 & 0.003\\ -0.015 & -1.84\end{bmatrix}\end{aligned} \tag{130}$$

Then, the controller parameters are

$$\begin{bmatrix}\mathbf{F}(\boldsymbol{\sigma}) & -\mathbf{G}(\boldsymbol{\sigma})\hat{\mathbf{C}}(\boldsymbol{\sigma})\\ -\mathbf{H}(\boldsymbol{\sigma}) & \mathbf{L}(\boldsymbol{\sigma})\hat{\mathbf{C}}(\boldsymbol{\sigma})\end{bmatrix}=\widetilde{\mathbf{A}}_F=\widetilde{\mathbf{F}}\left(\widetilde{\mathbf{P}}_0+\widetilde{\mathbf{P}}_1\boldsymbol{\sigma}\right)^{-1} \tag{131}$$

So, we obtain

$$
\begin{aligned}
F(\sigma) &= -1.5 - 0.75\frac{1}{\sigma(t)} \\
G(\sigma) &= -0.006 - 0.003\frac{1}{\sigma(t)} \\
H(\sigma) &= 0.03 + 0.015\frac{1}{\sigma(t)} \\
L(\sigma) &= -3.68 - 1.84\frac{1}{\sigma(t)}
\end{aligned}
\tag{132}
$$

All the controller parameters can be calculated on-line. Firstly, we compare this LPVSMC approach with the standard SMC in [14] by letting the maximum of control input be equal and choosing $k = 3$ and $\varepsilon = 0.01$.

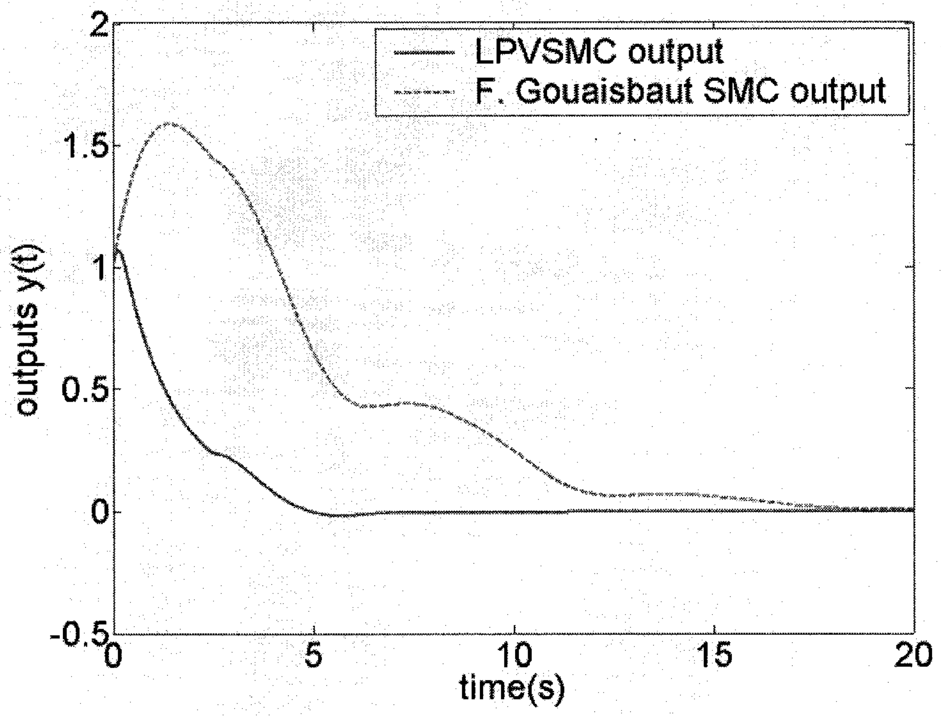

Figure 3-1 Outputs of LPVSMC and parameter-independent SMC

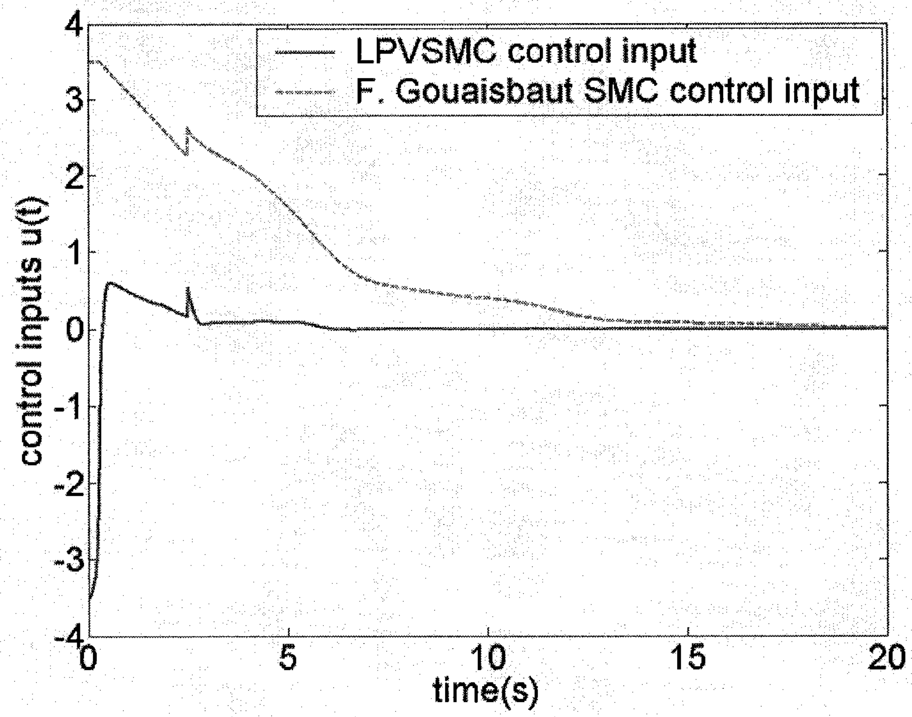

Figure 3-2 Control inputs of LPVSMC and. parameter-independent SMC

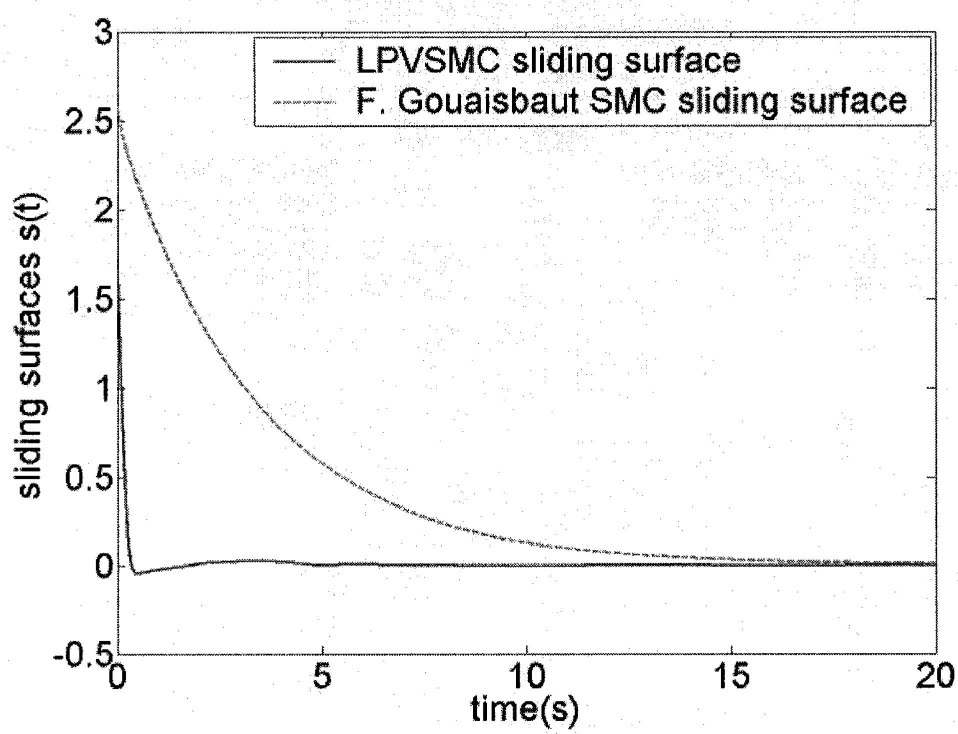

Figure 3-3 Sliding surfaces of LPVSMC and parameter-independent SMC

The simulation results show that the LPV sliding mode controller can improve the regulation of output with smaller overshoot and less setting time. The LPVSMC can achieve better performances than the F. Gouaisbaut Theorem 1 of [14].

Secondly, we have the following simulation results for the output, output error, states, sliding surface and the sliding surface parameters response to a unit-step input are shown as

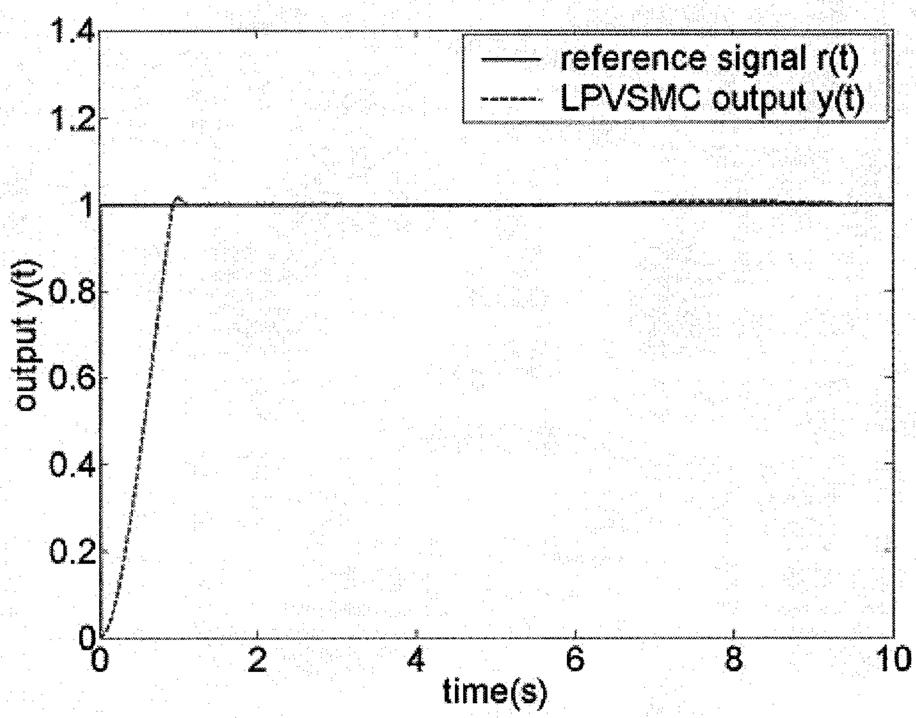

Figure 3-4 Output of LPVTDS response to a unit-step input

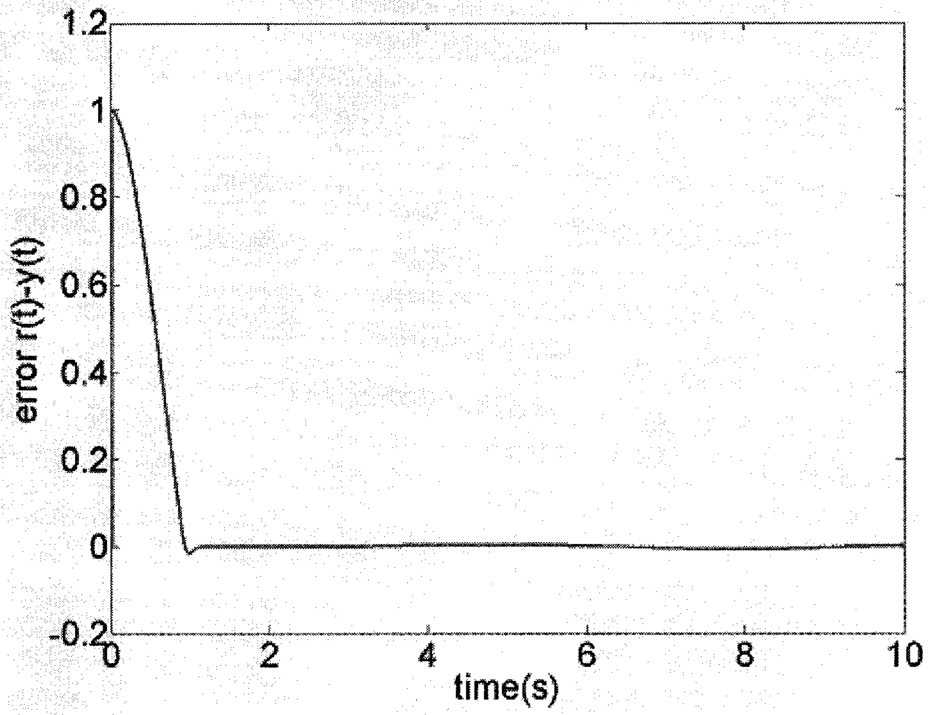

Figure 3-5 Output error of LPVTDS response to a unit-step input

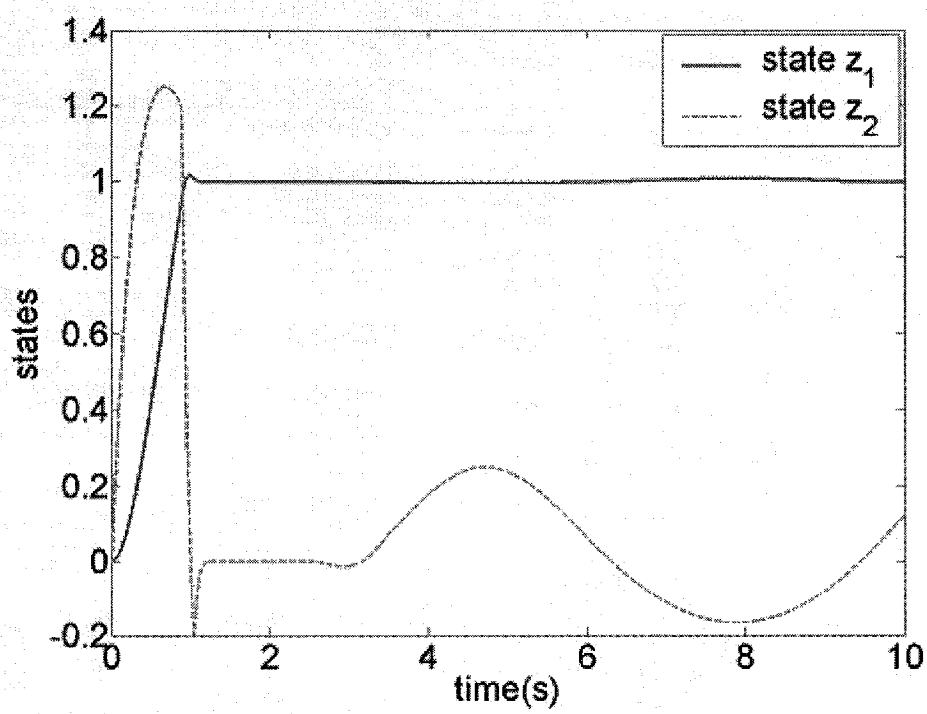

Figure 3-6 States of LPVTDS response to a unit-step input

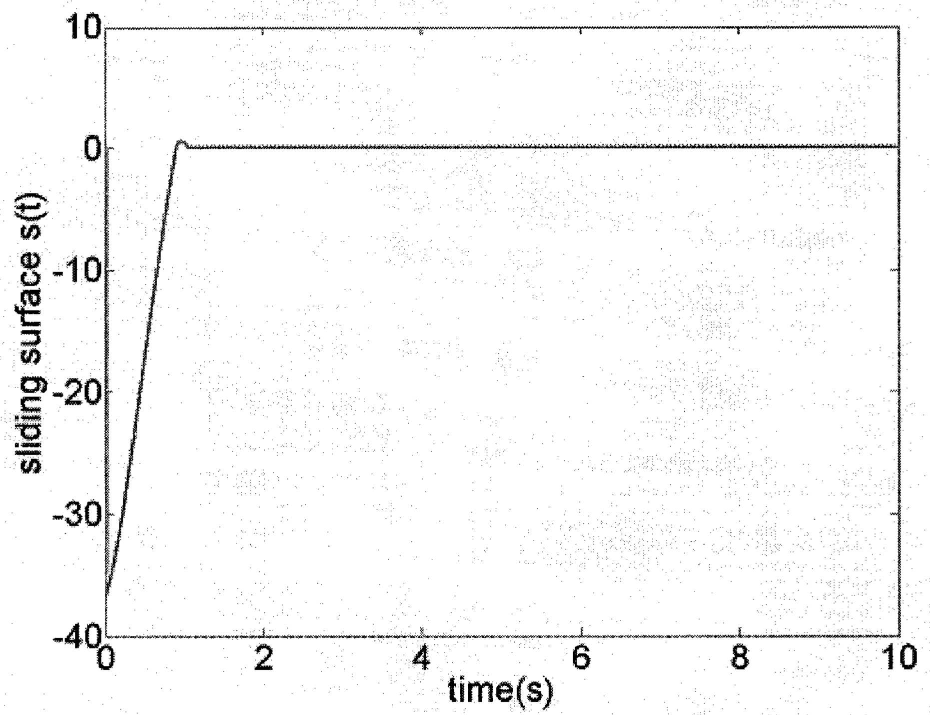

Figure 3-7 Sliding surface of LPVTDS response to a unit-step input

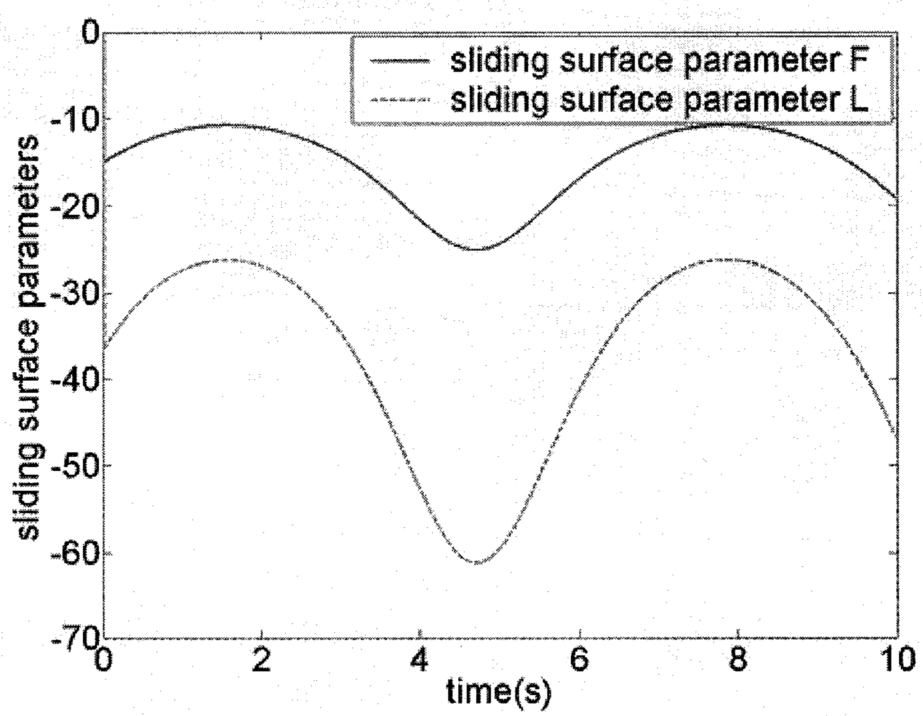

Figure 3-8 Sliding surface parameters F and L of LPVTDS

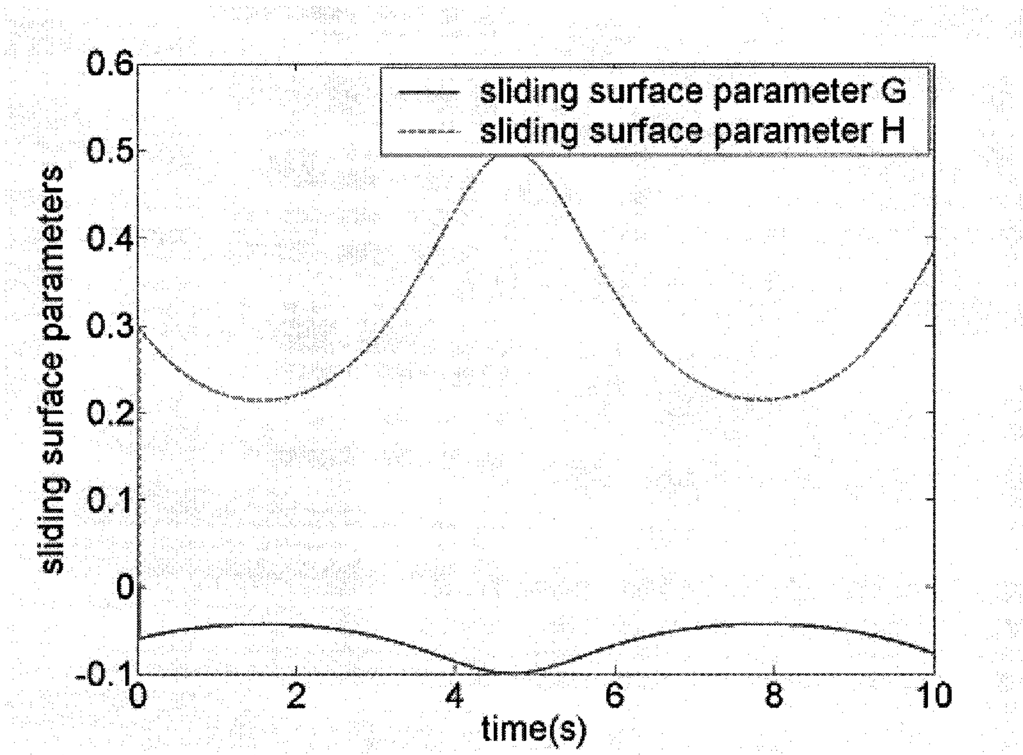

Figure 3-9 Sliding surface parameters G and H of LPVTDS

The following are the simulation results response to a sinusoidal input.

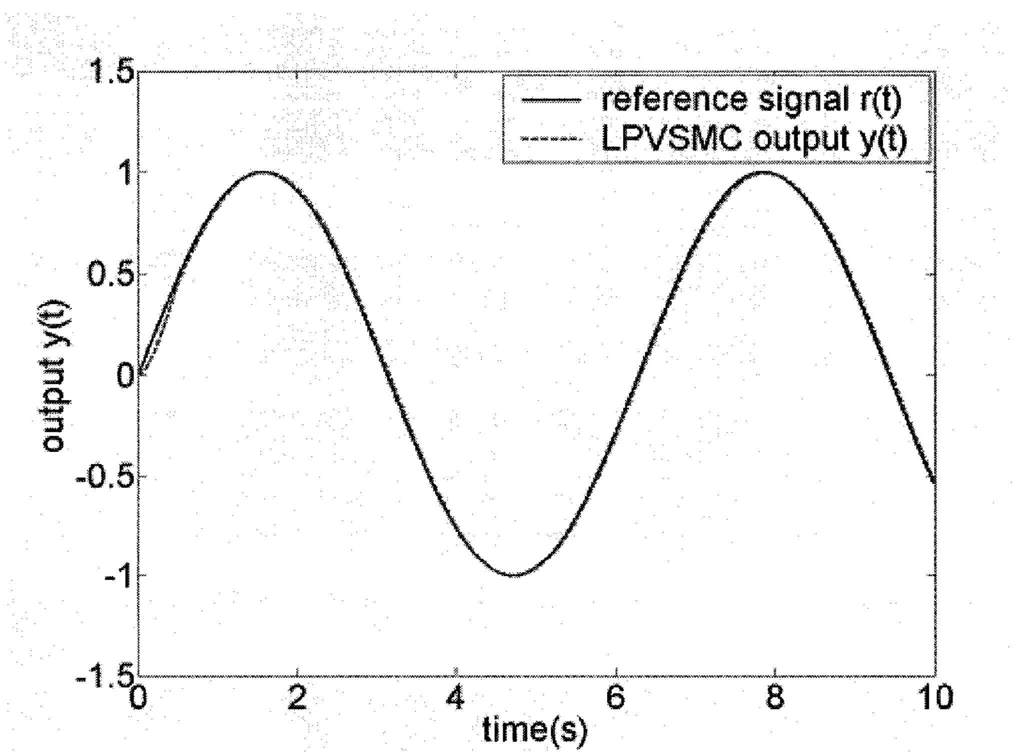

Figure 3-10 Output of LPVTDS response to a sinusoidal input

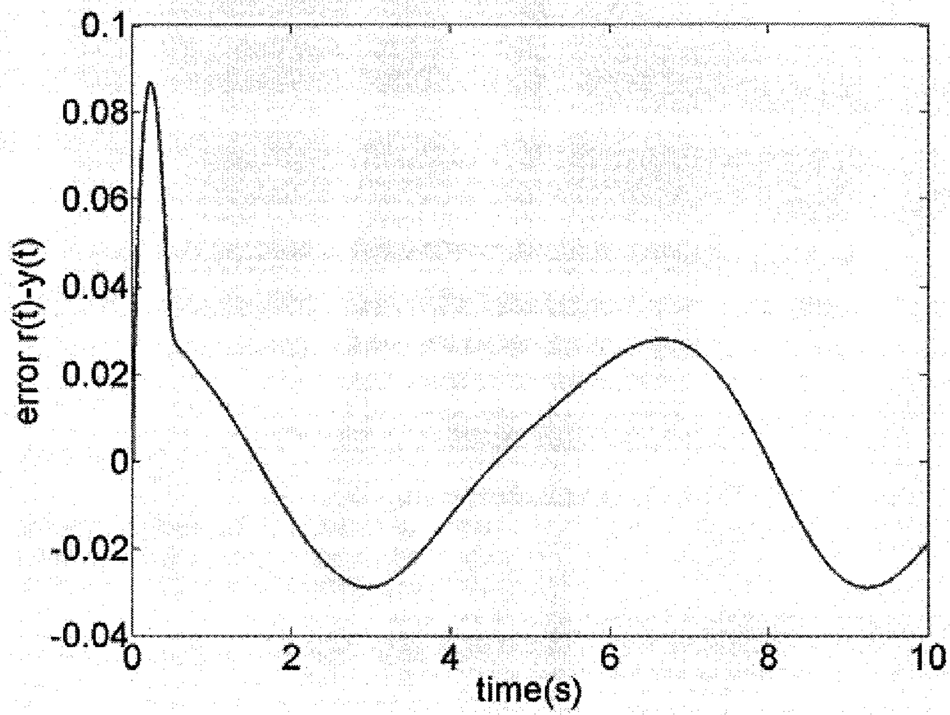

Figure 3-11 Output error of LPVTDS response to a sinusoidal input

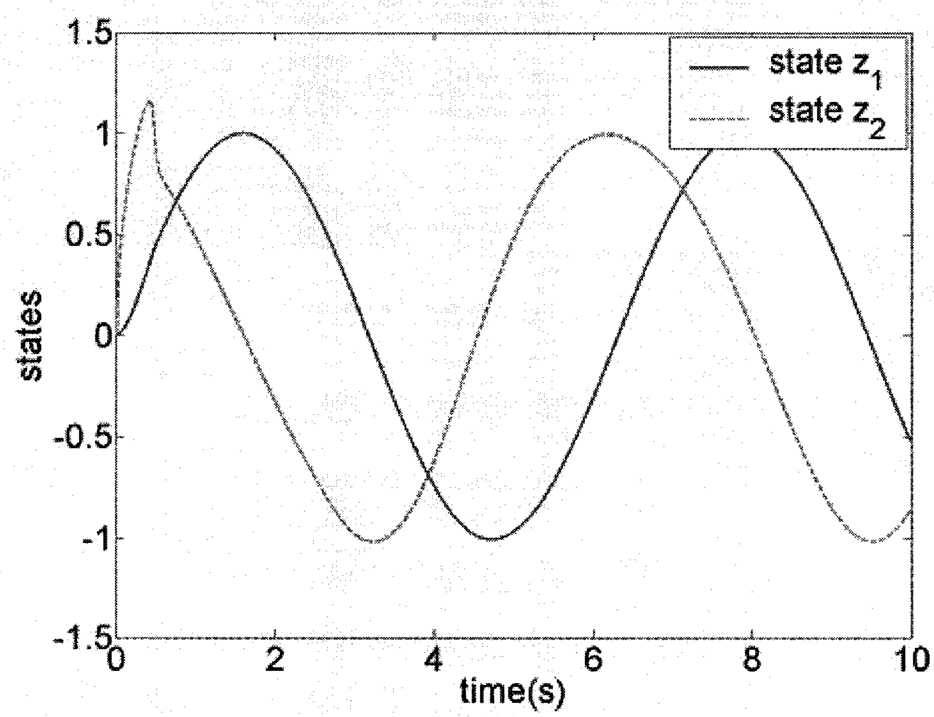

Figure 3-12 States of LPVTDS response to a sinusoidal input

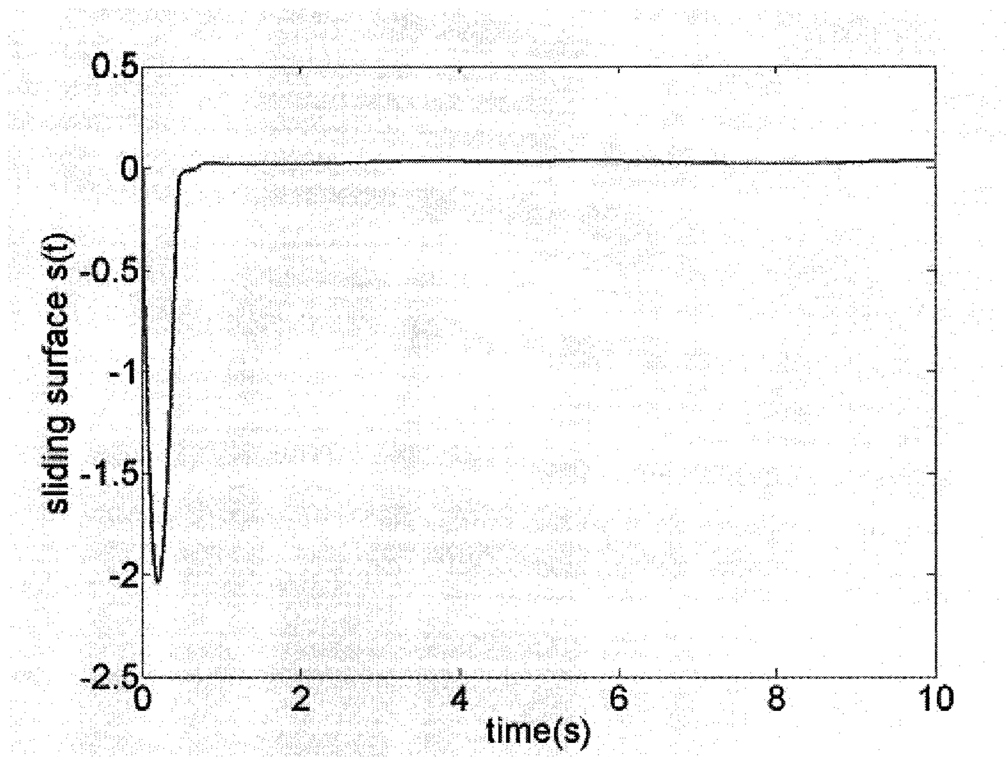

Figure 3-13 Sliding surface of LPVTDS response to a sinusoidal input

The simulation results show that the LPVSMC can track a unit-step input and a sinusoid input accurately. From the Equation (132), the sliding surface parameters are independent on the reference input, so the sliding surface parameters response to a sinusoid are identical to them response to a unit-step input as show in Figure 3-8 and Figure 3-9.

In summary, Theorem 1 gives a novel method to check out the stability of an LPVTDS, and Theorem 2 presents a systemitic procedure to synthesize an LPV sliding mode controller for an LPVTDS. At the end, the example is used to show that the LPVSMC can accomplish a high performance for regulation and tracking problems.

Chapter 4

Application of LPVSMC to Vortex-Coupled Delta Wing Dynamics

In the chapter, a LPV multiple time-delay model is built based on the aerodynamic model of vortex-coupled delta wing systems. Then, an LPV sliding mode controller is synthesized for the vortex-coupled delta wing system. Finally, we simulate the closed-loop system and make comparison with other control methods.

4.1. Quasi-LPV Modelling for Delta Wing Systems

At first, the integral of sinusoid in Equation (79) is approximated as a constant in several short intervals. Then, the integral is replaced by the sum of three time-delayed components. Next, a state equation is constructed. In addition, the time-varying parameters are defined and the LPV state equations of the delta wing systems are obtained.

In order to approximate the integral in Equation (79), the whole integral range, $t-T \le \tau \le t$, is divided into four equal intervals, i.e. $\begin{bmatrix} t & t\text{-}\frac{T}{4} \end{bmatrix}$, $\begin{bmatrix} t\text{-}\frac{T}{4} & t\text{-}\frac{T}{2} \end{bmatrix}$, $\begin{bmatrix} t\text{-}\frac{T}{2} & t\text{-}\frac{3T}{4} \end{bmatrix}$ and $\begin{bmatrix} t\text{-}\frac{3T}{4} & t\text{-}T \end{bmatrix}$. Since the size of each interval is very small (0.04sec), it is reasonable to consider the $\sin(\frac{\pi(t-\tau)}{T^*})$ term as a constant. Now, we can approximate the whole integral as

$$\int_{t-T}^{t}\sin(\frac{\pi(t-\tau)}{T^*})\dot{\Phi}(\tau)d\tau \tag{133}$$

$$\approx\frac{\sin(\frac{\pi(t-t)}{T})+\sin(\frac{\pi(t-(t-\frac{T}{4}))}{T})}{2}\int_{t-\frac{T}{4}}^{t}\dot{\Phi}(\tau)d\tau$$

$$+\frac{\sin(\frac{\pi(t-(t-\frac{T}{4}))}{T})+\sin(\frac{\pi(t-(t-\frac{T}{2}))}{T})}{2}\int_{t-\frac{T}{2}}^{t-\frac{T}{4}}\dot{\Phi}(\tau)d\tau$$

$$+\frac{\sin(\frac{\pi(t-(t-\frac{T}{2}))}{T})+\sin(\frac{\pi(t-(t-\frac{3T}{4}))}{T})}{2}\int_{t-\frac{3T}{4}}^{t-\frac{T}{2}}\dot{\Phi}(\tau)d\tau$$

$$+\frac{\sin(\frac{\pi(t-(t-\frac{3T}{4}))}{T})+\sin(\frac{\pi(t-(t-T))}{T})}{2}\int_{t-T}^{t-\frac{3T}{4}}\dot{\Phi}(\tau)d\tau$$

From the Leibniz-Newton formula

$$\int_{t-h}^{t}\dot{\mathbf{x}}(s)ds=\mathbf{x}(t)-\mathbf{x}(t-h) \tag{134}$$

, we can obtain the approximation of the integral terms

$$\int_{t-T}^{t}\sin(\frac{\pi(t-\tau)}{T^*})\dot{\Phi}(\tau)d\tau\approx 0.354\Phi(t)+0.5\Phi(t-T/4)-0.5\Phi(t-3T/4)-0.354\Phi(t-T) \tag{135}$$

For simplification, we define a new variable to represent the sum of these three time delays

$$\frac{1}{2}\delta=\left[0.5\Phi(t-T/4)-0.5\Phi(t-3T/4)-0.354\Phi(t-T)\right] \tag{136}$$

After replacing the integral terms by time-delayed representation, the vortex breakdown location can be represented as

$$X_{vbl}(t) = X_{sl} + \frac{1.65}{\tan\alpha(t)}\left(0.354\Phi(t) + \frac{1}{2}\delta\right) \tag{137}$$

$$X_{vbr}(t) = X_{sr} - \frac{1.65}{\tan\alpha(t)}\left(0.354\Phi(t) + \frac{1}{2}\delta\right) \tag{138}$$

By substituting Equations (137) and (138) into Equation (59), the roll moment coefficient $Cl(X_{vbl}, X_{vbl})$ can be represented as

$$Cl = e_0 + e_1 \cdot \left[(X_{sl} - X_{sr}) + \frac{1.65}{\tan\alpha(t)}\left(0.708\,\Phi(t) + \delta\right) \right] \tag{139}$$

The LPV modelling approach focuses on linearizing the nonlinear systems by hiding the nonlinear terms via defining them as time-varying parameters. Before we construct the LPV model for the roll motion of delta wing systems, the roll angle of delta wing is defined as

$$x_1 = \Phi(t) \tag{140}$$

and the roll angular velocity of delta wing as

$$x_2 = \dot{\Phi}(t) \tag{141}$$

It is hard to analyze the systems and to synthesize the controller for the steady terms X_{sl} and X_{sr}, since they are the solutions of the second-order Equation (64). Therefore, precise mathematical expressions do not exist for the terms X_{sl} and X_{sr}. However, $(X_{sl} - X_{sr})$ can be written as an LPV representation

$$X_{sl} - X_{sr} = p(x_1)x_1 \tag{142}$$

because this term is function of roll angle x_1. Moreover, the angle of attack $\alpha(t)$ is a function of the roll angle x_1. This term can be written as an LPV representation $m(x_1)$ defined as another time-varying parameter

$$\frac{1.65}{\tan\alpha(t)} = m(x_1) \tag{143}$$

The functions $p(x_1(t))$ and $m(x_1(t))$ can be obtained by curve fitting to the experimental results of [19] (see Figure 4-1 and Figure 4-2).

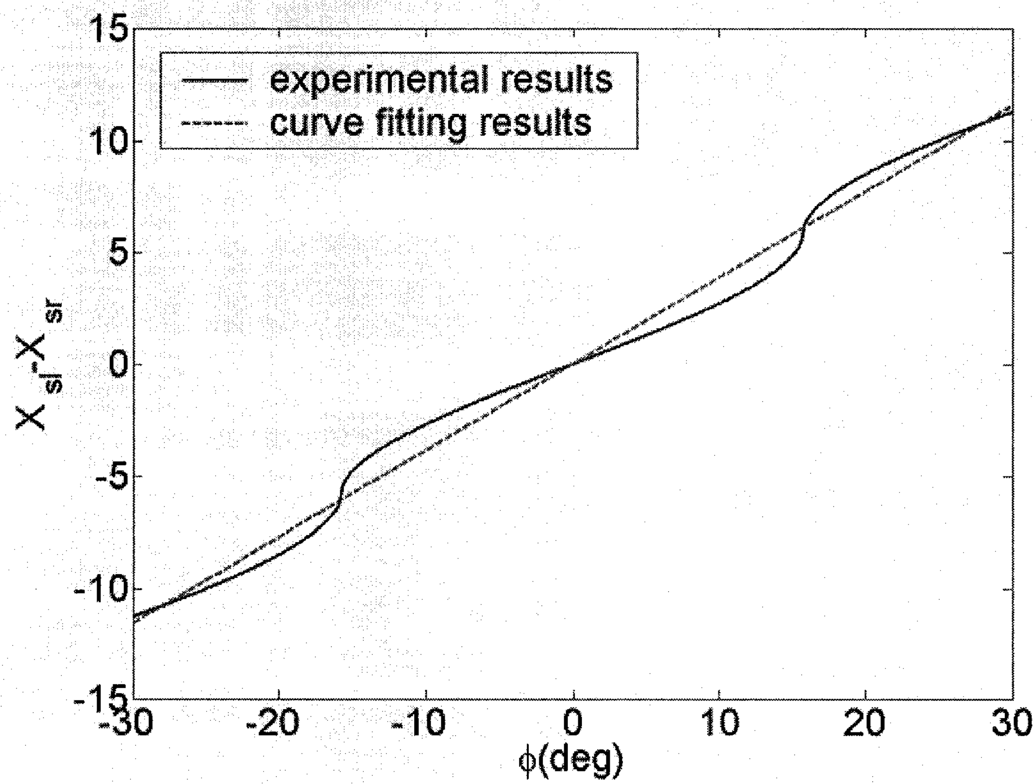

Figure 4-1 Curve fitting $X_{sl} - X_{sr}$ versus the roll angle ϕ

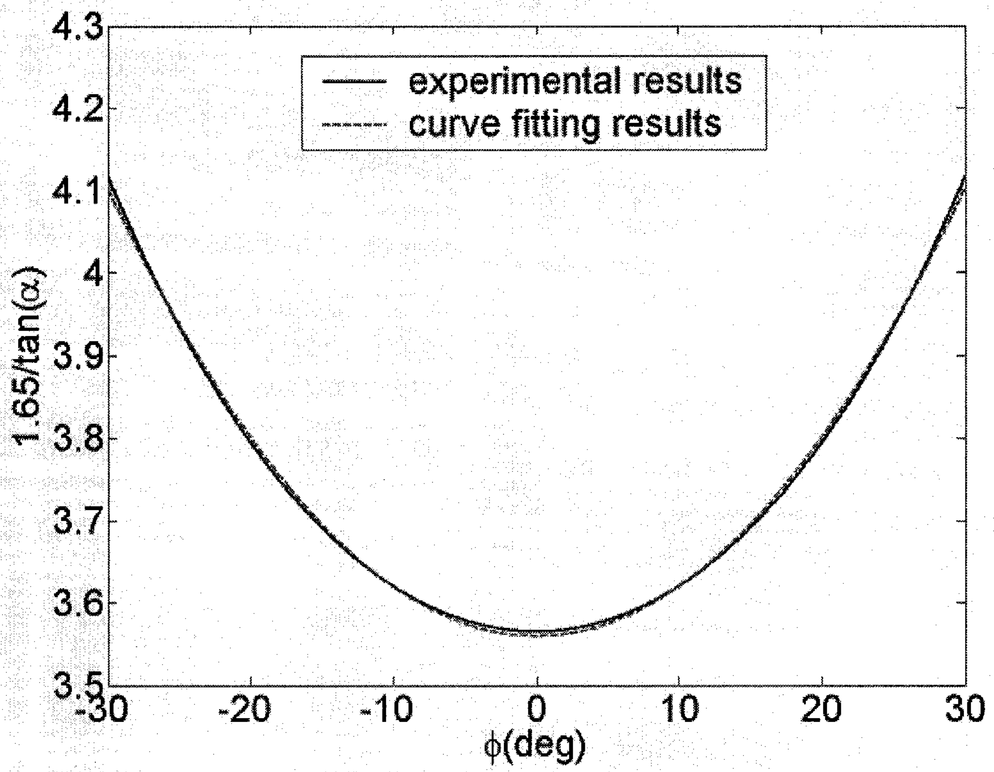

Figure 4-2 Curve fitting $\frac{1.65 \cdot T}{2 \cdot \tan(\alpha)}$ versus the roll angle ϕ

$m(x_1)$ is a time-varying parameter that can be defined as

$$m(x_1) = 3.5603 + 1.9760x_1^2 \tag{144}$$

and $p(x_1(t))$ is approximated as a constant

$$p = 22.0825 \tag{145}$$

Now, we only require to consider one time-varying parameter $m(x_1)$. The parameter box of $m(x_1)$ is

$$m(x_1) \in [3.5603, \quad 4.1049] \tag{146}$$

Then, the roll moment coefficient Cl is expressed as

$$Cl = e_0 + e_1[p(x_1)x_1 + m(x_1)(0.708x_1 + \delta)] \tag{147}$$

$$= e_0 + e_1[p(x_1) + 0.708m(x_1)]x_1 + e_1 \cdot m(x_1)\delta$$

The LPV representation of the dynamic for the roll motion of delta wing systems can be written as

$$\begin{bmatrix} \dot{x}_1 \\ \dot{x}_2 \end{bmatrix} = \begin{bmatrix} 0 & 1 \\ a_{21} & a_{22} \end{bmatrix} \begin{bmatrix} x_1(t) \\ x_2(t) \end{bmatrix} + \begin{bmatrix} 0 & 0 \\ a_{h121} & 0 \end{bmatrix} \begin{bmatrix} x_1(t-\frac{T}{4}) \\ x_2(t-\frac{T}{4}) \end{bmatrix} + \begin{bmatrix} 0 & 0 \\ a_{h221} & 0 \end{bmatrix} \begin{bmatrix} x_1(t-\frac{3T}{4}) \\ x_2(t-\frac{3T}{4}) \end{bmatrix} \tag{148}$$
$$+ \begin{bmatrix} 0 & 0 \\ a_{h321} & 0 \end{bmatrix} \begin{bmatrix} x_1(t-T) \\ x_2(t-T) \end{bmatrix} + \begin{bmatrix} 0 \\ 1 \end{bmatrix} u + \begin{bmatrix} 0 \\ c_{21} \end{bmatrix}$$

where

$$a_{21} = \frac{qs_a b}{I} e_1 [p + 0.708m(x_1)], \tag{149}$$
$$a_{22} = -\frac{f_c}{I},$$
$$a_{h121} = \frac{qs_a b}{I} e_1 m(x_1),$$
$$a_{h221} = -\frac{qs_a b}{I} e_1 m(x_1),$$
$$a_{h321} = -\frac{qs_a b}{I} 0.708 e_1 \cdot m(x_1),$$
$$c_{21} = \frac{qs_a b}{I} e_0$$

Figure 4-3 shows the comparison between experimental results of the delta wing systems and the LPV model. Figure 4-4 and Figure 4-5 show the states phase plot of the open-loop LPV model response to the initial condition of

$$\begin{aligned} x_1(0) &= 57.3 \text{ deg} \\ x_2(0) &= 0 \quad \text{deg/sec} \end{aligned} \tag{150}$$

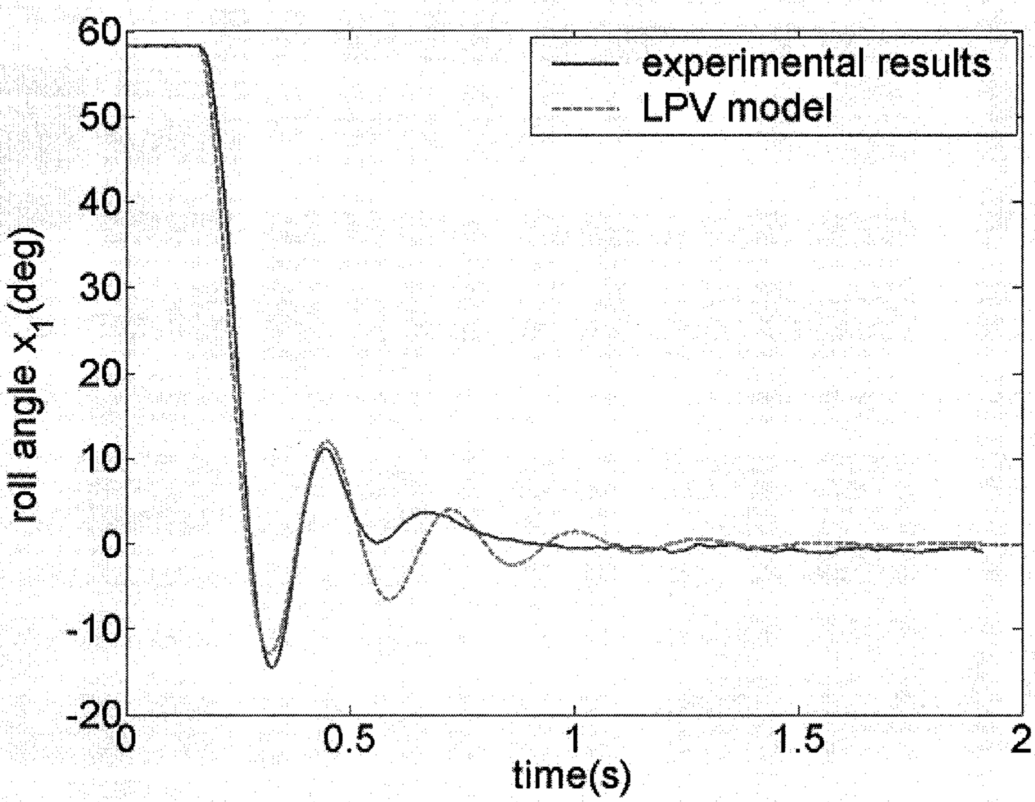

Figure 4-3 Open-loop response of the LPV model vs. experimental results

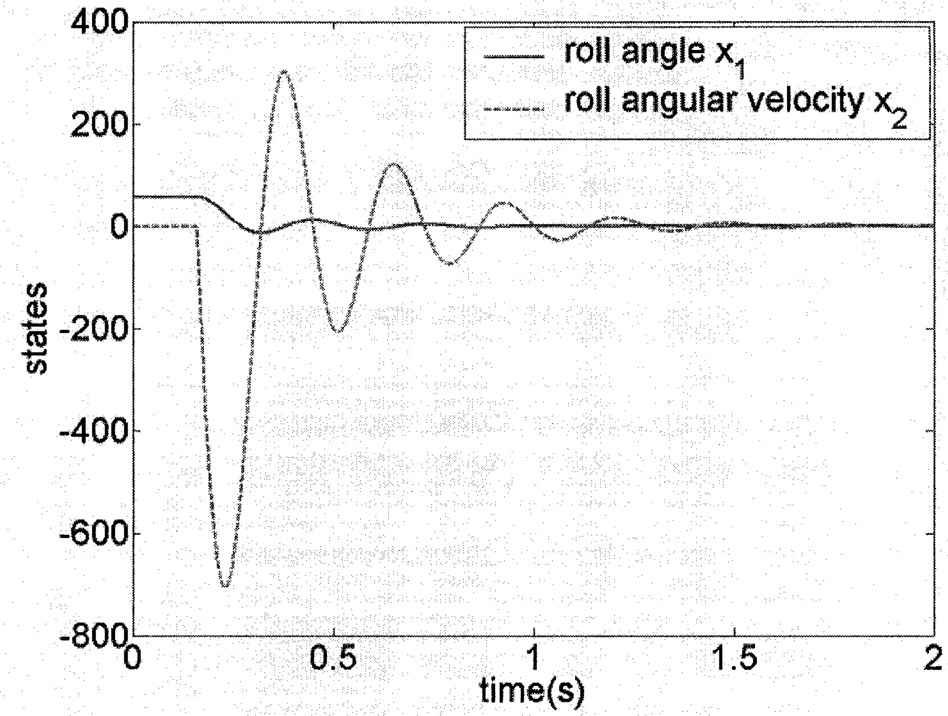

Figure 4-4 States of the open-loop LPV model

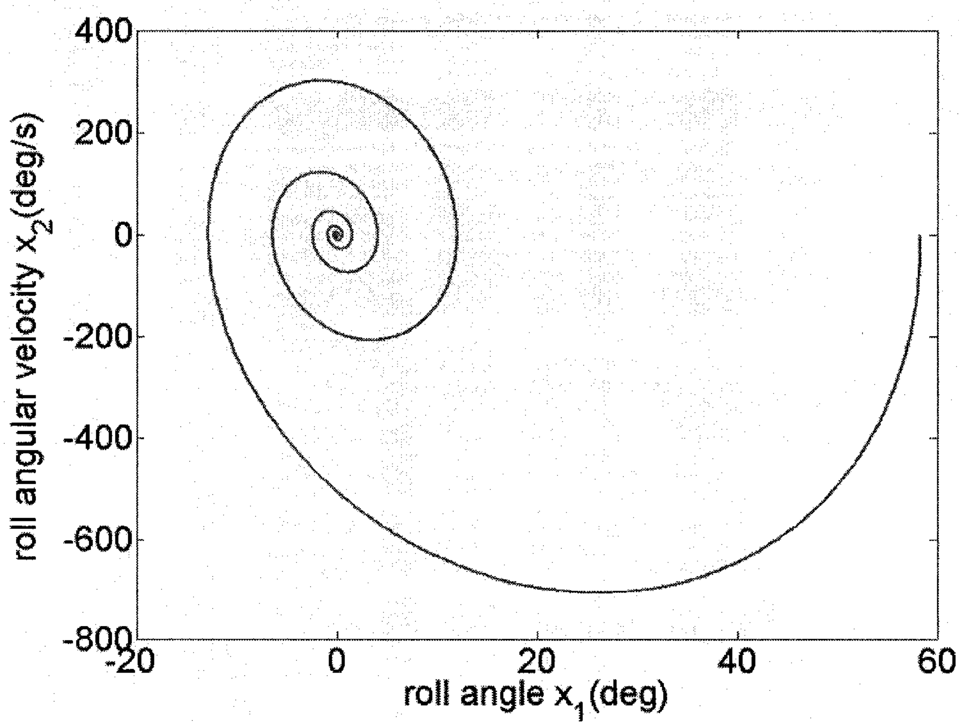

Figure 4-5 Phase diagram of the open-loop LPV model

Note that the quasi-LPV model developed in this section (148) is already in a regular form and satisfies **Assumption 1**. Thus we can use the LPVSMC synthesis procedure discussed in Chapter 3 to calculate the controller for this LPV model directly. The following section will present the LPVSMC synthesis procedure for the LPV delta wing system model.

4.2. LPVSMC for Delta Wing Systems

Given an LPVTDS, our sliding mode controller synthesis procedure is divided into three phases. The first phase is to transform the LPVTDS into the reduced form as Equation (101). Based on The reduced form of the roll motion of the delta wing systems (148) can be obtained as:

$$\begin{bmatrix} \dot{\mathbf{z}}_w \\ \dot{\mathbf{z}}_1 \end{bmatrix} = \left(\widetilde{\mathbf{A}}_0 + \widetilde{\mathbf{A}}_1 \widetilde{\mathbf{A}}_F\right) \begin{bmatrix} \mathbf{z}_w \\ \mathbf{z}_1 \end{bmatrix} + \left(\widetilde{\mathbf{A}}_{h0}\right) \begin{bmatrix} \mathbf{z}_w(t-h) \\ \mathbf{z}_1(t-h) \end{bmatrix} \tag{151}$$

where

$$\widetilde{\mathbf{A}}_0 = \begin{bmatrix} 0 & 0 \\ 0 & 0 \end{bmatrix},\ \widetilde{\mathbf{A}}_1 = \begin{bmatrix} 1 & 0 \\ 0 & 1 \end{bmatrix},\ \widetilde{\mathbf{A}}_F = \begin{bmatrix} \mathbf{F}(\sigma) & -\mathbf{G}(\sigma)\hat{\mathbf{C}}(\sigma) \\ -\mathbf{H}(\sigma) & \mathbf{L}(\sigma)\hat{\mathbf{C}}(\sigma) \end{bmatrix},$$
$$\widetilde{\mathbf{A}}_{h10} = \begin{bmatrix} 0 & 0 \\ 0 & 0 \end{bmatrix},\ \widetilde{\mathbf{A}}_{h20} = \begin{bmatrix} 0 & 0 \\ 0 & 0 \end{bmatrix},\ \widetilde{\mathbf{A}}_{h30} = \begin{bmatrix} 0 & 0 \\ 0 & 0 \end{bmatrix} \tag{152}$$

The second phase is to use **Theorem 2** to calculate the time-varying controller $\widetilde{\mathbf{A}}_F$, which guarantees the asymptotic stability of the closed-loop systems. We have one time-varying parameter

$$m(z_1) = 3.5603 + 1.9760 z_1^2 \tag{153}$$

where the parameter boxes of $m(z_1)$ and $\dfrac{\partial m(z_1)}{\partial z_1}$ are

$$m(z_1) \in [3.5603, \quad 4.1049] \text{ and } \left|\frac{\partial m(z_1)}{\partial z_1}\right| = |1.9760 \times 2z_1| \le 2.0691 \tag{154}$$

In order to find a parameter-dependent controller, we set the positive definite matrix functions as

$$\begin{aligned}\widetilde{\mathbf{P}}(\cdot) &= \widetilde{\mathbf{P}}_0 + \widetilde{\mathbf{P}}_1 m(z_1) > \mathbf{0}\\ \widetilde{\mathbf{Q}}(\cdot) &= \widetilde{\mathbf{Q}}_0 + \widetilde{\mathbf{Q}}_1 m(z_1) > \mathbf{0}\\ \widetilde{\mathbf{R}}(\cdot) &= \widetilde{\mathbf{R}}_0 + \widetilde{\mathbf{R}}_1 m(z_1) > \mathbf{0}\end{aligned} \tag{155}$$

After solving the Equation (123) on each vertex of the parameter box (146), we have

$$\begin{aligned}\widetilde{\mathbf{P}}_0 &= \begin{bmatrix} 40.5166 & 0 \\ 0 & 40.5166 \end{bmatrix}\\ \widetilde{\mathbf{P}}_1 &= \begin{bmatrix} 1 & 0 \\ 0 & 1 \end{bmatrix}\\ \widetilde{\mathbf{F}} &= \begin{bmatrix} -13.572 & -0.00415 \\ 0.01759 & -61.892 \end{bmatrix}\end{aligned} \tag{156}$$

Then, the controller parameters are

$$\begin{bmatrix} \mathbf{F}(\boldsymbol{\sigma}) & -\mathbf{G}(\boldsymbol{\sigma})\hat{\mathbf{C}}(\boldsymbol{\sigma}) \\ -\mathbf{H}(\boldsymbol{\sigma}) & \mathbf{L}(\boldsymbol{\sigma})\hat{\mathbf{C}}(\boldsymbol{\sigma}) \end{bmatrix} = \widetilde{\mathbf{A}}_F = \widetilde{\mathbf{F}}\left(\widetilde{\mathbf{P}}_0 + \widetilde{\mathbf{P}}_1 m(z_1)\right)^{-1} = \widetilde{\mathbf{F}}\widetilde{\mathbf{P}}_0^{-1} + \frac{1}{m(z_1)}\widetilde{\mathbf{F}} \tag{157}$$

The final phase is to synthesize the sliding mode controller based on the equilibrium input u_{eq}. According to Equation (91), we can derivate the equilibrium input for the LPV delta wing model

$$
\begin{aligned}
u_{eq} = -\hat{\mathbf{B}}^{-1}\Big\{ & \left[\frac{\partial \mathbf{H}(\boldsymbol{\sigma})}{\partial \boldsymbol{\sigma}}\dot{\boldsymbol{\sigma}} + \mathbf{H}(\boldsymbol{\sigma})\mathbf{F}(\boldsymbol{\sigma}) + \mathbf{L}(\boldsymbol{\sigma})\mathbf{C}(\boldsymbol{\sigma})\hat{\mathbf{A}}_{12}(\boldsymbol{\sigma})\mathbf{H}(\boldsymbol{\sigma}) - \hat{\mathbf{A}}_{22}(\boldsymbol{\sigma})\mathbf{H}(\boldsymbol{\sigma})\right]\mathbf{z}_w \\
& + \Big[-\mathbf{H}(\boldsymbol{\sigma})\mathbf{G}(\boldsymbol{\sigma})\mathbf{C}(\boldsymbol{\sigma}) - \frac{\partial \mathbf{L}(\boldsymbol{\sigma})}{\partial \boldsymbol{\sigma}}\dot{\boldsymbol{\sigma}}\mathbf{C}(\boldsymbol{\sigma}) - \mathbf{L}(\boldsymbol{\sigma})\frac{\partial \mathbf{C}(\boldsymbol{\sigma})}{\partial \boldsymbol{\sigma}}\dot{\boldsymbol{\sigma}} - \mathbf{L}(\boldsymbol{\sigma})\mathbf{C}(\boldsymbol{\sigma})\hat{\mathbf{A}}_{11}(\boldsymbol{\sigma}) \\
& \quad - \mathbf{L}(\boldsymbol{\sigma})\mathbf{C}(\boldsymbol{\sigma})\hat{\mathbf{A}}_{12}(\boldsymbol{\sigma})\mathbf{L}(\boldsymbol{\sigma})\mathbf{C}(\boldsymbol{\sigma}) + \hat{\mathbf{A}}_{21}(\boldsymbol{\sigma}) + \hat{\mathbf{A}}_{22}(\boldsymbol{\sigma})\mathbf{L}(\boldsymbol{\sigma})\mathbf{C}(\boldsymbol{\sigma})\Big]\mathbf{z}_1 \\
& + \left[\frac{\partial \mathbf{L}(\boldsymbol{\sigma})}{\partial \boldsymbol{\sigma}}\dot{\boldsymbol{\sigma}} + \mathbf{L}(\boldsymbol{\sigma})\mathbf{C}(\boldsymbol{\sigma})\hat{\mathbf{A}}_{12}(\boldsymbol{\sigma})\mathbf{L}(\boldsymbol{\sigma}) - \hat{\mathbf{A}}_{22}(\boldsymbol{\sigma})\mathbf{L}(\boldsymbol{\sigma}) + \mathbf{H}(\boldsymbol{\sigma})\mathbf{G}(\boldsymbol{\sigma})\right]\mathbf{r} \\
& + \sum_{i=1}^{n}\left\{\left[-\mathbf{L}(\boldsymbol{\sigma})\mathbf{C}(\boldsymbol{\sigma})\hat{\mathbf{A}}_{hi11}(\boldsymbol{\sigma}) + \hat{\mathbf{A}}_{hi21}(\boldsymbol{\sigma})\right]\mathbf{z}_1(t-h_i)\right\} \\
& + \sum_{i=1}^{n}\left\{\hat{\mathbf{A}}_{hi22}(\boldsymbol{\sigma})\mathbf{z}_2(t-h_i)\right\} \\
& + \mathbf{L}(\boldsymbol{\sigma})\dot{\mathbf{r}}(t)\Big\}
\end{aligned}
\tag{158}
$$

where $n = 3$. Thus, the sliding mode controller is Equation (96).

4.3. Simulation Results

Firstly, the resulting LPV controller is tested through time domain simulation by using two kinds of typical inputs: step and sinusoid. First, we choose a step input

$$
\begin{cases} r(t) = 0 & t < 0 \\ r(t) = 30 & t \geq 0 \end{cases} \tag{159}
$$

A compromise between the output performance and the chattering frequency gives us $k = 300$ and $\varepsilon = 0.05$. Using these coefficients, we have the following simulation results for the output, output error, states sliding surface and control input of closed-loop system for the step input as the reference signal.

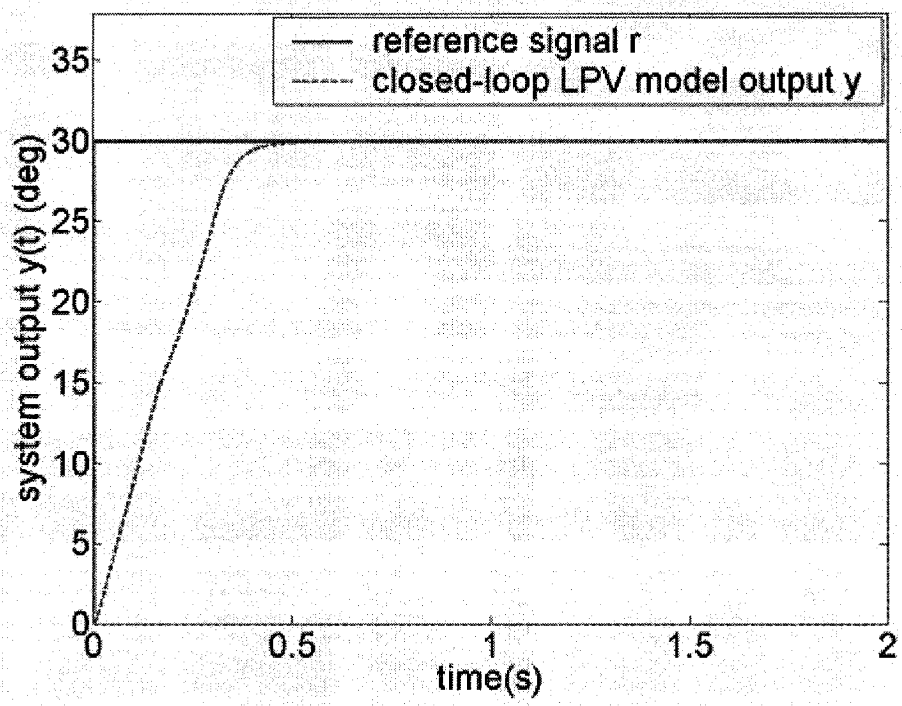

Figure 4-6 Output of LPV delta wing model response to a step input

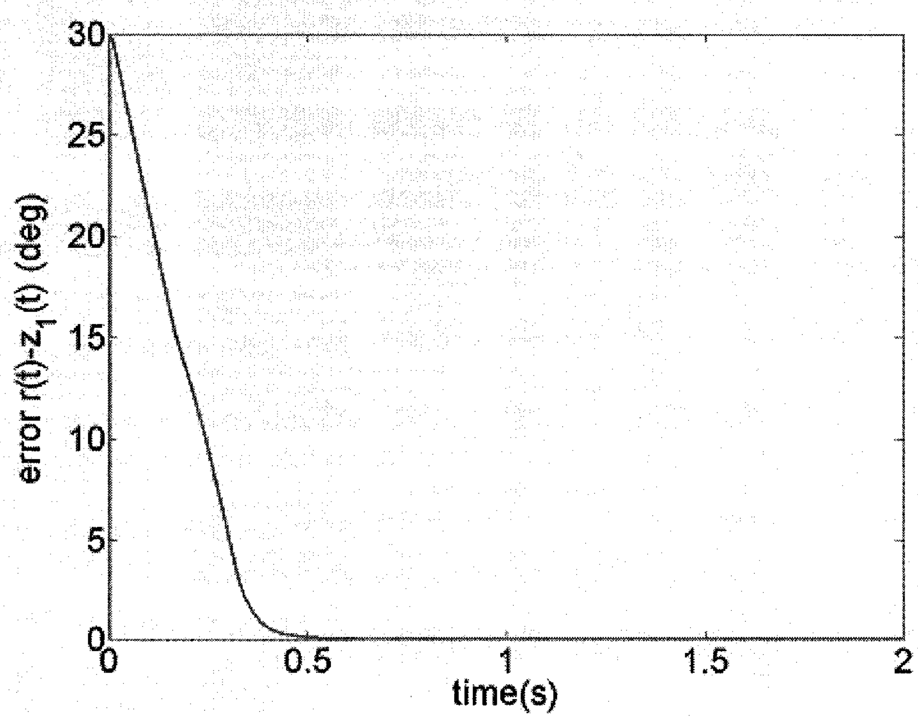

Figure 4-7 Output error of LPV delta wing model response to a step input

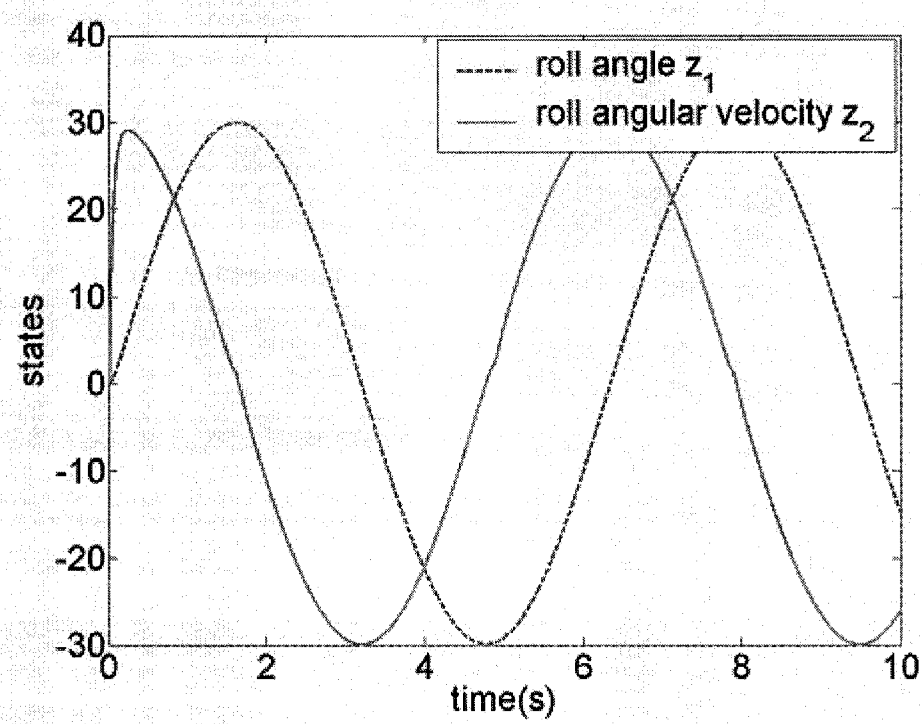

Figure 4-8 States of LPV delta wing model response to a step input

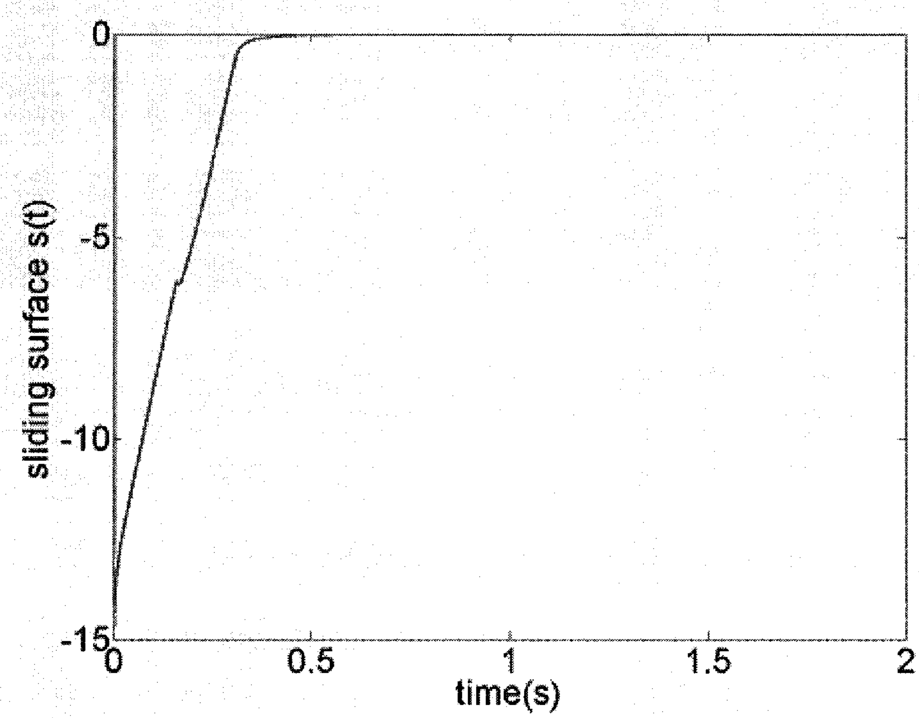

Figure 4-9 Sliding surface of LPV delta wing model response to a step input

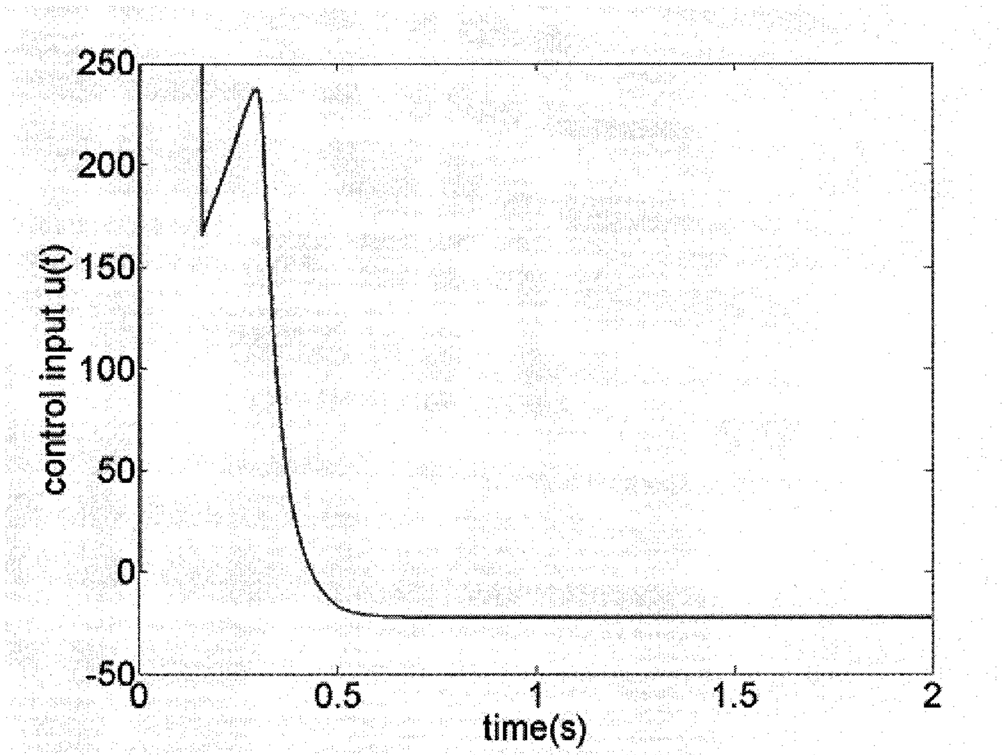

Figure 4-10 Control input of LPV delta wing model response to a step input

The simulation results show that the controller can track the step input very fast and the steady state error is zero. Then, we choose a sinusoid input

$$r(t) = 30\sin(t) \tag{160}$$

The following are the simulation results for the output, output error, states, sliding surface and control input of closed-loop system for the sinusoidal reference signal.

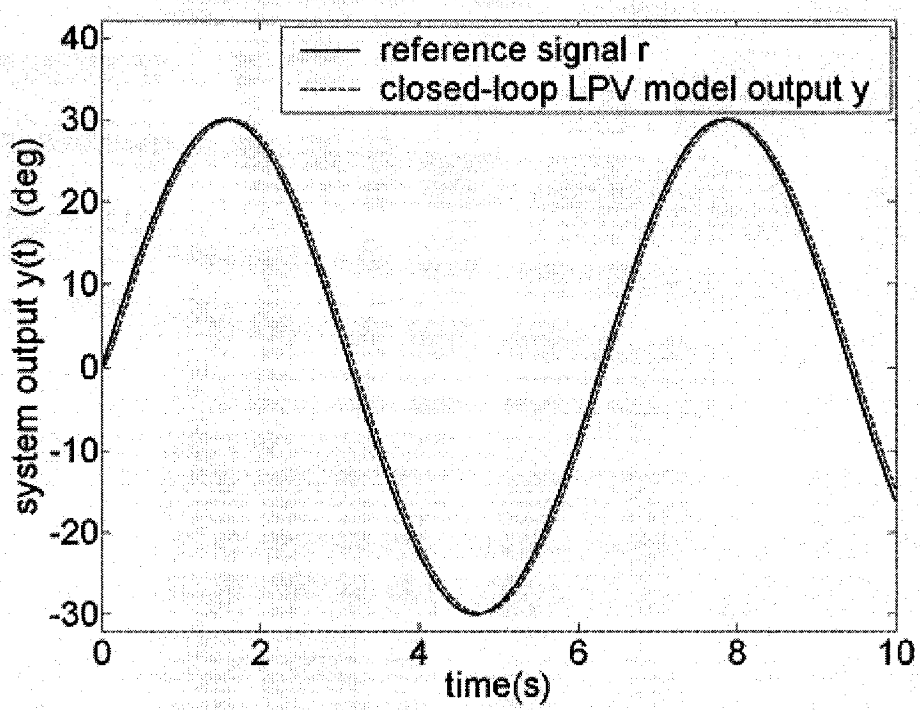

Figure 4-11 Output of LPV delta wing model response to a sinusoidal input

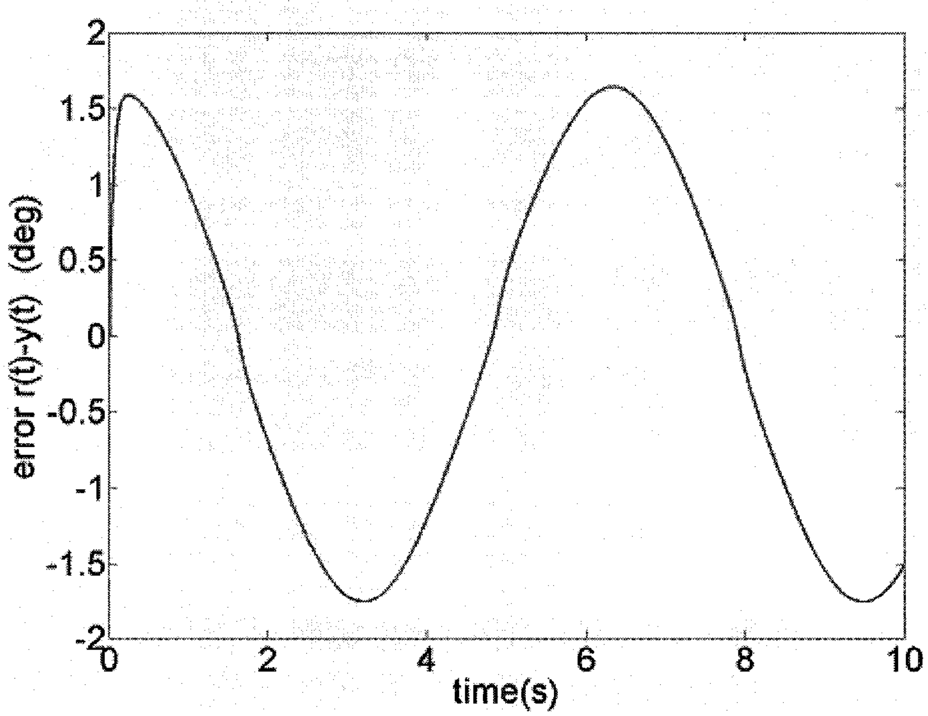

Figure 4-12 Output error of LPV delta wing model response to a sinusoidal input

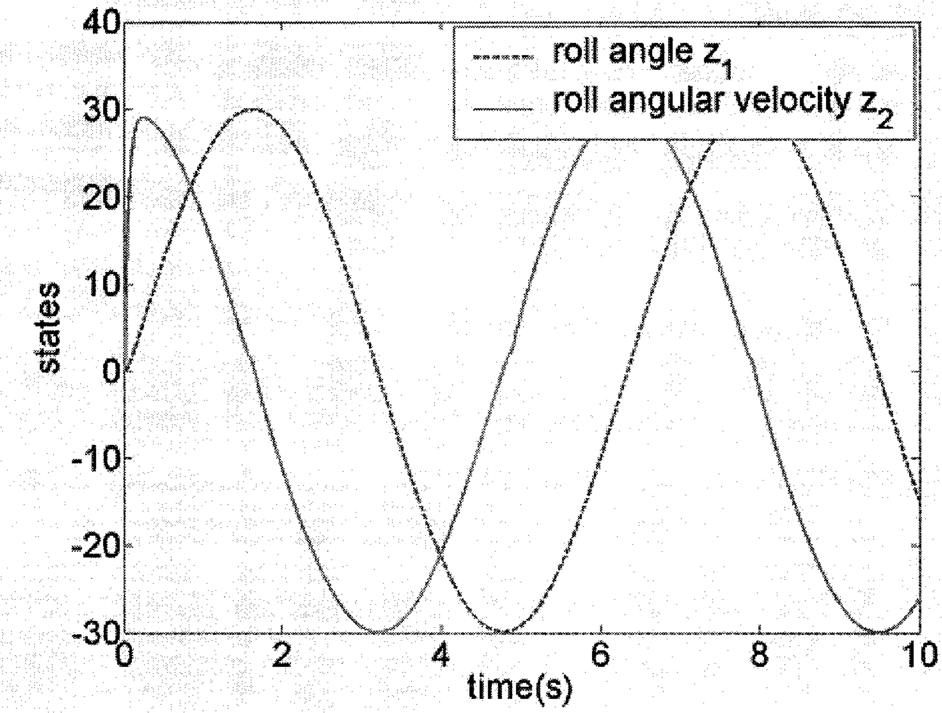

Figure 4-13 States of LPV delta wing model response to a sinusoidal input

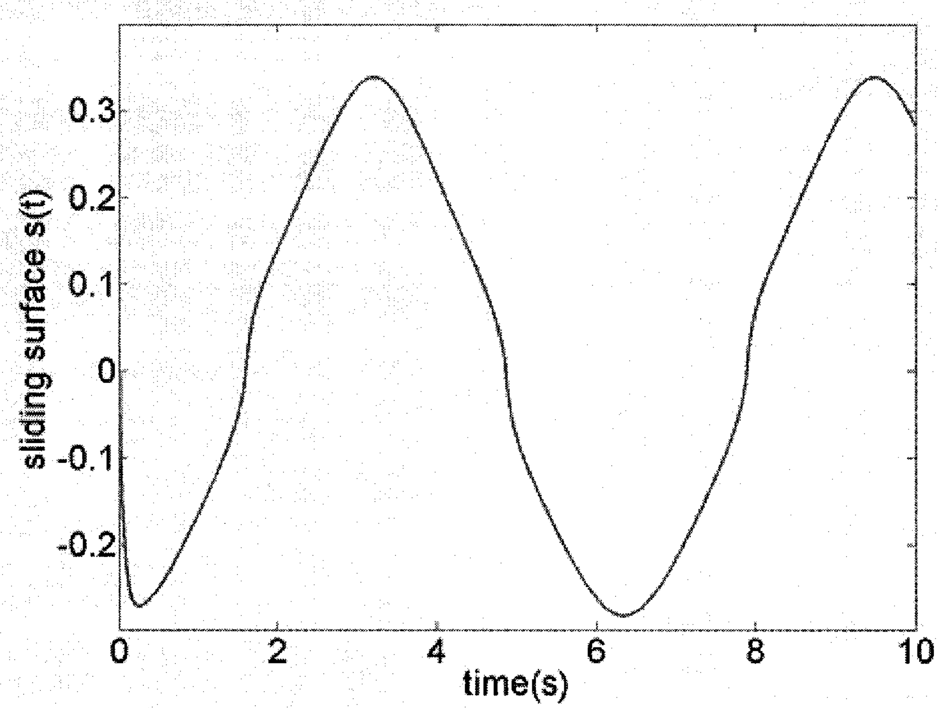

Figure 4-14 Sliding surface of LPV delta wing model response to a sinusoidal input

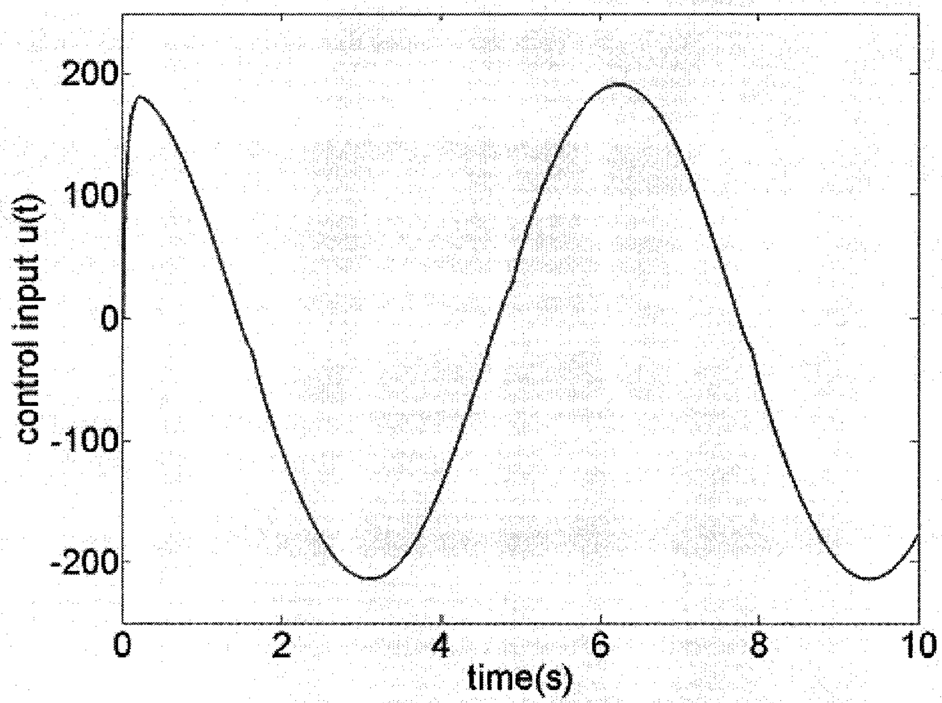

Figure 4-15 Control input of LPV delta wing model response to a sinusoidal input

The response to a sinusoidal input proves that the controller can track different reference input and achieve a good performance.

Secondly, we use the LPVSMC design procedure, and we implement it with a fixed parameter (the average parameter value).

$$m_{average} = \frac{m_{max} + m_{min}}{2} \tag{161}$$

Then, we compare between the LPVSMC and fixed parameter SMC with the initial values of roll angle and angular velocity of delta wing systems as

$$\begin{aligned} \mathbf{z}_1 &= 26\,\deg \\ \mathbf{z}_2 &= 0\,\deg/\sec \end{aligned} \tag{162}$$

Supposing the maximum of control input to be equal and choosing $k = 300$ and $\varepsilon = 0.05$, the following simulation results can prove our approach can achieve better performances than the SMC with the fixed parameters.

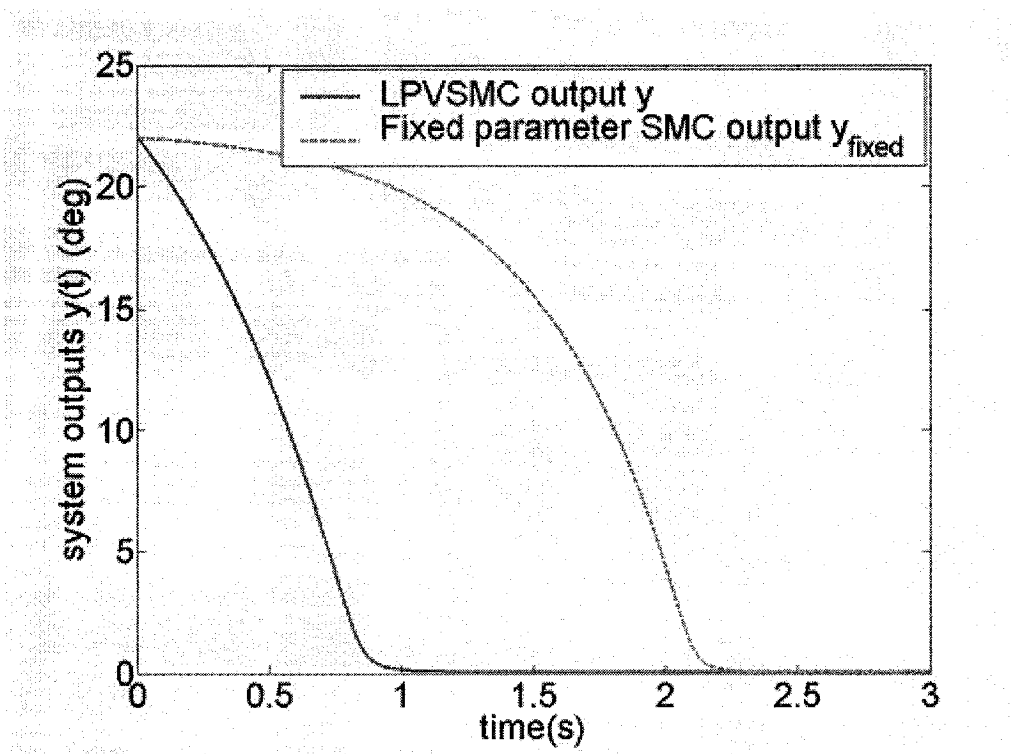

Figure 4-16 Outputs of LPVSMC and fixed parameter SMC

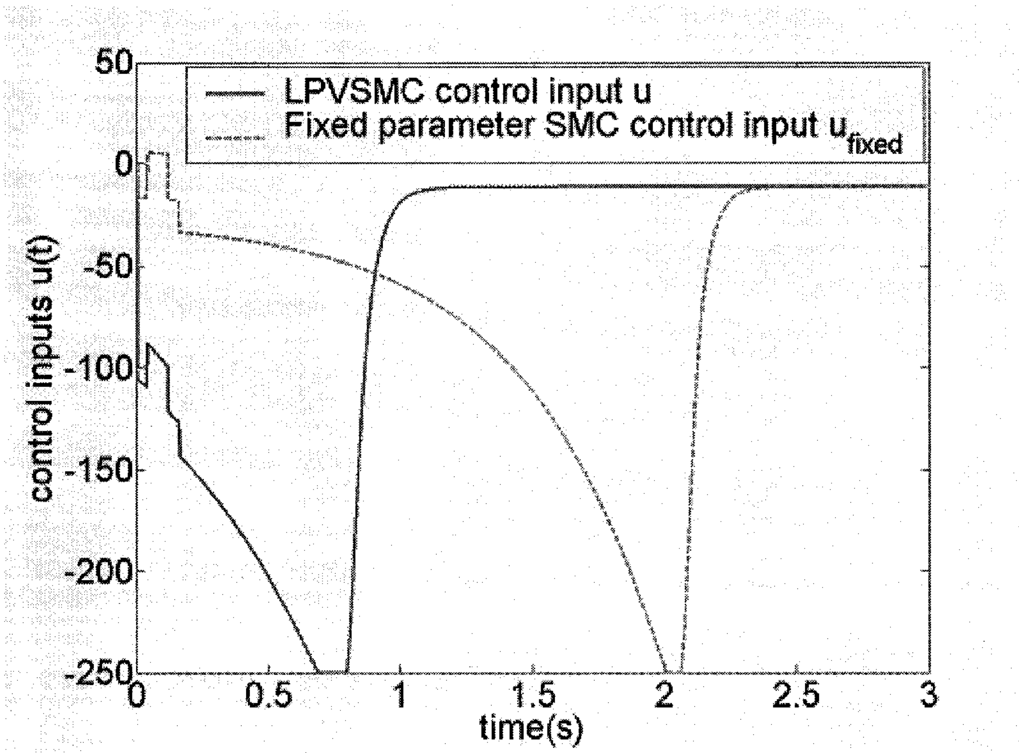

Figure 4-17 Control inputs of LPVSMC and fixed parameter SMC

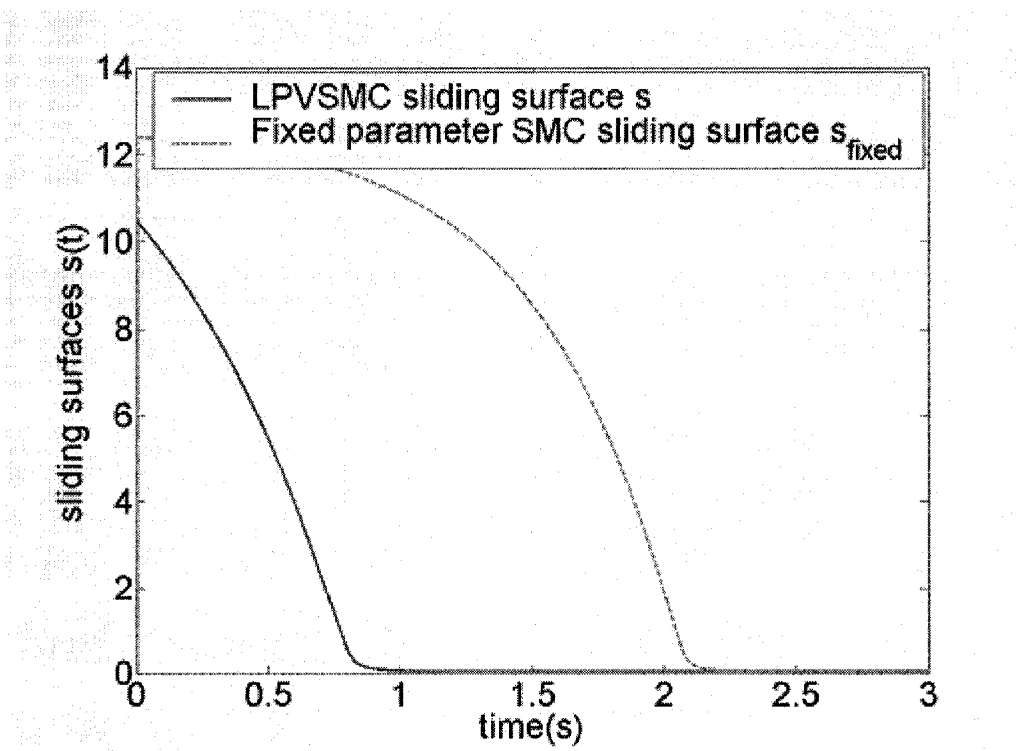

Figure 4-18 Sliding surfaces of LPVSMC and fixed parameter SMC

The simulation results show that the LPV sliding mode controller can get a better regulation than the SMC with the fixed parameters. It provides evidence that an LPVSMC, which consider the system time-varying parameters, is a suitable method for an LPVTDS control. By choosing different initial values of roll angles, we find out that the system with linear parameter-varying sliding mode controller is stable in the range of

$$-35 \sim 32\,\mathrm{deg} \tag{163}$$

when the initial roll angular velocity is zero. Moreover, the range of fixed parameter SMC system is

$$-24 \sim 22\,\mathrm{deg} \tag{164}$$

which is less than the stable range of LPVSMC approach.

A comparison was also attempted between the LPVSMC approach and the SMC approach in [14]. However, the LMI of Gouaisbaut's Theorem 4 for the delta wing systems are not feasible, so the approach cannot synthesize a stable controller for the delta wing problem.

To conclude the investigation, the LPVSMC controller was tested on the full nonlinear vortex-coupled model of delta wing systems given by (58). The following simulation shows the closed loop system response to the following step input

$$\begin{cases} r(t) = 0 & t < 0 \\ r(t) = 30 & t \geq 0 \end{cases} \tag{165}$$

From the simulation results (see Figures 4-19 and 4-20), the control performance for the nonlinear system is comparable or even better than for the quasi-LPV model (Figure 4-6 and Figure 4-10). This indicates the approach is also effective for the original nonlinear system.

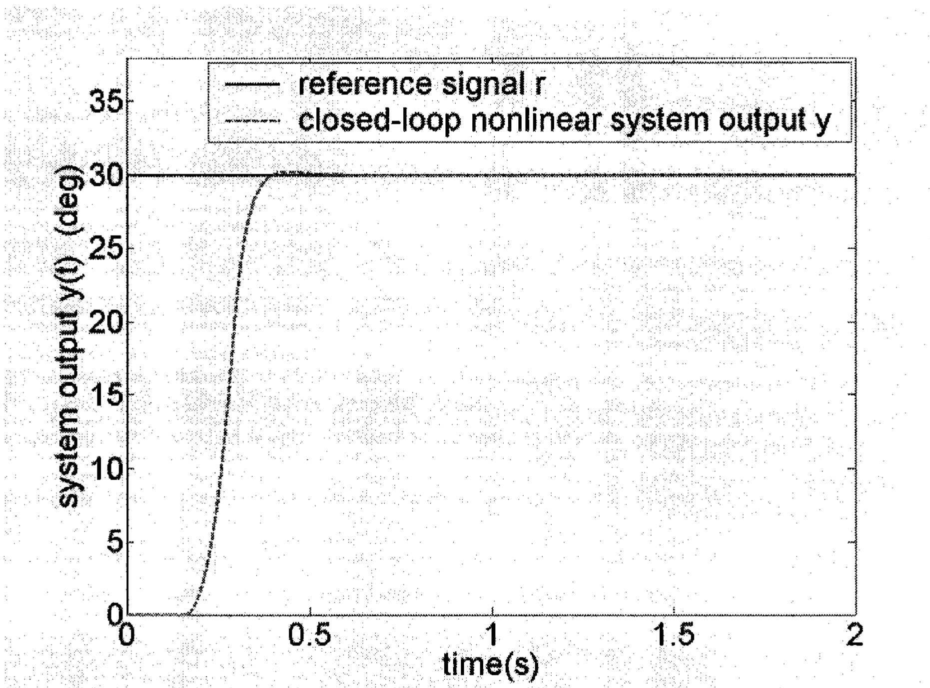

Figure 4-19 Output of nonlinear delta wing system response to a step input

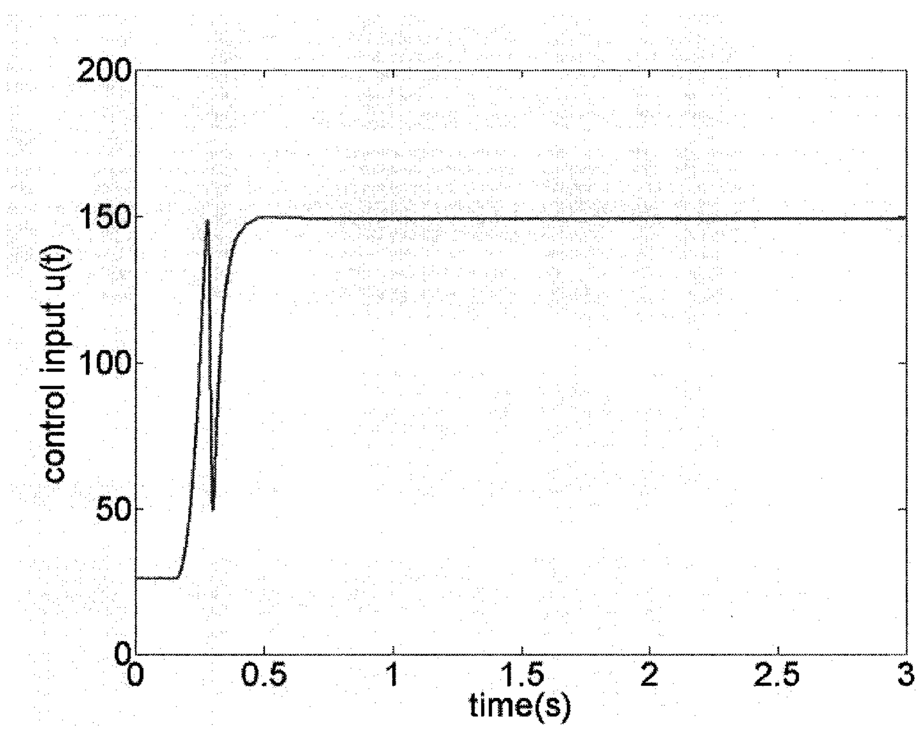

Figure 4-20 Control input of nonlinear delta wing system response to a step input

From the simulation results above, it is apparent that the linear parameter-varying sliding mode controller works effectively to control delta wing systems. The simulations show that the controller performs well for step and sinusoidal references in a stable manner with good performance. It is also evident that the LPVSMC approach is less conservation than fixed parameter SMC and Gouaisbaut's SMC approach.

To sum up, a LPV multiple time-delay model is construct for the vortex-coupled delta wing system. In the following, a controller is synthesized based on the systemic design procedure that is developed in chapter 3. All the simulations prove that the LPV sliding mode controller can implement the tracking of reference signal and regulation of the output with a good performance.

Chapter 5

Conclusions and Future Work

In this thesis a new LPVSMC synthesis approach for LPVTDS is developed that combines SMC theory, LPV control theory, and time delay stability analysis. The main original contributions of this thesis are as follows:

1) A new LPVSMC synthesis procedure for LPVTDS

A linear parameter-varying sliding surface is proposed to achieve the requirement of tracking or regulation. Using this surface a parameter-dependent Lyapunov-Krasovskiĭ functional analysis is used to guarantee asymptotic stability of the closed-loop system. The time-varying controller parameters are calculated from a set of LMIs, which can be readily solved using LMI solvers such as YALMIP, SeDuMi, or LMITool. Furthermore, the results are extended to the more general case of multiple time delay systems. This original contribution represents the first approach for LPV based SMC of time delay systems.

2) A new multiple time delay LPV model for vortex-coupled delta wing systems

This model is developed based on an approximation of an NIRISS representation of vortex-coupled dynamics proposed in the literature. This model is characterized by time-varying nonlinear terms and complex time-delayed components. Through curve fitting of the various coefficients and delay terms a new LPV description is developed. It is shown that the LPV model agrees closely with the full nonlinear model representation. This new LPV model can be used to develop and test new LPV, LPVSMC, and other nonlinear control methods. This work represents the first LPV based model for vortex coupled delta wing systems.

3) Application of the LPVSMC method to vortex-coupled delta wing systems

The LPVSMC approach is applied to an LPV representation of vortex-coupled delta wing system dynamics. The simulation results demonstrate that the LPVSMC provides improved stability and performance compared to SMC approaches without parameter variation. It is also demonstrated that the LPVSMC approach is less conservation than fixed parameter SMC and Gouaisbaut's SMC approach. Furthermore, it is shown from the simulation results that the LPVSMC performance for the nonlinear system is comparable or even better than for the LPV model. This indicates the approach is also effective for the original nonlinear system dynamics. The approach presented is one of the first applications of nonlinear control for vortex-coupled delta wing systems.

Future Work

Since the LPVSMC controller coefficients depend directly on parameters to be measured or estimated online, it is anticipated that filtering methods to deal with parameter measurement noise or rapid parameter variations might be necessary in the future. Modification of the method for digital control implementation might also be needed for certain applications. Another future work is to provide a more rigorous analysis of the robustness properties of the LPVSMC approach, since one of the advantages of SMC is to achieve robustness and disturbance rejection [56]. The robustness investigation can be divided into two steps: the robustness of the attraction of sliding surface and the robustness on the sliding surface. Generalization of the approach to remove the other assumptions used in this thesis should also be investigated. Finally, it is anticipated that this method will lead to significant improvement over existing SMC approaches in aerospace and automotive applications with parameter variations. The new method should be applied to such applications to get more experience and help guide the improvement of the method in the future.

REFERENCES

[1] Apkarian, Pierre and Adams, J. Richard, "Advanced Gain-Scheduling Techniques for Uncertain Systems," *IEEE Transactions on Control Systems Technology,* Vol. 6(1), pp. 21-32, January 1998.

[2] Apkarian, Pierre, Gahinet, Pascal and Becker, Greg, "Self-Scheduled $\mathbf{H}_\infty$ Control of Linear Parameter-Varying Systems: a Design Example," *Automatica,* Vol. 31(9), pp. 1251-1261, 1995.

[3] Boyd, Stephen, Ghaoui, Laurent El, Feron, Eric and Balakrishnan, Venkataramanan, "Linear Matrix Inequalities in System and Control Theory," Society for Industrial and Applied Mathematics (SIAM), Philadelphia, Pennsylvania, 1994.

[4] Boyd, Stephen and Vandenberghe, Lieven, "Convex Optimization," Cambridge University Press, Cambridge, United Kingdom, 2004.

[5] Brogan, William L., "Modern Control Theory," Third Edition, Prentice-Hall Inc., Englewood Cliffs, New Jersey, 1991.

[6] Bruzelius, F., Breitholtz, C. and Pettersson S., "LPV-Based Gain Scheduling Technique Applied to a Turbo Fan Engine Model," Proceedings of the 2002 IEEE International Conference on Control Applications, Glasgow, Scotland, U.K., September 2002.

[7] Chen, Wu-Hua, Guan, Zhi-Hong and Lu, Xiaomei, "Delay-dependent Output Feedback Guaranteed Cost Control for Uncertain Time-Delay Systems," *Automatica*, Vol. 40, pp. 1263-1268, 2004.

[8] DeCarlo, R. A., Żak, S. H. and Drakunov, S. V., "Variable Structure, Sliding-Mode Controller Design," The Control Handbook, pp. 941-951, CRC Press, New York, NY, 1996.

[9] Feng, Yong, Yu, Xing Hou and Man, Zhi Hong, "Non-Singular Terminal Sliding Mode Control of rigid Manipulators," *Automatica*, Vol. 38, pp. 2159-2167, 2002.

[10] Fridman, Emilia and Shaked, Uri, "Parameter Dependent Stability and Stabilization of Uncertain Time-Delay Systems," *IEEE Transactions on Automatic Control,* Vol. 48(5), May 2003.

[11] Fridman, Emilia and Shaked, Uri, "An Improved Stabilization Method for Linear Time-Delay Systems," *IEEE Transactions on Automatic Control,* Vol. 47(11), November 2002.

[12] Gordon, W. Brandon and Liu, W. Wei, "Report No. 2, Flow Model Development and simulation -Innovative Methods of Flight Control by Manipulation of the Flow Structure," Technical Report, March 2004.

[13] Gordon, W. Brandon and Liu, W. Wei, "Report No. 1, Flow Model Development and Simulation -Innovative Methods of Flight Control by Manipulation of the Flow Structure," Technical Report, December 2003.

[14] Gouaisbaut, F., Dambrine, M. and Richard, J. P., "Robust Control of Delay Systems: a Sliding Mode Control Design via LMI," *Systems & Letters*, 46 pp. 219-230, 2002.

[15] Gujjula, Sushma and Singh, Sahjendra N., "Variable Structure Control of Unsteady Aeroelastic System with Partial State Information," *Journal of Guidance, control, and Dynamics*, Vol. 28(3), pp. 568-573, 2005.

[16] He, Yong, Wu, Min, She, Jin Hua and Liu, Guo Ping, "Parameter-Dependent Lyapunov Function for Stability of Time-Delay Systems with Polytopic-Type Uncertainties," *IEEE Transactions on Automatic Control,* 49(5), May 2004.

[17] Hess, R. A. and Wells, S. R., "Sliding Mode Control Applied to Reconfigurable Flight Control Design," *Journal of Guidance, control, and Dynamics*, Vol. 26(3), pp. 733-739, 2002.

[18] Hu, J., Chu, J. and Su, H., "SMVSC for a Class of Time-Delay Uncertain Systems with Mismatching Uncertainties," *IEEE Transactions on Control Theory & Applications,* Vol. 147(6), 2000.

[19] Huang, Xing. Z., "Experimental Investigation of Leading-Edge Vortex Control via Microactuators," presentation in 'Missile Flight Control using Micro-actuated Flow Effectors' meeting, DRDC Valcartier TN 2004-066, May 2004

[20] Huang, Xing. Z., "Non-Linear Indicial Response and Internal State-Space (NIRISS) Representation and Its Application on Delta Wing Configurations," RTO Technical Report, RTO-TR-047, 2002.

[21] Huang, Xing. Z., Lou, H. Y. and Hanff, E. S., "Non-Linear Indicial Response and Internal State-Space Representation for Free-to-Roll Trajectory Prediction of a 65° Delta Wing at High Incidence," *AIAA Paper* 2002-4713, 2002.

[22] Huang, Xing. Z., Sun, Y.Z and Hanff, E. S., "Circulation Criterion to Predict Leading-Edge Vortex Breakdown Over Delta Wings," *AIAA Paper* 1997-2265, 1997.

[23] Ikeda, Masao and Ashida, Tomonori, "Stabilization of Linear Systems with Time-Varying Delay," *IEEE Transactions on Automatic Control,* Vol. 24(2), pp. 360-370, 1979.

[24] Kharitonov, V. L. and Zhabko, A. P., "Lyapunov-Krasovskiĭ Approach to the Robust Stability Analysis of Time-Delay Systems," *Automatica*, Vol. 39(1), pp. 15-20, 2003.

[25] Krasovskiĭ, N. N., "Stability of Motion: Application of Lyapunov's Second Method to Differential Systems and Equations with Delay," Stanford University Press, 1963.

[26] Lee, Joon Hwa, Kim, Sang Woom and Kwon, Wook Hyun, "Memoryless $\mathbf{H}_\infty$ Controllers for State Delayed Systems," *IEEE Transactions on Automatic Control,* Vol. 39(1), pp. 159-162, 1994.

[27] Lee, Jung Hoon and Youn, Myung Joong, "A New Improved Continuous Variable Structure Controller for Accurately Prescribed Tracking Control of BLLDD Servo Motors," *Automatica*, Vol. 40, pp. 2069-2074, 2004.

[28] Li, Xiao qiu and DeCarlo, R. A., "Memoryless Sliding Mode Control of Uncertain Time-Delay System," Proceedings of the American Control Conference, Arlington, VA, June, 2001.

[29] Lind, Rick, "Linear Parameter-Varying Modelling and Control of Structural Dynamics with Aerothermoelastic Effects," *Journal of Guidance, control, and Dynamics*, Vol. 25(4), pp. 733-739, 2002.

[30] Mackenroth, Uwe, "Robust Control Systems Theory and Case Studies," Springer-Verlag Berlin Heidelberg, Germany, 2004.

[31] Marcos, Andrés and Balas, Gary J, "Development of Linear-Parameter-Varying Models for Aircraft," *Journal of Guidance, control, and Dynamics*, Vol. 27(2), pp. 218-228, 2004.

[32] Moon, Young Soo, Park, Pogyeon, Kwon, Wook Hyun and Lee, Young Sam, "Delay-Dependent Robust Stabilization of Uncertain State-delayed Systems," *International Journal of Control*, Vol. 74(14), pp. 1447-1455, 2001.

[33] Park, Poo Gyeon, "A Delay-Dependent Stability Criterion for Systems with Uncertain Time-Invariant Delays," *IEEE Transactions on Automatic Control,* Vol. 44(4), pp. 876-877, 1999.

[34] Perruquetti, Wilfrid and Barbot, Pierre Jean, "Sliding Mode Control in Engineering," Marcel Dekker Inc., New York, 2002.

[35] Phoojaruenchanachai, Suthee and Furuta, Katsuhisa, "Memoryless Stabilization of Uncertain Linear Systems Including Time-Varying State Delays," *IEEE Transactions on Automatic Control,* Vol. 37(7), pp. 1022-1023, 1992.

[36] Pisano, Alessandro and Usai, Elio, "Output-Feedback Control of an Underwater Vehicle Prototype by Higher-Order Sliding Modes," *Automatica*, Vol 40, pp. 1525-1531, 2004.

[37] Powly, A. A. and Bhat, M. Seetharama, "Missile Autopilot Design Using Discrete-Time Variable Structure Controller with Sliding Sector," *Journal of Guidance, control, and Dynamics*, Vol. 27(4), pp. 634-646, 2004.

[38] Richard, Jean Piere, "Time-Delay Systems: an Overview of Some Recent Advances and Open Problems," *Automatica*, Vol. 39, pp. 1667-1694, 2003.

[39] Roh, Young Hoon and Oh, Jun Ho, "Robust Stabilization of Uncertain Input-Delay Systems by Sliding Mode Control with Delay Compensation," *Automatica*, Vol. 35, pp. 1861-1865, 1999.

[40] Rugh, J. Wilson and Shamma, S. Jeff, "Research on Gain Scheduling," *Automatica*, Vol. 36, pp. 1401-1425, 2000.

[41] Shamma, S. Jeff and Athans, Michael, "Guaranteed Properties of Gain Scheduled Control for Linear Parameter-Varying Plants," *Automatica*, Vol. 27(3), pp 559-564, May 1991.

[42] Shin, J. and Belcastro C, "Quasi-Linear Parameter Varying Representation Over Non-Trim Region," AIAA Guidance, Navigation, and Control Conference and Exhibit, Rhode Island, AIAA-2004-5423, August 2004.

[43] Sivrioglu, Selim and Nonami, Kenzo, "Sliding Mode Control With Time-Varying Hyperplane for AMB Systems," *IEEE Transactions on Mechatronics,* Vol. 3(1), pp. 51-59, 1998.

[44] Shyu, Kuo Kai, Liu, Wen Jeng and Hsu, Kou-Chen, "Design of Large-Scale Time-Delayed Systems with Dead-Zone Input via Variable Structure Control," *Automatica*, Vol. 41(7), pp. 1239-1246, 2005.

[45] Slotine, Jean Jacques and Li, Wei Ping, "Applied Nonlinear Control," Prentice Hall, Englewood Cliffs, New Jersey, 1991.

[46] Song, Young Sam, Kwon, Sung Ha, Park, Seung Kyu, Oh, Do-Chang and Jeung, Eun Tae, "Sliding Mode Control for Time-Delay System Using a Virtual State," Proceedings of the American Control Conference, Arlington, VA, June 2001.

[47] Tan, K., Grigoriadis, K. M. and Wu, F., "$\mathbf{H}_\infty$ and $\mathbf{L}_2$-to-$\mathbf{L}_\infty$ Gain Control of Linear Parameter-Varying Systems with Parameter-Varying Delays," *IEEE Proceedings: Control Theory and Applications*, Vol. 150(5), pp. 509-517, January 1998.

[48] Tan, Weehong, Packard, K. Andrew and Balas, J. Gary, "Quasi-LPV Modelling and LPV Control of a Generic Missile," Proceedings of the American Control Conference, Chicago, Illinois, June 2000.

[49] Wang, Jun Ling and Wang, Chang Hong, "Delay-dependent $\mathbf{H}_\infty$ Control for LPV Systems with Mixed Time-Varying Delays," Proceedings of the 3rd International Conference on Machine Learning and Cybernetics, Shanghai, August, 2004.

[50] Wu, Fen and Grigoriadis, Karolos M., "LPV Systems with Parameter-Varying Time Delays: Analysis and Control," *Automatica*, Vol. 37(2), pp. 221-229, 2001.

[51] Wu, Fen and Grigoriadis, Karolos M., "LPV Systems with Parameter-Varying Time Delays," Proceedings of the 36th Conference on Decision and Control, San Diego, California, USA, December 1997.

[52] Wu, Min, He, Yong, She, Jin Hua and Liu, Guo Ping, "Delay-Dependent Criteria for Robust Stability of Time-Varying Delay Systems," *Automatica*, Vol. 40(8), pp. 1435-1439, 2004.

[53] Xu, Haojian, Mirmirani, Maj. D. and Ioannou, Petros A., "Adaptive Sliding Mode Control Design for a Hypersonic Flight Vehicle," *Journal of Guidance, control, and Dynamics*, Vol. 27(5), pp. 829-838, 2004.

[54] Yang, Ming, Gordon, W. Brandon and Rabbath, C. A., "Dynamic Modelling and Linear Parameter-varying Control of Vortex Coupled Delta Wing Systems," to be submitted to the *AIAA Journal of Guidance, Control and Dynamics*, 2005.

[55] Yang, Ming and Gordon, W. Brandon, "Report No. 1, Survey of Linear Parameter-Varying Control Methods-Dynamic Modelling, Stability, and Performance of Linear Parameter-Varying Systems," Technical Report, October 2004.

[56] Young, K. David, Utkin, I. Vadim and Özgüner, Ümit, "A Control Engineer's Guid to Sliding Mode Conrol," *IEEE Transactions on Control Systems Technology*, Vol. 7(3), pp. 328-342, May, 1999.

[57] Young, K. David and Özgüner, Ümit, "Frequency Shaping Compensator Design for Sliding Mode Control," *International Journal of Control*, Vol. 57(5), pp. 105-1019, 1993.

[58] Young, K. David, "Controller Design for a Manipulator Using Theory of Variable Structure Systems," *IEEE Transactions on Systems, Man and Cybernetics*, Vol. 8, pp. 101-109, 1978.

[59] Zhang Xian Ming, Wu, Min, She, Jin-Hua and He, Yong, "Delay-dependent Stabilization of Linear Systems with Time-Varying State and Input Delays," *Automatica*, Vol. 41(8), pp. 1405-1412, 2005.

[60] Zhou, Kemin and Doyle, John C., "Essentials of Robust Control," Prentice Hall, Upper Saddle River, New Jersey, 1998.

[61] http://control.ee.ethz.ch/~joloef/yalmip.php.

APPENDIX A

Proof of Lemma 2. From the Leibniz-Newton formula

$$\mathbf{x}(t)-\mathbf{x}(t-h)-\int_{t-h}^{t}\dot{\mathbf{x}}(s)ds=\mathbf{0} \tag{166}$$

, the following equation holds for any $\mathbf{N}_1(\cdot),\mathbf{N}_2(\cdot)\in \mathbb{R}^{n\times n}$:

$$\begin{aligned}
&2\left[\mathbf{x}^T(t)\mathbf{N}_1^T(t)+\mathbf{x}^T(t-h)\mathbf{N}_2^T(t)\right]\times\left[\mathbf{x}(t)-\mathbf{x}(t-h)-\int_{t-h}^{t}\dot{\mathbf{x}}(s)ds\right]=\mathbf{0}\\
&\Rightarrow 2\begin{bmatrix}\mathbf{x}(t)\\ \mathbf{x}(t-h)\end{bmatrix}^T\begin{bmatrix}\mathbf{N}_1^T(t) & -\mathbf{N}_1^T(t)\\ \mathbf{N}_2^T(t) & -\mathbf{N}_2^T(t)\end{bmatrix}\begin{bmatrix}\mathbf{x}(t)\\ \mathbf{x}(t-h)\end{bmatrix}-2\int_{t-h}^{t}\begin{bmatrix}\mathbf{x}(t)\\ \mathbf{x}(t-h)\end{bmatrix}^T\begin{bmatrix}\mathbf{N}_1^T(t)\\ \mathbf{N}_2^T(t)\end{bmatrix}\dot{\mathbf{x}}(s)ds=\mathbf{0}
\end{aligned} \tag{167}$$

Applying **Lemma 1** with $\mathbf{a}=[\mathbf{x}(t)\quad \mathbf{x}(t-h)]$, $\mathbf{b}=\dot{\mathbf{x}}(s)$ and any bounded matrix function $\mathbf{X}(\cdot)\in \mathbb{R}^{2n\times 2n}$:

$$\begin{aligned}
&-2\int_{t-h}^{t}\begin{bmatrix}\mathbf{x}(t)\\ \mathbf{x}(t-h)\end{bmatrix}^T\begin{bmatrix}\mathbf{N}_1^T(t)\\ \mathbf{N}_2^T(t)\end{bmatrix}\dot{\mathbf{x}}(s)ds\\
&\le\int_{t-h}^{t}\begin{bmatrix}\mathbf{x}(t)\\ \mathbf{x}(t-h)\\ \dot{\mathbf{x}}(s)\end{bmatrix}^T\begin{bmatrix}\mathbf{X}(t) & \mathbf{Y}(t)-[\mathbf{N}_1(t)\quad \mathbf{N}_2(t)]\\ \mathbf{Y}^T(t)-[\mathbf{N}_1(t)\quad \mathbf{N}_2(t)]^T & \mathbf{Z}(s)\end{bmatrix}\begin{bmatrix}\mathbf{x}(t)\\ \mathbf{x}(t-h)\\ \dot{\mathbf{x}}(s)\end{bmatrix}ds\\
&=-\int_{t-h}^{t}\dot{\mathbf{x}}^T(s)\mathbf{Z}(s)\dot{\mathbf{x}}^T(s)ds-2\begin{bmatrix}\mathbf{x}(t)\\ \mathbf{x}(t-h)\end{bmatrix}^T\begin{bmatrix}\mathbf{N}_1^T(t) & -\mathbf{N}_1^T(t)\\ \mathbf{N}_2^T(t) & -\mathbf{N}_2^T(t)\end{bmatrix}\begin{bmatrix}\mathbf{x}(t)\\ \mathbf{x}(t-h)\end{bmatrix}\\
&\quad+\begin{bmatrix}\mathbf{x}(t)\\ \mathbf{x}(t-h)\end{bmatrix}^T 2\mathbf{Y}(t)^T[\mathbf{I}\quad -\mathbf{I}]\begin{bmatrix}\mathbf{x}(t)\\ \mathbf{x}(t-h)\end{bmatrix}+h\begin{bmatrix}\mathbf{x}(t)\\ \mathbf{x}(t-h)\end{bmatrix}^T\mathbf{X}(t)\begin{bmatrix}\mathbf{x}(t)\\ \mathbf{x}(t-h)\end{bmatrix}
\end{aligned} \tag{168}$$

with

$$\begin{bmatrix} \mathbf{X}(t) & \mathbf{Y}(t) \\ (*) & \mathbf{Z}(s) \end{bmatrix} \geq \mathbf{0} \tag{169}$$

After simple rearrangement, the following inequality can be obtained

$$\begin{aligned} \mathbf{0} &= 2\begin{bmatrix} \mathbf{x}(t) \\ \mathbf{x}(t-h) \end{bmatrix}^T \begin{bmatrix} \mathbf{N}_1^T(t) & -\mathbf{N}_1^T(t) \\ \mathbf{N}_2^T(t) & -\mathbf{N}_2^T(t) \end{bmatrix} \begin{bmatrix} \mathbf{x}(t) \\ \mathbf{x}(t-h) \end{bmatrix} - 2\int_{t-h}^{t} \begin{bmatrix} \mathbf{x}(t) \\ \mathbf{x}(t-h) \end{bmatrix}^T \begin{bmatrix} \mathbf{N}_1^T(t) \\ \mathbf{N}_2^T(t) \end{bmatrix} \dot{\mathbf{x}}(s)ds \\ &\leq -\int_{t-h}^{t} \dot{\mathbf{x}}^T(s)\mathbf{Z}(s)\dot{\mathbf{x}}^T(s)ds + \begin{bmatrix} \mathbf{x}(t) \\ \mathbf{x}(t-h) \end{bmatrix}^T 2\mathbf{Y}^T(t)[\mathbf{I} \quad -\mathbf{I}] \begin{bmatrix} \mathbf{x}(t) \\ \mathbf{x}(t-h) \end{bmatrix} + h\begin{bmatrix} \mathbf{x}(t) \\ \mathbf{x}(t-h) \end{bmatrix}^T \mathbf{X}(t) \begin{bmatrix} \mathbf{x}(t) \\ \mathbf{x}(t-h) \end{bmatrix} \end{aligned} \tag{170}$$

Thus,

$$-\int_{t-h}^{t} \dot{\mathbf{x}}^T(s)\mathbf{Z}(s)\dot{\mathbf{x}}^T(s)ds \leq \begin{bmatrix} \mathbf{x}(t) \\ \mathbf{x}(t-h) \end{bmatrix}^T 2\mathbf{Y}^T(t)[\mathbf{I} \quad -\mathbf{I}] \begin{bmatrix} \mathbf{x}(t) \\ \mathbf{x}(t-h) \end{bmatrix} + h\begin{bmatrix} \mathbf{x}(t) \\ \mathbf{x}(t-h) \end{bmatrix}^T \mathbf{X}(t) \begin{bmatrix} \mathbf{x}(t) \\ \mathbf{x}(t-h) \end{bmatrix} \tag{171}$$

By defining

$$\mathbf{Y}(\boldsymbol{\sigma}(t) = [\mathbf{Y}_1(t) \quad \mathbf{Y}_2(t)] \tag{172}$$

and

$$\begin{aligned} \mathbf{X}(\boldsymbol{\sigma}(t)) &= \mathbf{Y}^T(\boldsymbol{\sigma}(t)\mathbf{Z}^{-1}(\boldsymbol{\sigma}(t))\mathbf{Y}(\boldsymbol{\sigma}(t) \\ &= [\mathbf{Y}_1(\boldsymbol{\sigma}(t) \quad \mathbf{Y}_2(\boldsymbol{\sigma}(t)]\mathbf{Z}^{-1}(\boldsymbol{\sigma}(t))[\mathbf{Y}_1(\boldsymbol{\sigma}(t) \quad \mathbf{Y}_2(\boldsymbol{\sigma}(t)]^T \geq \mathbf{0} \end{aligned} \tag{173}$$

we obtain the following inequality

$$
\begin{aligned}
&-\int_{t-h}^{t}\dot{\mathbf{x}}^{T}(s)\mathbf{Z}(s)\dot{\mathbf{x}}^{T}(s)ds \\
&\leq\begin{bmatrix}\mathbf{x}(t)\\ \mathbf{x}(t-h)\end{bmatrix}^{T}2\begin{bmatrix}\mathbf{Y}_1^{T}(t)\\ \mathbf{Y}_2^{T}(t)\end{bmatrix}[\mathbf{I}\ \ -\mathbf{I}]\begin{bmatrix}\mathbf{x}(t)\\ \mathbf{x}(t-h)\end{bmatrix} \\
&\qquad +h\begin{bmatrix}\mathbf{x}(t)\\ \mathbf{x}(t-h)\end{bmatrix}^{T}\begin{bmatrix}\mathbf{Y}_1^{T}(t)\\ \mathbf{Y}_2^{T}(t)\end{bmatrix}\mathbf{Z}^{-1}(\sigma(t))\begin{bmatrix}\mathbf{Y}_1^{T}(t)\\ \mathbf{Y}_2^{T}(t)\end{bmatrix}^{T}\begin{bmatrix}\mathbf{x}(t)\\ \mathbf{x}(t-h)\end{bmatrix} \\
&=\begin{bmatrix}\mathbf{x}(t)\\ \mathbf{x}(t-h)\end{bmatrix}^{T}\begin{bmatrix}\mathbf{Y}_1^{T}(t)+\mathbf{Y}_1(t) & -\mathbf{Y}_1^{T}(t)+\mathbf{Y}_2(t)\\ -\mathbf{Y}_1(t)+\mathbf{Y}_2^{T}(t) & -\mathbf{Y}_2^{T}(t)-\mathbf{Y}_2(t)\end{bmatrix}\begin{bmatrix}\mathbf{x}(t)\\ \mathbf{x}(t-h)\end{bmatrix} \\
&\qquad +h\begin{bmatrix}\mathbf{x}(t)\\ \mathbf{x}(t-h)\end{bmatrix}^{T}\begin{bmatrix}\mathbf{Y}_1^{T}(t)\\ \mathbf{Y}_2^{T}(t)\end{bmatrix}\mathbf{Z}^{-1}(\sigma(t))\begin{bmatrix}\mathbf{Y}_1^{T}(t)\\ \mathbf{Y}_2^{T}(t)\end{bmatrix}^{T}\begin{bmatrix}\mathbf{x}(t)\\ \mathbf{x}(t-h)\end{bmatrix}
\end{aligned}
\tag{174}
$$

Also, we have

$$
\begin{bmatrix}\mathbf{X}(t) & \mathbf{Y}(t)\\ (*) & \mathbf{Z}(t)\end{bmatrix}=\begin{bmatrix}\mathbf{Y}(t)\mathbf{Z}^{-1}(t)\mathbf{Y}^{T}(t) & \mathbf{Y}(t)\\ \mathrm{Y}(*) & \mathbf{Z}(t)\end{bmatrix}=\begin{bmatrix}\mathbf{Y}(t)\mathbf{Z}^{-1/2}(t) & \mathbf{0}\\ \mathbf{Z}^{1/2}(t) & \mathbf{0}\end{bmatrix}\begin{bmatrix}\mathbf{Y}(t)\mathbf{Z}^{-1/2}(t) & \mathbf{0}\\ \mathbf{Z}^{1/2}(t) & \mathbf{0}\end{bmatrix}^{T}\geq\mathbf{0}
\tag{175}
$$

where

$$
\mathbf{Z}(t)=\mathbf{Z}^{T}(t)>\mathbf{0}
\tag{176}
$$

This completes the proof. □

APPENDIX B

Schur Complement. Supposing matrices $\mathbf{X} \in \boldsymbol{S}^{n_a}$, $\mathbf{Y} \in I\!R^{n_a \times n_b}$, $\mathbf{Z} \in \boldsymbol{S}^{n_b}$ and $\mathbf{W} \in \boldsymbol{S}^{n_a+n_b}$, the condition [3] and [4]

$$\mathbf{W}=\begin{bmatrix} \mathbf{X} & \mathbf{Y} \\ (*) & \mathbf{Z} \end{bmatrix} \leq \mathbf{0} \tag{177}$$

is equivalent to

$$\mathbf{Z} \leq \mathbf{0} \quad \text{and} \quad \mathbf{X} - \mathbf{Y}\mathbf{Z}^{-1}\mathbf{Y}^{T} \leq \mathbf{0} \tag{178}$$

where $(\mathbf{X} - \mathbf{Y}\mathbf{Z}^{-1}\mathbf{Y}^{T})$ is called the Schur complement of $\mathbf{X}$ in $\mathbf{W}$. Using Schur complement, we can convert nonlinear inequalities to LMIs.

APPENDIX C

Proof of Remark 2. Consider unforced LPV system with n time delays

$$\dot{\mathbf{z}}(t)=\mathbf{A}(\boldsymbol{\sigma}(t))\mathbf{z}(t)+\sum_{i=1}^{n}\left(\mathbf{A}_{hi}(\boldsymbol{\sigma}(t))\mathbf{z}(t-h_i)\right) \quad \boldsymbol{\sigma}(t)\in\Theta \tag{179}$$

Choose a parameter-dependent Lyapunov-Krasovskiĭ functional candidate as

$$V=V_1(\boldsymbol{\sigma}(t))+V_2(\boldsymbol{\sigma}(t))+V_3(\boldsymbol{\sigma}(t)) \tag{180}$$

where

$$\begin{aligned}
V_1(\boldsymbol{\sigma}(t),t)&=\mathbf{z}^T(t)\mathbf{P}(\boldsymbol{\sigma}(t))\mathbf{z}\\
V_2(\boldsymbol{\sigma}(t),t)&=\sum_{i=1}^{n}\int_{t-hi}^{t}\mathbf{z}^T(\theta)\mathbf{R}(\boldsymbol{\sigma}(\theta))\mathbf{z}(\theta)d\theta\\
V_3(\boldsymbol{\sigma}(t),t)&=\sum_{i=1}^{n}\int_{t-hi}^{t}\int_{s}^{t}\dot{\mathbf{z}}^T(\theta)\mathbf{Q}(\boldsymbol{\sigma}(\theta))\dot{\mathbf{z}}(\theta)d\theta ds
\end{aligned} \tag{181}$$

and $\mathbf{P}(\cdot),\mathbf{Q}(\cdot),\mathbf{R}(\cdot)\in\boldsymbol{S}^n$ are symmetric positive definite matrix functions with $\mathbf{P}(\cdot)>\mathbf{0}$, $\mathbf{Q}(\cdot)>\mathbf{0}$ and $\mathbf{R}(\cdot)>\mathbf{0}$. Calculating the derivative of V_1 along the trajectory of Equation (103) yields

$$\frac{dV_1}{dt}=\mathbf{z}^T\mathbf{A}^T\mathbf{P}\mathbf{z}+\sum_{i=1}^{n}\left(\mathbf{z}_{h_i}^T\mathbf{A}_{h_i}^T\mathbf{P}\mathbf{z}\right)+\mathbf{z}^T\mathbf{P}\mathbf{A}\mathbf{z}+\sum_{i=1}^{n}\left(\mathbf{z}^T\mathbf{P}\mathbf{A}_{h_i}\mathbf{z}_{h_i}\right)+\mathbf{z}^T\left(\sum_{i=1}^{s}\dot{\boldsymbol{\sigma}}_i\frac{\partial\mathbf{P}(\boldsymbol{\sigma}_i)}{\partial\boldsymbol{\sigma}_i}\right)\mathbf{z} \tag{182}$$

$\frac{dV_2}{dt}$ is represented as follows

$$\frac{dV_2}{dt}=\sum_{i=1}^{n}\left(\mathbf{z}^{T}\mathbf{R}\mathbf{z}-\mathbf{z}_{hi}^{T}\mathbf{R}_{hi}\mathbf{z}_{hi}\right) \tag{183}$$

and

$$\frac{dV_3}{dt}=\sum_{i=1}^{n}\left(\dot{\mathbf{z}}^{T}h_i\mathbf{Q}\dot{\mathbf{z}}\right)-\sum_{i=1}^{n}\left(\int_{t-h_i}^{t}\dot{\mathbf{z}}^{T}(s)\mathbf{Q}(\boldsymbol{\sigma}(s))\dot{\mathbf{z}}(s)ds\right) \tag{184}$$

By approximation the integral in the above equation and using **Lemma 2**,

$$-\int_{t-h_i}^{t}\dot{\mathbf{z}}^{T}(s)\mathbf{Q}(\boldsymbol{\sigma}(s))\dot{\mathbf{z}}(s)ds\leq\begin{bmatrix}\mathbf{z}\\ \mathbf{z}_{h_i}\end{bmatrix}^{T}\begin{bmatrix}\mathbf{Y}_1^T+\mathbf{Y}_1 & -\mathbf{Y}_1^T+\mathbf{Y}_2\\ (*) & -\mathbf{Y}_2^T-\mathbf{Y}_2\end{bmatrix}\begin{bmatrix}\mathbf{z}\\ \mathbf{z}_{h_i}\end{bmatrix}+h_i\begin{bmatrix}\mathbf{z}\\ \mathbf{z}_{h_i}\end{bmatrix}^{T}\begin{bmatrix}\mathbf{Y}_1^T\\ \mathbf{Y}_2^T\end{bmatrix}\mathbf{Q}^{-1}\begin{bmatrix}\mathbf{Y}_1^T\\ \mathbf{Y}_2^T\end{bmatrix}^{T}\begin{bmatrix}\mathbf{z}\\ \mathbf{z}_{h_i}\end{bmatrix} \tag{185}$$

we obtain the following inequality

$$\frac{dV_3}{dt}\leq\sum_{i=1}^{n}\left(\dot{\mathbf{z}}^{T}h_i\mathbf{Q}\dot{\mathbf{z}}\right)+\sum_{i=1}^{n}\left(\begin{bmatrix}\mathbf{z}\\ \mathbf{z}_{h_i}\end{bmatrix}^{T}\begin{bmatrix}\mathbf{Y}_1^T+\mathbf{Y}_1 & -\mathbf{Y}_1^T+\mathbf{Y}_2\\ (*) & -\mathbf{Y}_2^T-\mathbf{Y}_2\end{bmatrix}\begin{bmatrix}\mathbf{z}\\ \mathbf{z}_{h_i}\end{bmatrix}+h_i\begin{bmatrix}\mathbf{z}\\ \mathbf{z}_{h_i}\end{bmatrix}^{T}\begin{bmatrix}\mathbf{Y}_1^T\\ \mathbf{Y}_2^T\end{bmatrix}\mathbf{Q}^{-1}\begin{bmatrix}\mathbf{Y}_1^T\\ \mathbf{Y}_2^T\end{bmatrix}^{T}\begin{bmatrix}\mathbf{z}\\ \mathbf{z}_{h_i}\end{bmatrix}\right) \tag{186}$$

The quadratic form of the derivative of this parameter-dependent Lyapunov-Krasovskiĭ functional can be written as

$$\begin{bmatrix}\left\{\mathbf{A}^T\mathbf{P}+\mathbf{P}\mathbf{A}+\left(\sum_{i=1}^{s}\dot{\sigma}_i\frac{\partial\mathbf{P}(\sigma_i)}{\partial\sigma_i}\right)+n\left(\mathbf{R}+\mathbf{Y}_1+\mathbf{Y}_1^T\right)\right\} & \mathbf{P}\mathbf{A}_{h1}-\mathbf{Y}_1^T+\mathbf{Y}_2 & \cdots & \mathbf{P}\mathbf{A}_{hn}-\mathbf{Y}_1^T+\mathbf{Y}_2 & \mathbf{Y}_1^T\sum_{i=1}^{n}h_i\\ (*) & -\mathbf{R}_{h1}-\tilde{\mathbf{Y}}_2-\tilde{\mathbf{Y}}_2^T & \mathbf{0} & \mathbf{0} & h_1\mathbf{Y}_2^T\\ \vdots & \mathbf{0} & \ddots & \mathbf{0} & \vdots\\ (*) & \mathbf{0} & \mathbf{0} & -\tilde{\mathbf{R}}_{hn}-\tilde{\mathbf{Y}}_2-\tilde{\mathbf{Y}}_2^T & h_n\mathbf{Y}_2^T\\ (*) & (*) & \cdots & (*) & -\mathbf{Q}\sum_{i=1}^{n}h_i\end{bmatrix}\leq\mathbf{0} \tag{187}$$

Consider a reduced form of a closed-loop multiple time delay LPV system

$$\begin{bmatrix} \dot{\mathbf{z}}_w \\ \dot{\mathbf{z}}_1 \end{bmatrix} = \left(\widetilde{\mathbf{A}}_0 + \widetilde{\mathbf{A}}_1\widetilde{\mathbf{A}}_F\right)\begin{bmatrix} \mathbf{z}_w \\ \mathbf{z}_1 \end{bmatrix} + \sum_{i=1}^{n}\left(\widetilde{\mathbf{A}}_{hi}\right)\begin{bmatrix} \mathbf{z}_w(t-h_i) \\ \mathbf{z}_1(t-h_i) \end{bmatrix} \tag{188}$$

where

$$\widetilde{\mathbf{A}}_0 = \begin{bmatrix} \mathbf{0} & \mathbf{0} \\ \mathbf{0} & \hat{\mathbf{A}}_{11}(\boldsymbol{\sigma}) \end{bmatrix}, \qquad \widetilde{\mathbf{A}}_1 = \begin{bmatrix} \mathbf{I} & \mathbf{0} \\ \mathbf{0} & \hat{\mathbf{A}}_{12}(\boldsymbol{\sigma}) \end{bmatrix},$$
$$\widetilde{\mathbf{A}}_{hi} = \begin{bmatrix} \mathbf{0} & \mathbf{0} \\ \mathbf{0} & \hat{\mathbf{A}}_{h11i}(\boldsymbol{\sigma}) \end{bmatrix}, \qquad \widetilde{\mathbf{A}}_F = \begin{bmatrix} \mathbf{F}(\boldsymbol{\sigma}) & -\mathbf{G}(\boldsymbol{\sigma})\hat{\mathbf{C}}(\boldsymbol{\sigma}) \\ -\mathbf{H}(\boldsymbol{\sigma}) & \mathbf{L}(\boldsymbol{\sigma})\hat{\mathbf{C}}(\boldsymbol{\sigma}) \end{bmatrix},$$
$$i = 1, 2, \cdots, n \tag{189}$$

Submitting Equation (188) into Equation (187) and pre- and post-multiplying with $\mathrm{diag}(\mathbf{P}^{-1}, \mathbf{P}^{-1}, \mathbf{P}^{-1})$, we have

$$\begin{bmatrix} \left\{ \begin{array}{c} \widetilde{\mathbf{P}}\widetilde{\mathbf{A}}_0^T + \widetilde{\mathbf{A}}_0\widetilde{\mathbf{P}} + \widetilde{\mathbf{F}}^T\widetilde{\mathbf{A}}_1^T + \widetilde{\mathbf{A}}_1\widetilde{\mathbf{F}} \\ + \left(\sum_{i=1}^{s}\dot{\boldsymbol{\sigma}}_i \dfrac{\partial\widetilde{\mathbf{P}}(\boldsymbol{\sigma}_i)}{\partial\boldsymbol{\sigma}_i}\right) + n\left(\widetilde{\mathbf{R}} + \widetilde{\mathbf{Y}}_1 + \widetilde{\mathbf{Y}}_1^T\right) \end{array} \right\} & \widetilde{\mathbf{A}}_{h1}\widetilde{\mathbf{P}} - \widetilde{\mathbf{Y}}_1^T + \widetilde{\mathbf{Y}}_2 & \cdots & \widetilde{\mathbf{A}}_{hn}\widetilde{\mathbf{P}} - \widetilde{\mathbf{Y}}_1^T + \widetilde{\mathbf{Y}}_2 & \widetilde{\mathbf{Y}}_1^T\sum_{i=1}^{n}h_i \\ (*) & -\widetilde{\mathbf{R}} - \widetilde{\mathbf{Y}}_2 - \widetilde{\mathbf{Y}}_2^T & \mathbf{0} & \mathbf{0} & h_1\widetilde{\mathbf{Y}}_2^T \\ \vdots & \mathbf{0} & \ddots & \mathbf{0} & \vdots \\ (*) & \mathbf{0} & \mathbf{0} & -\widetilde{\mathbf{R}} - \widetilde{\mathbf{Y}}_2 - \widetilde{\mathbf{Y}}_2^T & h_n\widetilde{\mathbf{Y}}_2^T \\ (*) & (*) & \cdots & (*) & -\widetilde{\mathbf{Q}}\sum_{i=1}^{n}h_i \end{bmatrix} \leq \mathbf{0} \tag{190}$$

where $\widetilde{\mathbf{F}} = \widetilde{\mathbf{A}}_F\mathbf{P}^{-1}$, $\widetilde{\mathbf{Y}}_1 = \mathbf{P}^{-1}\mathbf{Y}_1\mathbf{P}^{-1}$, $\widetilde{\mathbf{Y}}_2 = \mathbf{P}^{-1}\mathbf{Y}_2\mathbf{P}^{-1}$ and $\widetilde{\mathbf{Q}} = \mathbf{P}^{-1}\mathbf{Q}\mathbf{P}^{-1}$. This completes the proof. □

APPENDIX D

For the problem given we have

$$m(z_1) \in [3.5603, \quad 4.1049] \text{ and } \left|\frac{\partial m(z_1)}{\partial z_1}\right| = |1.9760 \times 2z_1| \le 2.0691 \tag{191}$$

and the positive definite matrix functions as

$$\begin{aligned} \widetilde{\mathbf{P}}(\cdot) &= \widetilde{\mathbf{P}}_0 + \widetilde{\mathbf{P}}_1 m(z_1) > \mathbf{0} \\ \widetilde{\mathbf{Q}}(\cdot) &= \widetilde{\mathbf{Q}}_0 + \widetilde{\mathbf{Q}}_1 m(z_1) > \mathbf{0} \\ \widetilde{\mathbf{R}}(\cdot) &= \widetilde{\mathbf{R}}_0 + \widetilde{\mathbf{R}}_1 m(z_1) > \mathbf{0} \end{aligned} \tag{192}$$

The MATLAB / YALMIP results obtained below show that the matrix functions above are positive definite:

```
P0 =
   40.5166         0
         0   40.5166

P1 =
     1     0
     0     1

Eig(P0+P1*mmin )=
   44.0769
   44.0769

Eig(P0+P1*mmax )=
   44.6215
   44.6215

Q0 =
  245.8622    0.0057
    0.0057  245.8622

Q1 =
  -49.3019   -0.0011
   -0.0011  -49.3019

Eig(Q0+Q1*mmin )=
   70.3311
   70.3343

Eig(Q0+Q1*mmax )=
   43.4819
```

```
   43.4839

R0 =
  -97.8358   -0.0191
   -0.0191  -97.8358

R1 =
   34.4268    0.0049
    0.0049   34.4268
```

$Eig(R0+R1*m_{min})=$

```
   24.7324
   24.7357
```

$Eig(R0+R1*m_{max})=$

```
   43.4819
   43.4839
```